Development of an open-source and open-data energy system optimization model for the analysis of the European energy mix

Doctoral Dissertation
Doctoral Program in Energy Engineering (35th Cycle)

Development of an open-source and open-data energy system optimization model for the analysis of the European energy mix

By

Daniele Lerede

******

Supervisor:
Prof. Laura Savoldi

Doctoral Examination Committee:
Prof. Anderson Rodrigo de Queiroz, Ph.D., North Carolina State University
Prof. Pierluigi Leone, Ph.D., Politecnico di Torino
Prof. Marina Neophytou, Ph.D., University of Cyprus
Stefan Petrovic, Ph.D., Danish Energy Agency
Marco Piscitelli, Ph.D., Politecnico di Torino

Politecnico di Torino
2023

Declaration

I hereby declare that the contents and organization of this dissertation constitute my own original work and does not compromise in any way the rights of third parties, including those relating to the security of personal data.

Daniele Lerede

2023

* This dissertation is presented in partial fulfillment of the requirements for **Ph.D. degree** in the Graduate School of Politecnico di Torino (ScuDo).

Uomini forti, destini forti.
Uomini deboli, destini deboli.

Acknowledgment

At the end of this wonderful course, I sincerely need to thank the person who believed in me from the first moment. Laura, it has been a pleasure to share this experience with a tutor who has always encouraged me to give my best and to always see the positive side of things. I hope this is just the beginning of our fruitful professional collaboration.

To all the colleagues of the MAHTEP Group, and in particular to Matteo and Gianvito, your support in the everyday working life has been the fuel to allow me to get to this day with joy and satisfaction. Thank you for all the things you taught me and for all the time and the experiences spent together.

To all the members of the Evaluation Board of my PhD defense, thanks for your availability and for the opportunity to confront myself with this last challenge of my PhD course. In particular, thanks to Professor Anderson Rodrigo de Queiroz and Dr. Stefan Petrovic, who carefully reviewed my thesis and provided useful and stimulating comments to improve my work; I will surely take advantage of your suggestions to carry on my research activity at my best.

Also thanks to the EUROfusion WorkPackage for Socio-Economic Studies, for giving me the possibility to grow and confront everyday with experts in the field of energy modeling.

Abstract

In the context of strategical planning in support of the ongoing energy transition, energy system modeling tools allow to perform comprehensive analyses of the role of current and innovative technologies and their respective interactions.

Technology assessment requires a bottom-up approach calling for the adoption of least-cost optimization energy system models. Those models work with large techno-economic databases to provide a detailed description of the system under exam over a medium-to-long-term time scale and on large spatial scales. Therefore, the validity of the tool used for the analyses and the quality of the adopted technological database affect the analyses performed with energy system optimization models.

Proprietary energy system optimization models rely on source codes that can be easy to access but difficult to be modified and on input data usually not shared with the public. That contributes to undermining the reliability of such tools, especially when they are used for policy-relevant analyses. The results of energy system models are already subject to the impossibility of verification against actual future developments, and the inaccessibility to data represents an impassable barrier at least to ensuring that the results of the analyses are unbiased by the customers' requirements.

In a framework of increasing interest towards open-source modeling tools, the OSeMOSYS and TEMOA projects, considered mature enough to compete with either commercial or proprietary frameworks, are paving the way to increase the scientific validity of energy system modeling tools.

This work aims to develop an open-data and open-software model instance for the European continent on a long-term time scale up to 2100, TEMOA-Europe, mostly updated in the last few years with parameters coming from freely accessible sources and based on a completely accessible open database. As this work is developed taking advantage of the involvement in the EUROfusion Socio-Economic Studies WorkPackage, the assessment of the role of nuclear fusion in

future energy scenarios is indeed its main driver. Thus, the necessity of producing reliable studies to drive research and development and public investment choices cannot ignore the full accessibility and repeatability of the analyses.

That specific purpose presents a broader spectrum of activities involving the review of the techno-economic characterization modules for those sectors that will call for progressively larger electrification of end-uses, specifically transportation and industry (usually defined as “hard-to-abate sectors”), and for the hydrogen sector that may contribute to change the way energy is produced and used. Extensive databases for the mentioned sectors are presented and deeply analyzed in this work in terms of characterization and results obtained from TEMOA-Europe.

Moreover, as constraints for the development of the energy system are as important as parameters for the characterization of energy technologies and socio-economic trends, a method to compute possible trajectories for the capacity deployment of electricity generation technologies is presented. Such a method relates the historical development trends for the installed capacity to the widely accepted theory of the S-curves. Constraints based on the actual levels of electricity generation capacity building at the European level are obtained to implement maximum capacity constraint trajectories in TEMOA-Europe and then used for scenario analysis. Three nuclear fusion technological alternatives based on the ARC, EU-DEMO and Asian-DEMO reactor concepts are analyzed in this open model to guarantee a non-biased characterization of nuclear fusion technologies. Constraints based on the abovementioned S-curve theory were derived to reasonably bind the adoption of nuclear fusion, and the presented results show how fusion may not come too late to contribute to the energy transition in Europe when considering ambitious decarbonization targets. Moreover, a set of outputs is shown to present the capabilities of TEMOA-Europe to provide useful insights into future energy system developments.

Contents

List of acronyms

Acronym	Meaning
AAC	Alkali-activated concrete
ARC	Affordable, robust, compact
BAT	Best available technique
BDH	Bioethanol dehydration
BF-BOF	Blast furnace-basic oxygen furnace
BY	Base year
CCS	Carbon capture and storage
CREST	Compact Reversed Shear Tokamak
CSP	Concentrated solar power
DHE	Diesel hybrid-electric
DNE 21+	Dynamic New Earth 21+
DPH	Diesel plug-in hybrid-electric
DRI-EAF	Direct reduced iron-electric arc furnace
DST	Diesel
EFTA	European Free Trade Area
ELC	Full-electric
EPA	Environmental Protection Agency
ESM	Energy system model
ESOM	Energy System Optimization Modeling/Model
ETM	EUROfusion TIMES Model
ETP	Energy Technology Perspectives
ETSAP	Energy Technology Systems Analysis Program
EU	European Union
FCE	Fuel cell
G2G	Gas-to-gas
GDP	Gross Domestic Product
GHE	Gasoline-hybrid electric
GHG	Greenhouse gas
GPH	Gasoline plug-in hybrid-electric
GSF	Gasification
GSL	Gasoline

GVW	Gross Vehicle Weight
HDR	Hydrogen direct reduction
HDV	Heavy-duty vehicle
HVC	High-value chemical
IAEA	International Atomic Energy Agency
IAM	Integrated Assessment Model
ICE	Internal combustion engine
IEA	International Energy Agency
IIASA	Institute for Applied Systems Analysis
IRENA	International Renewable Energy Agency
L2G	Liquid-to-gas
L2L	Liquid-to-liquid
LDV	Light-duty vehicle
LNG	Liquified natural gas
LP	Linear programming
LPG	Liquified petroleum gas
M&R	Maintenance and repair
MEM	Macro Energy Model
MoMani	Model Management Infrastructure
MTO	Methanol-to-olefins
NCC	Naphtha catalytic cracking
NEDC	New European Driving Cycle
NEMS	National Energy Modeling System
NFPP	Nuclear fusion power plant
NG	Natural gas
O&M	Operation and maintenance
OEO	Open Energy Outlook
OSeMOSYS	Open-source energy modeling system
PDH	Propane dehydrogenation
PEMFC	Proton exchange membrane fuel cell
POX	Partial oxidation
PSA	Pressure swing adsorption
PV	Photovoltaic
R&D	Research and development
RES	Reference Energy System
SC	Steam cracking

SECTR	System Electrification and Capacity Transition
SR	Steam reforming
SUV	Sport-utility vehicle
TEMOA	Tools for Energy Model Optimization and Analysis
TES	Total energy supply
TIMES	The Integrated MARKAL-EFOM System
TRES	Transforming Energy Scenario
UCM	Unit Commitment Model
VPSA	Vacuum pressure swing adsorption
WE	Water electrolysis
WEO	World Energy Outlook
WPSES	WorkPackage for Socio-Economic Studies

Chapter 1

Introduction

Europe represents one-sixth of the global economy ($ 16.6 trillion nominal gross domestic product 2022) [1] and produces one-tenth of global energy consumption and CO_2 emissions [2]. The world, and Europe in particular, is currently experiencing one of the toughest periods in modern history. Price inflation was triggered by the different pace of demand and supply recovery after the COVID-19 pandemic [3]; in addition to that, the exacerbation of the Russia-Ukraine conflict in the first months of 2022 led to the crisis in the supply of primary energy and non-energy commodities (natural gas, above all).

1.1 Energy system optimization modeling

Once upon a time, there was a war to claim control of a disputed territory, and as in all wars, someone took sides to defend one of the two factions. In response to that, the faction which represented the greatest supplier of the most important primary commodity for the production system stopped supplies to those who had dared to interfere. The supply crisis led to subsequent price inflation and stagnant economic growth.

Although similar to recent events, the described situation dates back to the 1970s and concerns the 1973 oil crisis, resulting from the embargo introduced by Saudi Arabia on exports to the United States during the Arab-Israeli conflict [4].

That was the context leading to the birth of energy system models (ESMs). Indeed, resource allocation became to be very linked to the price of primary

commodities. ESMs were the only tools able to provide a reliable basis for beginning the discussion about resource dependence as linked to economic growth. The focus shifted to energy-environment interactions in the mid-1980s, producing models for 20-25 years-long forecasts. In the 1990s, major attention began to be paid to climate change-related issues, as the natural extension of previously produced models, and the cost of mitigation strategies for damages to the environment was introduced in the new energy models [5].

In the energy modeling field, bottom-up ESMs and characterized by a wide and detailed description of energy supply and demand technologies (the "technology-richness" peculiarity, deemed as necessary in, e.g. [1] and [2]). Their peculiarity is to allow the analysis of inter-sectoral and technology-specific details where other types of models, such as those adopting a top-down economic approach, fail. This comes at the price of accurate characterization of the various processes or parts of them composing the energy system under exam.

Europe is now experiencing a similar scenario with respect to what occurred during the oil crisis in the 1970s, with the necessity of a progressive change in the paradigms dominating the energy field, summarized in the three pillars of the REPowerEU plan: diversification, savings and acceleration in clean energy production and consumption [6]. Moreover, considering the pressing need for climate change mitigation and greenhouse gas (GHG) emission abatement [7], energy system modeling reveals itself as a crucial approach once again.

The possible future developments of the energy system, needed to mitigate climate change effects, are widely studied using the energy scenario approach [8]. Institutions, international organizations and governments worldwide strongly rely on energy scenario comparison based either on energy system simulation or on optimization-based models. That is the case of e.g., the World Energy Model [9], the main tool used by the International Energy Agency (IEA) to generate long-term simulations aimed at driving global institutions in the transition towards net-zero emissions; or optimization models like those of The Integrated MARKAL-EFOM (TIMES) family (for instance the TIMES-Italy [10], adopted to support the Italian Energy Strategy [11], or the JRC-EU-TIMES, a multi-regional model for Europe built on a time scale up to 2050 [12]), developed in the framework of the IEA's Energy Technology Systems Analysis Program (ETSAP) [13]; or the MESSAGE family, first developed by the International Atomic Energy Agency (IAEA) [14] and then integrated with macro-economic and environmental

modules by the Institute for Applied Systems Analysis (IIASA) to give the Integrated Assessment Model (IAM) framework [15].

Specifically, energy system optimization models (ESOMs) apply different techniques, including mathematical programming (especially linear programming), econometrics and related methods of statistical analysis, and eventually network analysis with the main aim of emphasizing the necessity for coordinated developments between all the components of the energy system, to build cost-effective strategies [5]. Indeed, ESOMs aim to produce the least-cost configuration of the energy system over a medium-to-long-term time scale [16].

As ESOMs are particularly suited for the study of the role of current and innovative energy technologies in the energy system [17], research and development (R&D) programs cannot disregard the use of such models to understand the large-scale integration of their innovations. In particular, technological advancement must act to enhance and support the adoption of low-carbon options across supply and end-use sectors to achieve a transition towards a cleaner and more sustainable energy system [18]. Whereas the development and integration of renewable energy technologies is an ongoing process, especially in the electricity generation sector [19], and the peak in global GHG emissions from the power (electricity and heat) sector has just been reached in 2018 [20], mainly two innovative options are gaining increasing interest in the energy sector: plants equipped with carbon capture and storage (CCS) [21] and nuclear fusion [22]. While some plants already exist envisaging the adoption of the former technology (almost 30 power plants equipped with CCS were commissioned between 2020 and 2021) [23], which would allow a substantial reduction of vented CO_2 emissions in plants relying on fossil fuels, the feasibility of the latter still has to be demonstrated, despite considerable progress in recent years and a growing number of projects contributing to make fusion energy achievable [24]. Indeed, the main challenge for nuclear fusion is to achieve a positive balance between the energy injected into the plasma and the heat emitted by that, necessary to produce steam and – by way of turbines and alternators – electricity. Fusion fuel (the fusion reaction involves two hydrogen isotopes, deuterium and tritium) must be heated at extreme temperatures and must be kept stable under intense pressure, requiring confinement for long enough to allow the realization of the fusion reaction [24]. Nuclear fusion is deemed as a game changer mainly due to being a zero-carbon and dispatchable electricity source, therefore joining the strong benefits of renewable energy technologies, but with the possibility of a (quasi-)continuous operation as they intrinsically work as pulsed machines [25].

Discussions about CCS have been around for quite some time in the ESOM universe, as even the IEA considers it among the disruptive technologies to allow reaching net-zero emissions by 2050 [26] including it in both the Energy Technology Perspectives (ETP) model [27] and the World Energy Model for the production of the World Energy Outlook [26].

1.1.1 Nuclear fusion in energy system models

In the current framework of strong commitments to fight climate change [28], technological advancement to enhance and support the adoption of existing low-carbon options across supply and end-use energy sectors must go on to achieve a transition towards a cleaner and more sustainable energy system [18]. Nuclear fusion is deemed one of the possible groundbreaking zero-emission technologies to be effective on the large scale, provided that its feasibility for commercial purposes is demonstrated in the coming years.

The research on magnetic confinement nuclear fusion is mainly focused on the tokamak configuration, notwithstanding a few running projects concentrating on spherical tokamaks [29] and stellarators [30]. In this framework, the ITER reactor [31] is under construction in France. ITER is an international program gathering China, the European Union, India, Japan, South Korea and the United States in a 35-year collaboration to demonstrate an energy gain for fusion ("10 times as much thermal output power as thermal power absorbed by the plasma", see [31]) and the capability to sustain the fusion reaction for long periods of time (hundreds of seconds). The potential success of the research project will lead to the design, construction and operation of demonstration (DEMO) reactors to lay the foundations for the commercialization of nuclear fusion power plants in the second half of this century expected in Europe [32], China [33], Japan [34] and South Korea [35]. In the USA, the ARC project [36] is also based on the tokamak configuration but targets a compact machine at a higher magnetic field than DEMO. It has, instead, the aim of building an affordable, robust, compact (ARC) fusion reactor, able to produce three times the electricity required to operate the machine. Moreover, ARC would rely on high-temperature superconducting magnets [37] in place of ITER's low-temperature superconducting magnets [38] allowing comparable performances with reduced plant dimensions (thus lower construction effort). Furthermore, the target set for ARC's commercial availability is at 2035, thus at least 15 years before the ITER-based commercial reactors, according to the aggressive timeline set out in [25] to put fusion electricity in the grid in the early 2030s.

Despite being considered a fully clean and sustainable technology itself, issues regarding the life cycle of nuclear fusion-related materials, their availability and the activation of components at the end of life of the reactor are still to be fully clarified. From the environmental point of view, the CO_2 footprint of fusion materials (steel, cement, lithium, copper and vanadium, among others) is generally shown to be low if compared to renewable technologies, especially in the case of compact reactor concepts (i.e. ARC) [39]. Nonetheless, the construction of fusion reactors requires a huge amount of steel and cement. Low-carbon alternative options (e.g. based on electrolysis) are supposed to be available on the commercial scale soon [40] and widely adopted until the commercialization phase of fusion machines. In any case, such materials are widely required for the majority of energy supply and demand facilities. Considering reserves of crucial materials for fusion, deuterium is abundant in seawater, while the limited and uneven availability of lithium (required to breed tritium) and rare earths, among others, may cause equity issues, especially for the first generation of fusion reactors, when some industrial chains will not be fully developed [39]. From a safety point of view, the absence of a chain reaction guarantees the impossibility of catastrophic accidents [41]. Concerning radioactive wastes or residues, an appropriate selection of the material and the adoption of accurate procedures for management and disposal should limit the generation of activated waste to a low or very low level [42], and the technologies already developed for the nuclear fission plants could easily cope with them. The plans for the decommissioning of the ITER reactor, relying on the French expertise in the decommissioning of nuclear fission plants, go indeed in that direction.

Concerning the ESOM universe, nuclear fusion is still quite out of the radars, especially due to the (sometimes very) long time frame expected for its development and commercialization. However, the EUROfusion Consortium – and specifically the WorkPackage for Socio-Economic Studies (WPSES) – is in charge of understanding the future role of ITER-based reactor concepts [43] in the global energy mix. In particular, the WPSES relies on the EUROfusion TIMES Model (ETM) [44], a global energy system with 17 regions acting on a long time run until 2100. A three-year involvement in the EUROfusion WPSES for maintenance and further development of ETM, jointly with the production of energy scenario analyses, provided the experience and some useful insights to achieve the realization of this PhD research program.

Regarding the study of possible penetration of nuclear fusion in the energy mix using quantitative models, besides ETM under development within the EUROfusion WPSES, some studies have been carried out throughout the last two decades using different quantitative models:

- In [45], the PLANELEC-Pro global electricity system model is used by the Swiss Federal Institute of Technology to assess the global potential for the development of fusion power elaborating 6 multi-regional electricity market scenarios until 2100. No details are given concerning the technical and economic parameters adopted to characterize nuclear fusion power plants (NFFPs).
- In [46], the World-TIMES multiregional global energy system model is adopted by the GERAD Research Center (Canada) to compute results in two scenarios with different CO_2 concentration levels by 2100 (450 ppm and 550 ppm). In both cases, nuclear fusion achieved considerable installation levels despite the high installation costs. Fusion is considered available starting from 2048 considering a cost of ~ 6 – 9 $ per MW based on estimates dating back to 1998 [47], while technical parameters are not provided. Nonetheless, lithium to breed tritium is considered to be the only input commodity leading to electricity generation.
- The analysis presented in [48] is one of the most recent examples of quantitative assessment analyses to study the possible role of fusion given the climate prescriptions of the Paris Agreement. The authors of the Research Institute of Innovative Technology for the Earth (Japan) [48] use the Dynamic New Earth 21+ (DNE 21+) global multi-regional nonlinear least-cost optimization energy system model [49] and develops 3 socio-economic development pathways analyzed in 4 global emission pathways and considering scenarios dealing with the uncertainty in fusion energy development. DNE 21+ is also a bottom-up energy model involving the characterization of about 300 technologies to explore their possible role in climate change mitigation. Concerning nuclear fusion, it only considers a single nuclear fusion technology representative of the Compact Reversed Shear Tokamak (CREST) [50] and SlimCS [51] reactor concepts, both based on the developments of the ITER project and considered as economically and engineering viable small-size fusion technology options. The only technical parameters provided are represented by the annual capacity factor and the operational lifetime of the plant, while constraints for the development of fusion technologies are based on the same

trajectory depicted by historical data for nuclear fission capacity, despite being unequivocally influenced by the low social acceptance due to well-known severe accidents [52].

A characterization is provided in this work for the European DEMO and the Asian-DEMO (based on the features of CREST and SlimCS technologies, and on the K-DEMO that will be possibly developed in Korea for a pre-commercialization stage) but also, for the first time in an ESM, for an ARC-based reactor.

However, this work is not intended to highlight the features of fusion energy and to present it as the solution to the issues the world is facing, but rather to fill the gap in the existing literature concerning a comprehensive analysis of its possible role in the future energy system.

1.2 Main features of the ESOM framework

Since ESOMs are devoted to technology assessment in future energy scenarios, the first step is the identification of the reference energy system (RES), a properly detailed network description of the energy system ("all the components related to the production, conversion, delivery and end-use of energy" [53]), starting from the description of the main energy consumption and supply sectors [54].

The approach allows accounting for existing and future technologies In the system and has the fundamental advantage to allow the adoption of optimization techniques to analyze alternative system configurations, which use alternative technologies and energy sources to meet a given set of end-use demands.

The typical RES in **Figure 1** is thus composed of:

- supply module: the supply side is represented by the upstream sector, including extraction, transformation and import of primary resources (e.g. fossil fuels and uranium) and renewable energy potential, according to their availability. Extracted and renewable commodities are then used for power (electricity and heat) and hydrogen production;
- demand module: end-use is represented by the industrial, transport, buildings (residential and commercial) and agriculture sectors.

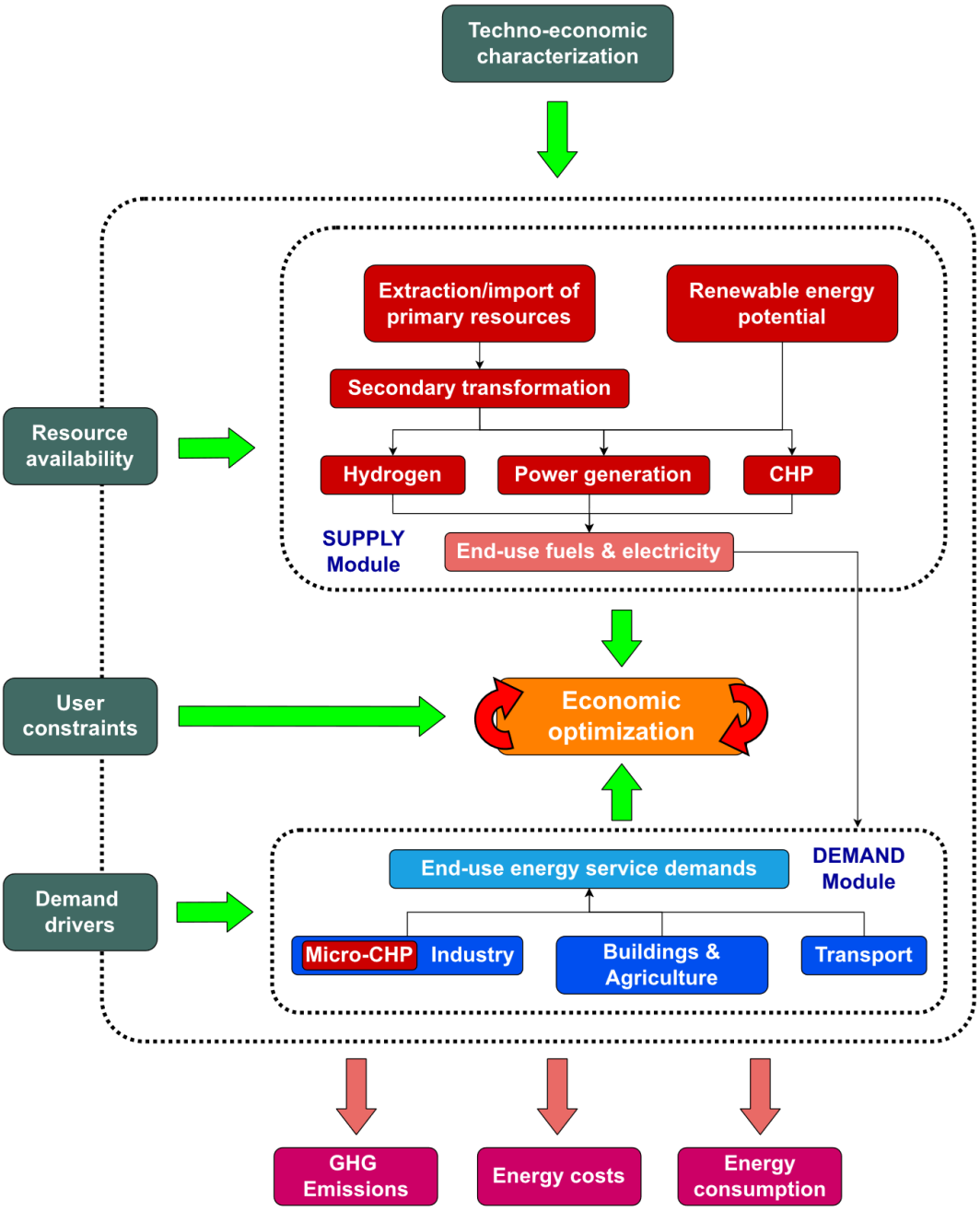

Figure 1. Schematic of RES inputs and outputs, elaborated by the authors, based on [13].

Demand levels are defined a priori according to a specified set of drivers, including gross domestic product (GDP), GDP based on purchasing power parity, GDP per capita, average number of household members, population and value-

added for each industrial subsectors and the service sector. End-use demands must be satisfied at the minimum cost for the model to obtain a solution, subject to a number of constraints to represent policy targets or existing limits for system performances and technology adoption.

ESOMs of the TIMES family, and generally bottom-up energy models, work in partial equilibrium, i.e. they simultaneously configure commodity production and consumption and their price according to the maximization of producers' and consumers' surplus. In case demands are not affected by commodity prices (i.e. user-specified for the entire time horizon of the model), the minimization of the total cost of the system is equivalent to the maximization of the total surplus [16]. Moreover, they work in the assumption of perfectly competitive markets, meaning that a single consumer/producer cannot decide the quantity and price at which each commodity can be bought/sold. Nonetheless, the presence of constraints influencing the availability of specific commodities inevitably introduces imperfections in the market computed by the model [16]. Eventually, competitive markets are characterized by perfect information, extended in ESOMs to the entire planning horizon, so that each agent has perfect foresight, i.e. complete knowledge of present and future market parameters [16].

The relationship between the supply and the demand side is constructed over three basic entities [13]:

- Technologies (also defined as processes) are representations of physical devices that transform commodities into other commodities. Technologies may be sources of commodities (e.g., mining/import processes), or transformation activities, such as conversion plants for electricity production, or end-use demand devices, like cars, steel production plants, etc.;
- Commodities include all energy carriers, energy services, materials, emission and demand commodities and may be either consumed or produced by technologies;
- Commodity flows are the links between technologies and commodities (e.g. electricity generation from wind), thus they correspond to the way a commodity is used by a technology.

Technologies are usually described according to a limited set of technical and economic parameters (techno-economic characterization) to allow the definition of specific energy production/consumption levels, economic features and

environmental performances, all concurring to the determination of the optimal objective function [16], as reported in **Table 1**. Note that a more extensive set of parameters is available in complex ESOMs like, for instance, TIMES [55], to provide descriptions of very specific techno-economic features (e.g., the maximum non-operational time before the transition to next-stand-by condition, or the ramp-up/ramp-down cost per unit of load change) which are uncommonly used.

Constraints are also fundamental in the ESOM formulation [56] and can be defined by the user to model:

- the real life mechanisms of technological substitution. For instance, old capacity at the end of its operational lifetime should be substituted avoiding abrupt investment in new capacity [16] through, e.g., minimum/maximum capacity constraints or limiting growth rates;
- physical and operational real-world phenomena through, e.g., minimum/maximum activity (production) constraints;
- trajectories to limit GHG emissions in future scenarios.

Although constraints are widely adopted for the definition of the different energy scenarios, it is commonly suggested not to adopt many restrictive constraints to avoid "railroading" the model, which should instead respond to its optimization paradigm [16]. Indeed, constraints should be used just to replicate either real life constraints on technological adoption and evolution, or the availability of resources, thus not to force model results to obtain the desired outcomes.

As a common approach in forecasting models, technological substitution throughout the considered time horizon is taken into account distinguishing between two kinds of technologies [57]:

- Base year technologies, used to model the demand and the energy use at the beginning of the time horizon. The base year demand is calculated by combining energy statistics concerning total energy consumption with dummy efficiency values and coefficients associated to the generic technologies for which an existing capacity is there. In this way, base year energy consumption is allocated to the existing capacity (see **Table 1**) of a specific technology.

- New technologies, used to model the energy use throughout the model time horizon, are added to the existing fleet of base year technologies from the second time-step on.

Table 1. Main parameters for the characterization of energy technologies in ESOMs.

Type of parameter	Definition	Description
Technical	Efficiency	Input-to-output transformation parameter
	Capacity factor	Utilization factor to define the available capacity fraction during a specific time slice
	Technical lifetime	Operational lifetime
	Capacity to activity	Conversion factor to be used in case capacity units differ from activity units
	Existing capacity	Capacity installed prior to the beginning of the time periods set for the optimization
Economic	Investment cost	Total cost of investment in new capacity
	Annual fixed operation and maintenance cost	-
	Variable operation and maintenance cost	-
	Technology-specific discount rate (optional)	Interest rate on investment for a specific technology
Environmental	Emission activity	Emission rate for the specific technology

Commodities are essential as they represent the inputs and outputs of the technologies. They can be labeled as physical, emission, or demand commodities [56]. Physical commodities can be transformed by technologies to obtain either other physical or emission or demand commodities. They represent energy-intensive materials (e.g. clinker or alumina), fuels (e.g. gasoline or gas oil) or other energy carriers (e.g. electricity or hydrogen). Emission commodities are mainly produced as outputs from technologies involving combustion of fossil fuels or take into account other process-related emissions (e.g. CO_2 emissions from calcination in clinker production): usually, CO_2 is the main emission commodity taken into account for the definition of energy scenarios as it is considered the main climate-altering agent [58], but any ESOM user may decide whether to also include other emission commodities like, e.g., methane CH_4 or nitrogen dioxide NO_2 for both accounting purposes and the definition of emission

targets related to other commodities than CO_2 alone. Demand commodities are either given pre-assigned values or may be elastic to the computed price. In the former case, demand levels must be satisfied at each step of the time scale. Demand commodities generally represent energy services supplied by energy-intensive processes: they may represent several needs ranging, for instance, from the heated surface in a residential building to the quantity of produced steel or the driven distance by a car in a year.

Commodity flows are represented according to the way commodities are used and produced by the technologies of the RES, so that the assigned commodity-specific efficiencies connect commodities and technologies to define the whole chain from extraction of natural resources to the final service demands.

1.3 ESOMs in the framework of open science

Among the wide range of existing ESOMs [59], one of the most relevant example of bottom-up, technology-rich energy modeling framework [60] is represented by the TIMES model generator [13] (and its ancestor MARKAL [61]). TIMES combines a technical engineering approach to macroeconomic ingredients, using a linear programming formulation to produce the least-cost optimized composition of the energy system under exam over a medium-to-long term time scale under the assumption of partial equilibrium of competitive markets in a perfect foresight approach [16]. Specific combinations of different policies and developments of the energy system allow the definition of different scenarios under a set of constraints on technologies, commodities, or demand evolution.

Out of the different applications of TIMES, the JRC-EU TIMES Model is an example of policy-relevant modeling tool used by the European Commission for the anticipation and evaluation of technology policy at the European level [12]. At the global level, the TIMES framework is at the basis of the analyses carried out by the IEA for the periodical publication of the ETP, first issued in 2006 [62], a periodical technology assessment to understand the future role of innovative technologies in a low-carbon energy system. Although the (technological) databases used in the JRC-EU TIMES Model (the full dataset is available at [63]) and ETP (parts of its dataset are available in [64], for instance) are open and publicly available, the TIMES generator relies on proprietary software to read the input data, solve the optimization problem, and postprocess the results.

Recently, a growing awareness is spreading in the scientific community about open science, i.e., the possibility to freely disseminate data and results of scientific research, increasing responsiveness and spreading knowledge regardless of the economic status of the recipients [65]. The importance of that issue is so relevant that it falls within the priorities of the European Commission [66]. In particular, the open science purpose can be realized in the field of energy modeling providing open access to both models and data, leading not only to higher quality, reliability, and recognition of the results of energy projection tools [67], but also to attempts for expanding the capabilities of traditional models. Nonetheless, energy scenarios have been criticized mostly for their lack of realism, as they are not able to fully reproduce the actual behavior of the energy market and can be strongly biased by external assumptions about its developments [68].

TIMES cannot be currently defined part of an open modeling environment, as being part of a complex environment based on commercial and proprietary software. Therefore, several open-source tools or frameworks have been developed in the recent years for ESOM analyses, with some focusing on the optimization of the electricity system alone, e.g., Balmorel [69], pyPSA [70], Switch [71] and some others referring to the entire energy system. Two main tools fall in the second category, namely the Open-Source Energy Modelling System (OSeMOSYS [72]) and Tools for Energy Model Optimization and Analysis (TEMOA) [73], both aimed at replicating the TIMES optimization algorithm using linear programming techniques to minimize the system-wide cost of energy supply by optimizing the deployment and utilization of energy technologies over a user-specified time horizon to meet fixed end-use demands [74].

As of today, OSeMOSYS has been used to develop a large body of model instances used for deterministic scenario analyses to assess optimal energy transition pathways at different national and international scales. The tool has been adopted as a support for several research questions. For instance, the OSeMOSYS-SAMBA has been developed and used for the analysis of energy security issues in South American countries [75]. Models based on OSeMOSYS have been developed for the analysis of future electrification pathways in Tanzania to decarbonize the power sector and ensure universal energy access [76] or for the study of the integration of renewable energy sources in the power system in Tunisia [77]. An interesting attempt to expand the OSeMOSYS formulation is shown in [78], where power plant retrofitting is modeled expanding the mathematical equations of the source code considering, for instance, possible change of plant (or operation) characteristics, or lifetime extension, with an

application to the Korean RES. Another attempt for the expansion of the model formulation is presented in [79], where the potential of different demand-response strategies in the balance between electricity supply and demand is assessed for the case of the Portuguese power system in three scenarios. Note, however, while no applications of OSeMOSYS have so far attempted the adoption of objective functions different from the one implemented in TIMES, the only attempt to compare the two tools on the same case study is limited just to the power sector [80].

On the other hand, the set of publications involving applications of TEMOA to real case studies is still limited to a few countries or regions. The main focus of works concerning TEMOA is devoted to the presentation of the modeling framework [73] and its uncertainty analysis tool for multi-stage stochastic optimization [81], which is also available in TIMES [82]. An example of application of TEMOA for the analysis of the United States energy system is presented in [83]. There, the US is presented as a single region and projections are drawn from 2015 to 2040 to assess the impact of the absence of federal climate policies, in response to the withdrawal of the US government from the Paris Agreement, first announced in 2017, then formalized in 2020 [84] and finally revoked after the settlement of the President Biden administration at the beginning of 2021 [85]. The dataset used in the cited work is based on the United States Environmental Protection Agency (EPA) MARKAL model [86] and represents the basis for the Open Energy Outlook (OEO) project. The OEO is a non-policy biased analysis for the assessment of possible U.S. energy futures to inform future energy and climate policy efforts [87]. In [88], future electricity generation, CO_2 emission trajectories and CO_2 abatement costs are analyzed for the North Carolina electric power sector using a state-level TEMOA model instance over time frame until 2050. Other TEMOA-based applications adopt its stochastic optimization feature: in [89], that is used to explore South Sudan electricity planning strategies, producing a near-term hedging strategy on a time horizon of 20 years from 2017 on; besides, stochastic optimization is also used in [90] to assess the role of uncertainties in influencing the total cost of the energy system in different decarbonization pathways for the US. The modeling framework has been also compared against other open ESOM tools: the Carnegie Institution for Science's Macro Energy Model (MEM), the energyRt model developed and used by the Environmental Defense Fund and the System Electrification and Capacity Transition (SECTR). Indeed, in [91] the differences of the four mentioned models are deeply analyzed to highlight the importance of the benchmarking process, so that different models can benefit from each other in the representation of specific

model structures. However,Ie only work presenting a benchmarking between a TEMOA-based model against an equivalent TIMES instance is based on the comparison between TEMOA-Italy and TIMES-Italy [92] and demonstrated how the two tools provide comparable results in a business-as-usual scenario. Another application of TEMOA [93] concerns its coupling with a multi-reservoir model (GRAPS) to co-optimize water supply and the power system according to a minimum cost paradigm. TEMOA is also used in [94] for seasonal planning, by adapting its standard mathematical formulation to accommodate the operational characteristics of the power system. The ESOM is shown to obtain high-quality performances when compared to Unit Commitment Models (UCM), particularly devoted to consider the hour-by-hour commitment and dispatch of generating units. Eventually, TEMOA has also found space in assessing the effects of extreme weather risks (in addition to the typical climate change mitigation policies generally addressed with ESOMs) considering the impact of hurricane trends on the costs of the energy system for Puerto Rico [95].

1.3.1 Selection of the open-source framework

Table 2 presents an overview of the main features of the OSeMOSYS and TEMOA open tools against TIMES. Concerning the input data management system, OSeMOSYS provides the Model Management Infrastructure (MoManI), an open-source browser-based platform which allows model development and the editing and update of the underlying OSeMOSYS equations [96]. Also TEMOA provides an online user interface for model creation and management [97][98]. Anyway, the input dataset for any TEMOA model instance can be constructed either as a text file or a relational database (preferred in case of larger datasets). Relational databases for TEMOA include the structure of the different tables filled with input data for the model and are stored in a text file in .sql format. Once the .sql text file is complete, it is converted into a .sqlite database in order to be interpreted by the TEMOA source code.

On the other hand, the TIMES input data system is articulated over two passages: the set of Excel files containing input data for the model, built following a precise structure and syntax (the number and complexity of the Excel database can increase a lot with model size and degree of detail) [57] are fed to the VEDA Front-End [99] model user interface that recalls the TIMES source code and the solver (generally the CPLEX Optimizer [100]). Differently from TEMOA, OSeMOSYS and TEMOA share the impossibility to set interpolation rules for the future evolution of parameters during the time frame selected for the analysis.

Concerning the possibility to modify the model structure (possible without any limitations with OSeMOSYS and TEMOA), the TIMES source code can be downloaded for free after having signed a Letter of Agreement and requested credentials [101]. More in detail, the optimization problem (maximization of the consumer and producer surplus or equivalently the minimization of the cost of the energy system) is formulated in a way that cannot be modified without the ETSAP approval (that obtains the intellectual property of any approved changes [101]).

The source code for the three modeling frameworks under analysis is based on high-level programming languages: among them, OSeMOSYS alone provides three different versions of the source code in GNU [102], Python [103], and GAMS [104], while TEMOA is only written in Python and TIMES in GAMS. In particular, the choice of Python (and in particular of the Pyomo open-source package for the implementation and solution of linear programming problems), with its verbosity, its easy access to a rich ecosystem of supporting modeling tools and the support of a wide user community and documentation is deemed as the most appropriate choice to reduce the learning curve for new modelers [73].

On the other hand, one of the main differences between OSeMOSYS and TEMOA regards the availability of open-source solvers, thus the complexity of the energy system that can be optimized by the model. Indeed, using the freely available GLPK [102] solver coupled with OSeMOSYS, only relatively simple energy systems can be optimized with acceptable computational cost. On the contrary, with TEMOA there is the possibility to use freely also solvers allowing the optimization of larger-size energy systems, such as CPLEX [105] or Gurobi [106]; GLPK can be nevertheless used for simpler study cases. TIMES, instead, requires a commercial license in order to use CPLEX or other solvers. The other important difference between OSeMOSYS and TEMOA is that the latter is provided with an extension of the deterministic code that allows performing a stochastic optimization. This allows conducting uncertainty analysis with large and complex models to evaluate the accuracy of the obtained results.

All in all, the OSeMOSYS and TEMOA open-source tools have already proved to be mature enough to be comparable to TIMES, even though the continuous extension of their functionalities (which is also partly taken on in [92]) would be beneficial to increase their reliability [67].

In this work, the choice of TEMOA for the development of the case-study, i.e., an open-source model for the European energy system, is mainly due to three reasons: 1) the possibility to use freely powerful open-source solvers as CPLEX and Gurobi; 2) the use of Python, allowing to rely on numerous software packages and libraries developed in that programming language; and 3) the possibility to model large-scale energy systems.

1.4 Aim of the work

Energy system modeling is the most suitable approach to assess the optimal evolution of the energy mix and identify the role of innovative mitigation technologies in a framework of changing priorities in view of the fight against climate change. In this framework, Europe is also facing a period of great uncertainty, coupling the crisis of supply of both energy and non-energy commodities and the target of reaching carbon neutrality by 2050 [107]. Moreover, research is focusing on low-carbon energy projects, above all nuclear fusion, deemed as a game changer for the energy sector once it will be demonstrated and commercialized. Indeed, it shall be able to contribute to baseload energy production as a zero-emission technology independently on climate conditions (differently from renewable energy sources). As research on nuclear fusion involves both private and public expensive and high-risk projects [108], an unbiased framework to investigate the feasibility of the claimed targets and to understand whether huge expenditures in R&D are justified by its expected role in the energy system is necessary. Fully transparent – open data and open software – ESOM provides a solution for this problem.

The aim of this work is to develop the first-of-a-kind open-database and open-software model instance for the European continent on a long-term time scale up to 2100 including nuclear fusion technologies, by the name of TEMOA-Europe. TEMOA-Europe is a single-region model merging data for the European Union (EU), the European Free Trade Area (EFTA) countries and the United Kingdom, thus providing a picture of a broad energy system, considered as a whole rather than composed of individual realities acting independently. This activity takes advantage of the involvement in the EUROfusion WPSES with a three-year experience in the development and maintenance of technological modules for ETM. Indeed, TEMOA-Europe is mainly based on the work carried out within the WPSES to present an alternative model for the assessment of the future role of nuclear fusion in the future energy mix and, more in general, for long-term inter-sectoral energy scenario analysis.

The thesis is structured as follows. In the viewpoint of developing an open database, **Chapter 2** presents the techno-economic characterization for the transportation, industrial, hydrogen and nuclear fusion technologies included in TEMOA-Europe. **Chapter 3** presents TEMOA-Europe and its main features, showing its potentiality in terms of outcomes that can be obtained by the use of the tool. Eventually, **Chapter 4** presents the conclusions and perspectives of this work.

Note that some of the contents of this thesis are already part of works either published or submitted by the candidate to international journals. In particular, the construction of a techno-economic database for road transport technologies in **Section 2.1** is taken from "Analysis of the Effects of Electrification of the Road Transport Sector on the Possible Penetration of Nuclear Fusion in the Long-Term European Energy Mix" [109] by D. Lerede, C. Bustreo, F. Gracceva, Y. Lechón and L. Savoldi, published on Energies in 2020; the database for industrial energy-intensive subsectors in **Section 2.3** was published on Renewable and Sustainable Energy Reviews by the title "Techno-economic and environmental characterization of industrial technologies for transparent bottom-up energy modeling" [40] by D. Lerede, C. Bustreo, F. Gracceva, M. Saccone and L. Savoldi in 2021; those parts related to the characterization of nuclear fusion technologies in **Section 2.5** are taken from "Analysis of the possible contribution of different nuclear fusion technologies to the global energy transition" [110], submitted by D. Lerede, M. Nicoli, L. Savoldi and A. Trotta to Energy Strategy Reviews and currently under review; eventually, the calculation of constraints for electricity generation technologies in **Section 3.6** partially refers to "Might future electricity generation suffice to meet the global demand?" [52] by D. Lerede and L. Savoldi, to be published soon on Energy Strategy Reviews.

Table 2. Comparison of available tools for macro-scale energy system optimization.

Feature \ Tool	OSeMOSYS	TEMOA	TIMES
Features of the input data entering tool	Several steps are required for the definition of the time scale, space-scale, and technological characterizations, but allows a prompt visualization of the RES network	Complexity increases with the complexity of the energy system, but the code formulation makes it straightforward	Complexity increases with the complexity of the energy system (especially with the number of regions), due to the large number of Excel files to be managed
Future evolution of parameters	The required values must be declared at each desired time-step	The required values must be declared at each desired time-step	The required values must be declared at each desired time-step, with the possibility of assigning different interpolation rules
Type of programming language	High-level	High-level	High-level
Programming language(s)	GNU open-source Python open-source GAMS commercial	Python open-source	GAMS commercial
Optimization software (solver)	GLPK for GNU open-source GLPK for Python open-source CPLEX for GAMS commercial	GLPK for Python open-source CPLEX for Python commercial (but can be run on an external server) Gurobi for Python commercial (but available with free academic license) COIN-OR CBC open-source*	CPLEX for GAMS commercial
Features of the optimization software	Suitable for simple energy systems if using-open-source solvers	Suitable for large-scale energy systems	Suitable for large-scale energy systems
Possibility to modify/improve the code	Possible	Possible	Possible, but requires approval by ETSAP
Possibility to perform stochastic optimization	Impossible at present state, but an extension can be formulated	Possible with an already implemented Python module	Possible, but time-consuming and complex due to the difficult data handling

* Not available for Windows.

Chapter 2

Development of a techno-economic database for TEMOA-Europe

In response to the scarcity of available updated and comprehensive databases, a new open-source techno-economic demand technology database is presented here, aiming at providing a comprehensive description of the main current and future technologies supposed to be available in the (road and non-road) transport and the industrial sectors to populate the energy system generated by the ESOM instance in which they are adopted. A comprehensive account concerning hydrogen production, storage, distribution and utilization technologies is reported in this section, alongside with an assessment about nuclear fusion technologies included in TEMOA-Europe. Since transparency of data in non-open models is often hindered by non-disclosure agreements and assumptions, sources and methodology for data gathering and processing are unclear [111], in this work it is deliberately decided to use only freely accessible sources, as that choice was deemed fundamental for pursuing full transparency and reproducibility of the results. **Section 2.1** presents the techno-economic database for road transport technologies (also currently adopted in ETM) and published in [109]. On the other hand, **Section 2.2** deals with the techno-economic characterization of non-road transport vehicles. **Section 2.3** presents an extensive database of currently available and innovative (even still at the R&D stage) energy-intensive technologies in five industrial subsectors (iron and steel, non-ferrous metals, non-metallic minerals, chemicals, pulp and paper) as from [40], while the construction of an hydrogen modules is described in **Section 2.4**. Eventually, **Section 2.5**

presents a first attempt to characterize a broad range of nuclear fusion technological options based on [110]. Note that all the techno-economic databases presented here report data adopted for new technologies in TEMOA-Europe.

2.1 Road transport

Road transport technologies are subdivided into 8 transport modes, shown in **Table 3**: as TEMOA-Europe only deals with energy-intensive technologies and cannot analyze behavioral aspects such as modal change, other transport modes like, e.g., walking and cycling, are not taken into account. **Table 4** shows the road vehicle technologies currently considered in this database. Taking as reference model the JRC-EU-TIMES [63], that also considers a broad range of different vehicles and almost the same transport modes envisaged in the TEMOA-Europe, with the only exceptions of medium trucks and three-wheelers. Indeed, medium trucks are included in a more general "Heavy-duty trucks" transport mode, while three-wheelers are not taken into account. On the other hand, a more detailed modeling is performed for cars, considering different size categories in place of a single kind of vehicle (medium car) representative of a wider range of cars. That is the reason why a punctual comparison will be not assessed, while taking [63] as a reference for future improvements to the TEMOA-Europe transport module.

The initial availability date of the different vehicle technologies for each transport mode varies according to the expected commercialization year (e.g. fuel cell cars are already available on the market, while fuel cell trucks are expected in the next 5-10 years).

In this database, road transport technologies are characterized by four parameters:

- Efficiency;
- Lifetime;
- Investment cost;
- Fixed operation and maintenance (O&M) cost.

Table 3. Transport modes of the road transport processes, and associated features. The identification code, used in the TEMOA-Europe database, is composed by two parts: the first part (TRA_ROA) stands for "road transport", while the last part of the code (e.g. CAR) uniquely identifies the transport mode.

Road transport mode	Code	Features
Passenger car	TRA_ROA_CAR	-
Light truck	TRA_ROA_LTR	Including SUVs and pick-ups
Van	TRA_ROA_LCV	Up to 3.5 t gross vehicle weight (GVW), for urban/regional freight transport
Two-wheeler	TRA_ROA_2WH	-
Three-wheeler	TRA_ROA_3WH	-
Medium truck	TRA_ROA_MTR	From 3.5 t up to 12 t GVW, for regional/national freight transport
Heavy truck	TRA_ROA_HTR	From 12 t up to 60 t GVW, for national/international freight transport
Bus	TRA_ROA_BUS	-

For each kind of possible transport mode, all or some vehicle technologies reported in **Table 4** have been selected and characterized at each time step after the base year, prescribing the trends for their future development.

Table 4. Vehicle technologies considered for new technologies in the road transport module; *** is a placeholder for the part of the last part of the code in **Table 3** identifying the specific transport mode.

Technology	Description	Fuel(s)
TRA_ROA_***_GSL_N	Gasoline (GSL) vehicle	Gasoline
TRA_ROA_***_DST_N	Diesel (DST) vehicle	Gas oil
TRA_ROA_***_NGA_N	Natural gas (NG) vehicle	Natural gas
TRA_ROA_***_LPG_N	Liquified petroleum gas (LPG) vehicle	LPG
TRA_ROA_***_ELC_N	Full-electric (ELC) vehicle	Electricity
TRA_ROA_***_GHE_N	Gasoline hybrid-electric (GHE) vehicle	Gasoline
TRA_ROA_***_DHE_N	Diesel hybrid-electric (DHE) vehicle	Gas oil
TRA_ROA_***_GPH_N	Gasoline plug-in hybrid-electric (GPH) vehicle	Gasoline + electricity
TRA_ROA_***_DPH_N	Diesel plug-in hybrid-electric (DPH) vehicle	Gas oil + electricity
TRA_ROA_***_FCE_N	Fuel cell (FCE) vehicle	Gaseous hydrogen

2.1.1 Efficiency

Fuel economy specifications, or equivalently the energy efficiency of a particular vehicle, given as a ratio of the distance travelled per unit of fuel consumed, are widely accessible for light-duty vehicles (LDVs) only. A database based on [112], including 66 cars, 33 vans and 54 light trucks, has been built, subdividing vehicles into "size categories": Mini, Small, Medium, Large for cars; Small, Medium, Large for vans; Small sport-utility vehicle (SUV), Compact SUV, Full-size SUV and pick-ups for light trucks, each one corresponding to a specific weight range. The fuel economy specifications are provided by manufacturers, on the basis of the New European Driving test Cycle (NEDC), in $\mathrm{l}/100$ vehicle $-$ kilometers (vkm) for gasoline, gas oil and LPG, $\mathrm{kg}/100$ vkm for natural gas and hydrogen or $\mathrm{kWh}/100$ km for electricity. These values are then properly translated in vkm/MJ, or equivalently Bvkm/PJ, as per the model convention for efficiency, using the fuel energy content properties retrieved from [113] and **Equation 1**:

$$\eta^* = \frac{100}{E_c \cdot \mathrm{LHV}} \qquad 1$$

In **Equation 1**, η^* is the vehicle efficiency ($\mathrm{Bvkm}/\mathrm{PJ}$), E_c is the declared fuel economy (either in $\mathrm{l}/(100$ vkm) or $\mathrm{kg}/(100$ vkm) or $\mathrm{kWh}/(100$ vkm)) and LHV is the fuel lower heating value (either in MJ/l or MJ/kg or MJ/kWh).

The fuel economy data collection highlights a decreasing efficiency trend with weight. For cars and light trucks, an average occupancy of 1.5 passengers was considered (since they are mostly used for passenger transport) [114], while vans have been supposed to be always driven at 80% of their maximum allowable capacity (since they are mostly suited for freight transport), according to **Equations 2** and **3**:

$$\mathrm{Weight}_{\mathrm{car/light\ truck}} = \mathrm{Curb\ \ weight} + 1.5 \cdot \mathrm{Passenger\ \ weight} \qquad 2$$

$$\mathrm{Weight}_{\mathrm{van}} = \mathrm{Curb\ \ weight} + 0.8 \cdot \mathrm{GVW}_{\mathrm{max}} \qquad 3$$

Then, a factor (f_{RD} = 1.39) is applied to get the efficiency trends as a function of the vehicle weight for cars/light trucks. It considers the average gap between official fuel consumption figures and actual fuel use for new cars in the EU, which is actually 39% higher than official values [115]. The efficiency trends

reported in **Figure 2a** for gasoline and diesel cars/light trucks, **Figure 2b** for LPG and natural gas cars/light trucks, **Figure 2c** for full-electric and fuel cell cars/light trucks and **Figure 2d** for gasoline hybrid-electric and plug-in hybrid electric cars/light trucks are retrieved from the DAT database [112] and are used as base for the efficiencies of new vehicles technologies.

The database for vans is not sufficiently detailed, for some technologies, to provide separate trends. Nevertheless, the few available data points show to be well reproduced by the car and light truck trends. Since no trends can be retrieved for diesel hybrid-electric cars/light trucks, but this technology is considered for vans, trucks and buses, an average diesel-to-gasoline efficiency-correlation factor $k_{DST/GAS}$, given by the ratio of gasoline and diesel car efficiencies, has been retrieved from the vehicle market database, highlighting a 20% higher efficiency for diesel cars ($k_{DST/GAS}$ = 1.2), with respect to gasoline cars. The ratio $k_{DST/GAS}$, reported in **Table 5**, is used to increase the efficiency of gasoline hybrid-electric vehicles to obtain the efficiency of diesel hybrid-electric vehicles.

Average efficiency values are then defined for each size category, and shown in **Table 6**, in order to get values for two- and three-wheelers (scaled down from Medium and Small cars respectively).

Table 5. Efficiency ratios with respect to diesel cars/light trucks.

Efficiency ratio	Value
$k_{DST/GSL}$	1.20
$k_{DST/LPG}$	1.27
$k_{DST/NGA}$	1.20
$k_{DST/ELC}$	0.36
$k_{DST/GHE}$	0.84
$k_{DST/DHE}$	0.78
$k_{DST/GPH}$	0.57
$k_{DST/FCE}$	0.67

For heavy-duty vehicles (HDVs), i.e. trucks and buses, an official document by Volvo Trucks [116] states guide values for fuel consumption of their diesel trucks. Based on such data, and merging them to those for diesel LDVs, a new efficiency trend for HDVs is calculated according to a polynomial fitting of the available data, as reported in **Equation 4** – where Weight (t) corresponds to the

selected representative weight for each HDV transport mode – and displayed in **Figure 3**.

$$\eta_{\mathrm{HDV\,DST}} = \{f_{\mathrm{RD}} \cdot [2.41 \cdot \ln(\mathrm{Weight}) - 15.96]\}^{-1} \qquad 4$$

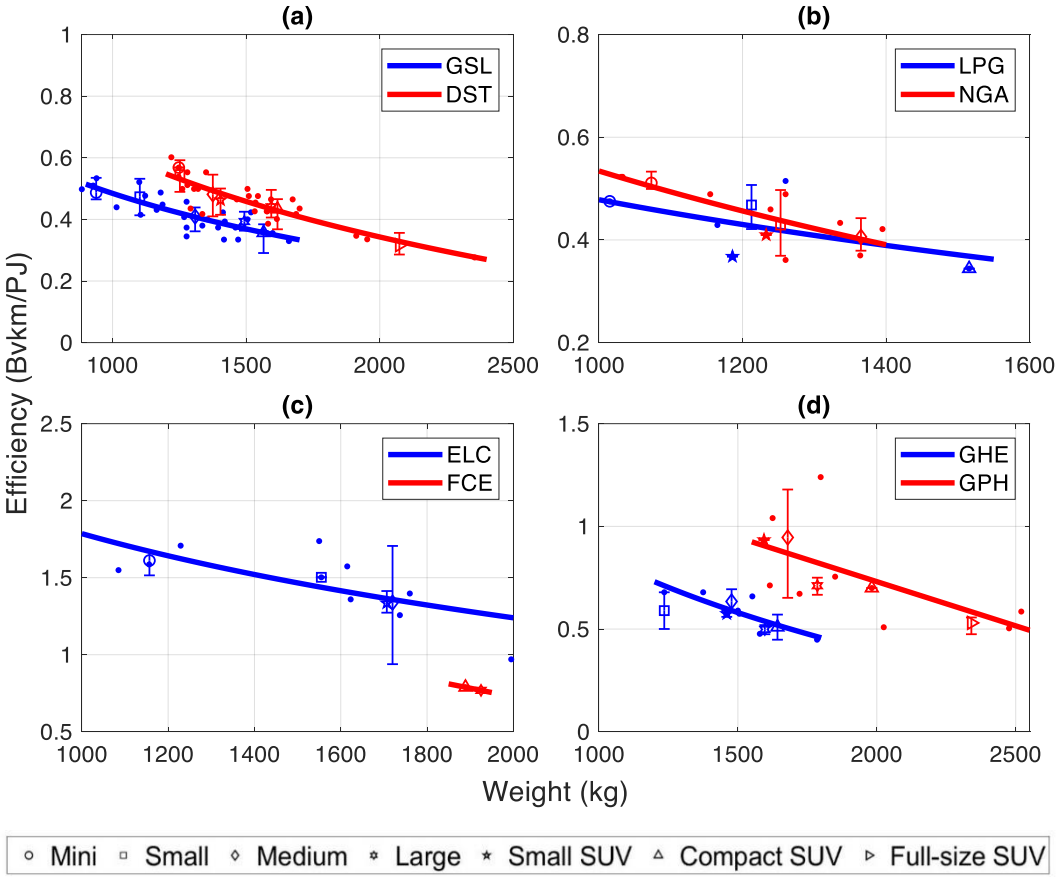

Figure 2. Efficiency trends as a function of vehicle weight for gasoline and diesel cars/light trucks (a), for LPG and natural gas cars/light trucks (b), for full-electric and fuel cell cars/light trucks (c) and for gasoline hybrid-electric and gasoline plug-in hybrid-electric cars/light trucks (d), respectively: data-points represent the collected efficiency data, while the different size categories (Mini, Small, Medium, Large, Small SUV, Compact SUV and Full-Size SUV) are represented by the mean values of their respective weight-efficiency couple.

Using **Equation 4**, the efficiency can be computed for medium trucks (8 t), heavy trucks (30 t) and buses (16.5 t, including curb weight and 20 passengers, each one weighting 75 kg), respectively. For all the other technologies, the *diesel-*

to-other technology ratios observed from the average car, van and light truck efficiencies, as reported in **Table 5**, are adopted.

In order to reduce the level of disaggregation of the model, which would inevitably increase the computational time, representative size categories are then selected for cars (Medium car, e.g. Volkswagen Golf, for all kinds of cars except for 2020 fuel cell cars, which are actually larger cars, but will be considered as medium-size cars from 2030 on, assuming an extension of the size range expected for that technology), light trucks (Compact SUV, e.g. Toyota RAV4) and vans (Medium van, e.g. Ford Transit Connect). Two- and three-wheelers are described by a single size category each. **Table 7** shows efficiency values in year 2020.

Table 7 shows that, for all transport modes, the full-electric technologies (ELC) are the most energy efficient: they are on average ~ 3 times more efficient than the corresponding gasoline and diesel technologies. Moreover, the modelled gasoline hybrid-electric car allows a significant gasoline fuel saving with respect to a traditional gasoline car (~ 30%), reaching thus a higher efficiency. Caution should be used in the comparison between transport modes which are strictly adopted for passenger transport, namely cars and buses: diesel buses show a 13-times higher consumption with respect to diesel cars, but the modelled car efficiency is calibrated on 1.5 passengers, against the 20 passengers accounted for in the calculation of bus efficiency: this means that more than 13 cars are needed for transporting 20 people, then consuming around 60% more than a single bus.

Table 6. Average efficiency values (in Bvkm/PJ) for all car and light truck size categories.

Size category	GSL	DST	LPG	NGA	ELC	GHE	GPH	FCE
Mini	0.49	-	0.46	0.48	1.68	-	-	-
Small	0.44	0.51	0.41	0.42	1.37	0.68	-	-
Medium	0.39	0.47	0.37	0.39	1.29	0.56	0.83	-
Large	0.36	0.42	-	-	1.09	0.52	0.76	0.70
Small SUV	0.39	0.46	0.41	0.43	1.30	0.56	0.83	-
Compact SUV	0.35	0.42	0.36	-	1.04	0.47	0.67	0.71
Full-size SUV	0.30	0.35	-	-	-	-	0.54	-
Pick-up	0.27	0.30	0.27	0.28	0.98	0.36	-	-

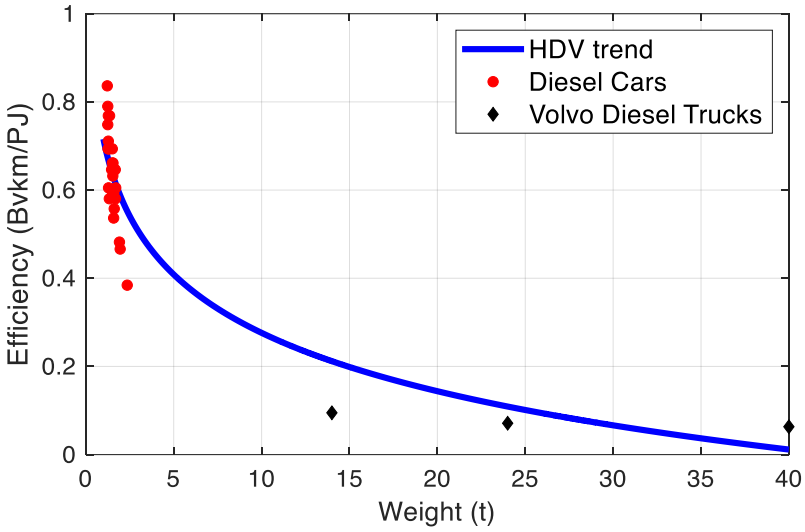

Figure 3. Efficiency trend for heavy-duty vehicles.

Table 7. Efficiency (Bvkm/PJ) of new technologies for the different modes in the TEMOA-Europe road transport module for the year 2020.

	GSL	DST	NGA	LPG	ELC	GHE	DHE	GPH	DPH	FCE
Passenger car	0.39	0.47	0.37	0.39	1.29	0.56	-	0.83	-	0.70
Light truck	0.32	0.38	-	0.33	0.94	0.43	-	0.61	-	-
Van	0.27	0.31	0.27	0.26	1.08	-	0.30	-	0.98	-
Two-wheeler	1.08	1.28	-	-	3.47	1.61	-	-	-	-
Three-wheeler	1.02	1.23	-	-	3.28	-	-	-	-	-
Medium truck	-	0.10	0.08	0.08	0.28	-	-	-	0.32	-
Heavy truck	-	0.04	0.03	0.04	-	-	-	-	0.14	-
Bus	-	0.06	0.04	0.04	0.15	-	-	-	0.19	-

The evolution of the efficiency over the time horizon analyzed in the present paper is assigned exogenously, keeping as reference the values assigned in the JRC-EU TIMES [63] for European LDVs, based on recent market trends. In JRC-EU TIMES, the full-electric LDVs are subdivided in 3 categories, according to their battery size (15 kWh, 30 kWh, 60 kWh), due to the fact that the vehicle demand is subdivided into long- and short-distance, making some technologies suited for a specific demand category. That aspect is not reflected in the database presented here, as demand disaggregation would require several assumptions

about future market trends, especially for cars. The evolutions assigned to 30 kWh BEVs has been taken into account for ETM full-electric LDVs. The efficiency variations, with respect to 2020 values, adopted in the present analysis are represented in **Figure 4**: the same ratios, for such parameter, between the characteristics of present and future technologies as in the JRC-EU TIMES have been applied throughout the time scale of this dataset. From 2050 on, all efficiencies are kept constant until the end of the time scale, due to the lack of reliable estimations. Note that, as in the JRC-TIMES, the efficiency is considered as constant for HDVs during the entire time horizon that we consider, mainly due to poor literature.

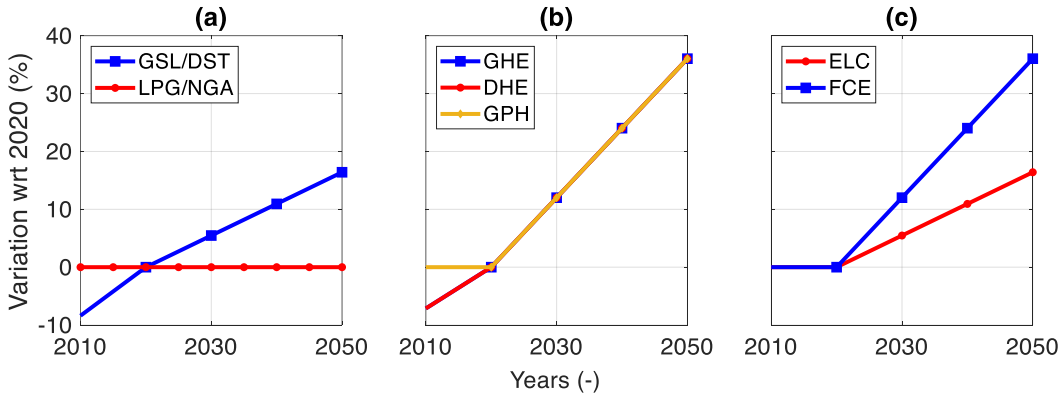

Figure 4. Efficiency variation with respect to 2020 applied to a) gasoline, diesel, LPG and natural gas LDVs; b) full-hybrid and plug-in hybrid LDVs; c) electric and fuel cell LDVs based on [63].

2.1.2 Lifetime

Standard vehicle lifetimes for each transport mode and technology are difficult to be retrieved from literature, then the same assumptions as in JRC-TIMES [63] are adopted here. A 12 years-long lifetime is generally considered for LDVs (two- and three-wheelers not included). On the other hand, full-electric and fuel cell technologies in the mentioned class are assigned a 10 years-long lifetime. Concerning two- and three-wheelers, a 10 years-long lifetime is generally given, excluding full-electric two-wheelers (6.5 years) and three-wheelers (8 years). A 15 years-long lifetime is taken into account for all HDVs excluding full-electric and fuel cell technologies (12 years).

2.1.3 Investment cost

The sum of Manufacturer's Suggested Retail Price and a 21.3% V.A.T. (average European value [117] in 2019, as TEMOA-Europe is a single-region model) gives the purchase price of a single vehicle (thus in €/vehicle), translated into the yearly cost dividing by the assigned vehicle lifetime.

Also the evolution of the investment costs, on the time horizon considered in our analysis, is assigned exogenously, keeping as reference the same ratios between present and future costs of European LDVs as assigned in [63], based on recent market trends, see **Figure 5**.

Moreover, since the 2020 full-electric Compact SUV retraces the characteristics of a luxury-class vehicles (Tesla Model X), the costs of full-electric TRLs have been adjusted from 2030 on so as to become representative of standard-class vehicles. The same applies to fuel cell cars, which are assumed to be Medium cars (instead of Large cars only, as currently on the market) starting from 2030. No variations for the investment cost of traditional HDVs are considered, while the same trends in **Figure 5** are applied to plug-in hybrid, full-electric and fuel cell technologies.

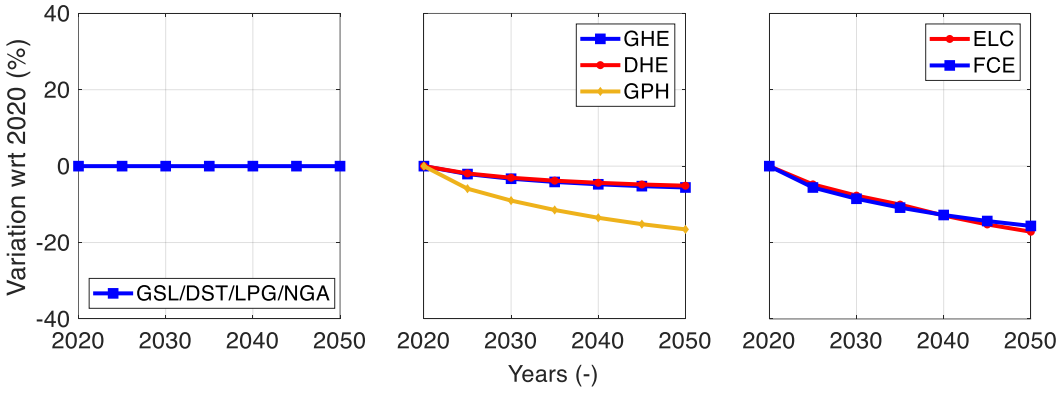

Figure 5. Investment cost variation with respect to 2020 applied to a) gasoline, diesel, LPG and natural gas LDVs; b) full-hybrid and plug-in hybrid LDVs; c) electric and fuel cell vehicles for all road transport modes.

Table 8 reports the yearly investment costs for all the vehicles considered in this database for the year 2020.

As expected, the annual price of full-electric, plug-in hybrid-electric and fuel cell technologies is still far from being comparable with that of "traditional" technologies. One may think this is only due to the lower lifetime with respect to the other technologies (as explained in **Section 2.1.2**), but even considering the same lifetime for gasoline and full-electric cars, e.g. electric cars would still cost 60% more than gasoline cars. Instead, investment cost for a gasoline hybrid-electric car is 20% higher than a conventional gasoline car (against a 40% fuel saving, as reported in the comments to **Table 7**). Similar observations are applicable to all other transport modes.

2.1.4 Fixed O&M cost

The fixed O&M cost corresponds to maintenance and repair (M&R) costs and it is here derived from the analysis in [118], where M&R costs were evaluated for year 2020 Medium cars. In [118], the definition of internal combustion engine (ICE) includes gasoline and diesel vehicles only. For LPG and natural gas cars, slightly increased costs are then adopted, due to the need for additional components with respect to a conventional ICE. The values obtained from [118] for cars, in $/vkm, are then properly scaled according to the difference observed in the investment cost difference between transport modes to be representative of all other vehicle types and reported in **Table 8**. For instance, the investment cost of gasoline light trucks is the 46% higher than for gasoline cars, and the same difference is reflected in Fixed O&M costs. Full-electric and plug-in hybrid electric vehicles allow substantial savings with respect to the other technologies. When fuel cell vehicles are assumed to be size-comparable with other technologies (e.g. for buses), they are ~ 30% cheaper than conventional ICEs. The fixed O&M costs have not been modified during the time scale of our analysis, except for fuel cell cars, since size range extension has been forecast, so that the fixed O&M have been adapted to be consistent with a Medium fuel cell car.

Table 8. Investment cost (in $/year) for the different modes/technologies in the TEMOA-Europe road transport module for the year 2020.

	GSL	DST	NGA	LPG	ELC	GHE	DHE	GPH	DPH	FCE
Passenger car	2200	2400	2400	2200	4300	2700	-	4200	-	9000
Light truck	3200	3600	-	3200	5500	3800	-	-	-	-
Van	2800	2800	3300	2800	5500	-	3400	-	4900	-
Two-wheeler	880	1000	-	-	2200	1500	-	-	-	-
Three-wheeler	330	360	-	-	-	-	-	-	-	-
Medium truck	-	5900	5800	5500	11300	-	-	-	11200	-
Heavy truck	-	11100	11000	10300	-	-	-	-	19800	-
Bus	-	8300	8700	8100	16800	-	-	-	15800	-

Table 9. Fixed O&M cost (in $/vkm) for the different modes/technologies in the TEMOA-Europe road transport module.

Transport mode	GSL	DST	NGA	LPG	ELC	GHE	DHE	GPH	DPH	FCE
Passenger car	0.081	0.081	0.083	0.083	0.066	0.080	-	0.077	-	0.090
Light truck	0.138	0.131	-	0.129	0.113	0.127	-	0.097	-	-
Van	0.096	0.095	0.087	0.087	0.090	-	0.096	-	0.094	-
Two-wheeler	0.011	0.010	-	-	0.008	0.009	-	-	-	-
Three-wheeler	0.031	0.029	-	-	0.022	-	-	-	-	-
Medium truck	-	0.469	0.486	0.460	0.307	-	0.431	-	-	-
Heavy truck	-	1.759	1.822	1.726	-	-	1.615	-	-	-
Bus	-	0.968	1.002	0.949	0.634	-	0.888	-	-	-

2.2 Non-road transport

Non-road transport technologies are subdivided into 6 transport modes, shown in **Table 10**; **Table 11** reports the road vehicle technologies currently considered in this database for the different transport modes. Note that no full-electric vehicles are taken into account for aviation and navigation, considering the complexity that such a solution would require for large distances to cover. It has to be also highlighted that non-road vehicles are rarely included in detail in ESOM databases and that literature is very poor regarding the kind of data required to produce techno-economic databases of this kind. Therefore, the characterization presented here will provide an extended range of alternative technologies, although with poor detail in terms of quantitative information.

Nonetheless, the comparison of the dataset presented here with respect to the ETM non-road transport module used to generate scenarios presented in [119] and the one included in the JRC-EU-TIMES [63] highglights a marked improvement. Indeed, the ETM non-road transport module considers demands expressed in energy terms (specifically PJ) and just a fixed trend for the evolution of the base year market shares of aircrafts, trains and ships. Such a modeling strategies makes it impossible to optimize fuel consumption and to envisage new investments in vehicles. In particular, the last feature makes the non-road transport sector not involved at all in the economic optimization process at the basis of the ESOM in exam. On the other hand, the JRC-EU-TIMES presents details for the passenger and freight trains alone in the category of non-road transport vehicles, and considers the possibility to perform investments in new technologies. Yet it does not takes into account any difference in fuel performances for diesel and electric trains (the only ones present in the database), mainly due to data unavailability.

Non-road transport technologies are characterized by the same parameters as for road transport technologies in this database.

2.2.1 Efficiency

The energy efficiency of non-road transport technologies is set at a single value based on 2020 data provided by the POTEnCIA database [120], thus no future improvements are expected for those vehicles. Specifically, the analysis started from base year efficiency values computed using the relationship between energy consumption and demand showed in **Equation 5**, where $\eta_{t,BY}$ represents the efficiency of technology t in the base year (BY), D_{BY} is the total base year

demand for transport mode m obtained from [120], $x_{t,BY}$ is the demand share of technology t in the base year and $E_{f,BY}$ is the consumption of fuel f in the base year (as all non-road transport technologies consume a single fuel and that is not used by any other technology in the same transport mode), both computed starting from the IEA energy balances for the year 2005 [121].

$$\eta_{t,BY} = (D_{m,BY} \cdot x_{t,BY})/E_{f,BY} \quad (5)$$

Table 10. Transport modes of the road transport processes, and associated identification code, used in the TEMOA-Europe database. The first part of the code generically indicates the transport mode (TRA_AVI for aviation, TRA_RAIL for trains and TRA_NAV for navigation), while the second part stands for a specific feature (DOM for domestic, INT for international, PAS for passenger and FRG for freight).

Road transport mode	Code
Domestic aviation	TRA_AVI_DOM
International aviation	TRA_AVI_INT
Passenger train	TRA_RAIL_PAS
Freight train	TRA_RAIL_FRG
Domestic navigation	TRA_NAV_DOM
International navigation	TRA_NAV_INT

The database in [120] presents the time series of the fuel efficiencies for the non-road vehicle fleet for each transport mode starting from 2000 and with future projections until 2025. The improvement of base year efficiency was computed comparing the 2020 values to efficiencies in 2005, considering the improved figure as the representative data for all the new vehicles installed after the base year. It has to be underlined that due to the poor detail of fuel consumption specifications for the different technologies in [120], the same values were used as representative for groups of vehicles using 1) fossil fuels (gas oil, heavy fuel oil, jet kerosene and LNG), methanol and ammonia in internal combustion engines; 2) electricity and 3) liquid or gaseous hydrogen and ammonia in fuel cell-based engines [122]. In particular, values for hydrogen- and fuel cell-based vehicles are computed according to the difference between diesel and fuel cell technologies in the road transport module, due to the absence of any information in the literature.

All the efficiency values for non-road transport technologies adopted in TEMOA-Europe are reported in **Table 12**.

Table 11. Vehicle technologies considered within the non-road transport module; *** is a placeholder for the part of the last part of the code identifying the specific transport mode.

Transport mode(s)	Technology	Description	Fuel(s)
Domestic aviation	TRA_AVI_DOM_JTK_N	Jet kerosene vehicle	Jet kerosene
	TRA_AVI_DOM_LH2_N	Liquid hydrogen-powered internal combustion engine vehicle	Liquid hydrogen
International aviation	TRA_AVI_INT_JTK_N	Jet kerosene vehicle	Jet kerosene
	TRA_AVI_INT_LH2	Liquid hydrogen-powered internal combustion engine vehicle	Liquid hydrogen
Passenger train / Freight train	TRA_RAIL_***_DST_N	Diesel vehicle	Gas oil
	TRA_RAIL_***_ELC_N	Full-electric vehicle	Electricity
	TRA_RAIL_***_GH2_N	Fuel cell vehicle	Gaseous hydrogen
Domestic navigation	TRA_NAV_DOM_DST_N	Diesel vehicle	Gas oil
	TRA_NAV_DOM_LNG_N	LNG vehicle	LNG
	TRA_NAV_DOM_DUAL_N	Dual fuel vehicle	Heavy fuel oil + ammonia
	TRA_NAV_DOM_AMM_N	Ammonia vehicle	Ammonia
	TRA_NAV_DOM_MTH_N	Methanol vehicle	Methanol
	TRA_NAV_DOM_LH2_FCE_N	Liquid hydrogen-powered internal combustion engine vehicle	Liquid hydrogen
	TRA_NAV_DOM_AMM_FCE_N	Ammonia fuel cell vehicle	Ammonia
International navigation	TRA_NAV_INT_HFO_N	Heavy fuel oil-fueled vehicle	Heavy fuel oil
	TRA_NAV_INT_LNG_N	LNG vehicle	LNG
	TRA_NAV_INT_DUAL_N	Dual fuel vehicle	Heavy fuel oil + ammonia
	TRA_NAV_INT_AMM_N	Ammonia internal combustion engine vehicle	Ammonia
	TRA_NAV_INT_MTH_N	Methanol vehicle	Methanol
	TRA_NAV_INT_LH2_N	Liquid hydrogen-powered internal combustion engine vehicle	Liquid hydrogen
	TRA_NAV_INT_AMM_FCE_N	Ammonia fuel cell vehicle	Ammonia

2.2.2 Lifetime

The lifetimes of non-road technologies are retrieved from the ETSAP Technology Briefs for aviation [123], rail [124] and navigation [125] technologies and are all attested at 30 years.

2.2.3 Investment cost

Investment costs in use for non-road transport technologies in TEMOA-Europe are again based on the capital costs indicated in the ETSAP Technology Briefs for aircrafts [123], considering 80 M$ as capital cost for domestic aviation vehicles and 240 M$ for international aviation vehicles. Those values are then reported to 140 million (domestic aviation) and 830 million (international aviation) available seat km per aircraft, considering 80% and 75% average load factor, respectively. The investment cost values expressed in $ per passenger kilometers ($/pkm) are reported in **Table 13**.

Concerning diesel trains, instead, the investment cost per km is computed as the 6% of that corresponding to diesel heavy trucks, as from the JRC-EU-TIMES [63], while [124] does not present any data. The same value is adopted for both passenger and freight trains and also assumed as representative for navigation technologies, due to the of any relevant data for this analysis. Since hydrogen internal combustion and fuel cell-based engines are not envisaged in any capital cost analysis, the same ~ 70% cost differences observed between fuel cell and traditional vehicles for road transport technologies are reported here for all the concerned non-road transport technologies. **Table 13** also reports costs for passenger (in $/pkm), freight (in $/fkm) trains and ships (in $/vkm).

2.2.4 Fixed O&M cost

Fixed O&M costs for non-road vehicles are calculated as a percentage of the investment costs listed in **Table 13**. The JRC-EU-TIMES Model suggests to consider a 2% of the investment cost for trains [63], while a more conservative 5% is assumed for aircrafts and ships.

Table 12. Efficiency (Mvkm/PJ) for the different modes/technolgies in the non-road transport module for the year 2020.

	Fossil fuels, methanol and ammonia in internal combustion engines							**Electricity**	**Gaseous or liquid hydrogen and ammonia in fuel cell-based engines**		
	JTK	**DST**	**HFO**	**LNG**	**DUAL**	**AMM**	**MTH**	**ELC**	**GH2**	**AMM_FCE**	**LH2_FCE**
Domestic aviation	3.97	-	-	-	-	-	-	-	-	-	8.73
International aviation	4.72	-	-	-	-	-	-	-	-	-	10.38
Passenger train	-	3.73	-	-	-	-	-	11.2	7.46	-	-
Freight train	-	3.54	-	-	-	-	-	10.6	7.09	-	-
Domestic navigation	-	0.510	-	0.510	0.510	0.510	0.510	-	-	0.919	0.919
International navigation	-	-	0.153	0.153	0.153	0.153	0.153	-	-	0.275	0.275

Table 13. Investment cost (in $/pkm for aircrafts and passenger trains, in $/fkm for freight trains and in $/vkm for ships) for the different modes/technologies in the TEMOA-Europe non-road transport module.

	Fossil fuels, methanol and ammonia in internal combustion engines	**Electricity**	**Gaseous or liquid hydrogen and ammonia in fuel cell-based engines**
Domestic aviation	710	-	1300
International aviation	390	-	710
Passenger train	300	300	500
Freight train	300	300	500
Domestic navigation	300	-	500
International navigation	300	-	500

2.3 Energy-intensive industrial subsectors

Given the large technical and economic detail required for technological characterization in ESOMs, a comprehensive characterization of industrial energy-intensive technologies for TEMOA-Europe is presented here.

The ETSAP database [126] of supply [127] and demand [128] technologies contains technical and economic characteristics also used in this work, but the latest update dates back to 2013 (for some end-use sectors, while for some others it dates back to 2011 or 2012) and, at the steady pace of development the current world is witnessing, this represents in some cases a strong limitation (e.g. most of the technologies considered in this work are considered in this work for the first time).

Also the JRC-EU-TIMES provides a very extensive dataset [63] for supply and demand technologies in all sectors. However, the JRC-EU-TIMES industrial module only includes well-established technologies, and it mainly relies on the MATTER database. The main issue with that source is that it is no longer available, or at least not so easily accessible – to the best of our knowledge – and

on the other hand it lacks explanations about the formulation of parameters included in it, for its validation was mainly based on expert-based reviews.

In the EFDA-TIMES Model [129], a mix of sources, including the MATTER database, was used for the latest update of the industry sector. With respect to that, here more up-to-date sources and a larger set of technologies are considered to describe, above all, future possibilities for the developments of a low-carbon industry sector.

The database presented here is in line with the technology portfolio available in the IEA ETP Model, for which, however, full data access is restricted, so that only qualitative evaluations for a wide range of existing and innovative technologies are available in [27]. For this reason, a comparison with the detailed characterization adopted in the ETP Model is not possible here. Since transparency of data is often limited by non-disclosure agreements, whereas, in non-open models, assumptions, sources and methodology for data gathering and processing are unclear [111], it is deliberately decided to use for this work only freely accessible sources (documents and datasets), as that choice is deemed fundamental for pursuing data transparency and result reproducibility.

In this section, the focus is on 5 energy-intensive industrial subsectors: the iron and steel subsector, in which steel and ferroalloys are produced; the non-ferrous metals subsector, producing aluminum, copper and zinc; the non-metallic minerals subsector, which presents cement, ceramics, glass and lime production technologies; the chemicals subsector, giving ammonia, chlorine, high value chemicals (HVC) and methanol as end-use products; and the pulp and paper subsector that satisfies paper demand. For each of those subsectors, the analysis of the consumption of fuels and other energy carriers, along with economic and environmental features, is carried out, giving a broad picture of the RES for the energy-intensive production processes in the industrial sector. Each of the subsectors includes a set of technologies for the production of bulk industrial products, identified as material commodities, each one with a general structure as in **Figure 6**. Such way of modeling energy-intensive technologies allows for radical technological change to be represented in the model, as large detail can be provided for all the stages of the technological routes contributing to the satisfaction of each demand commodity.

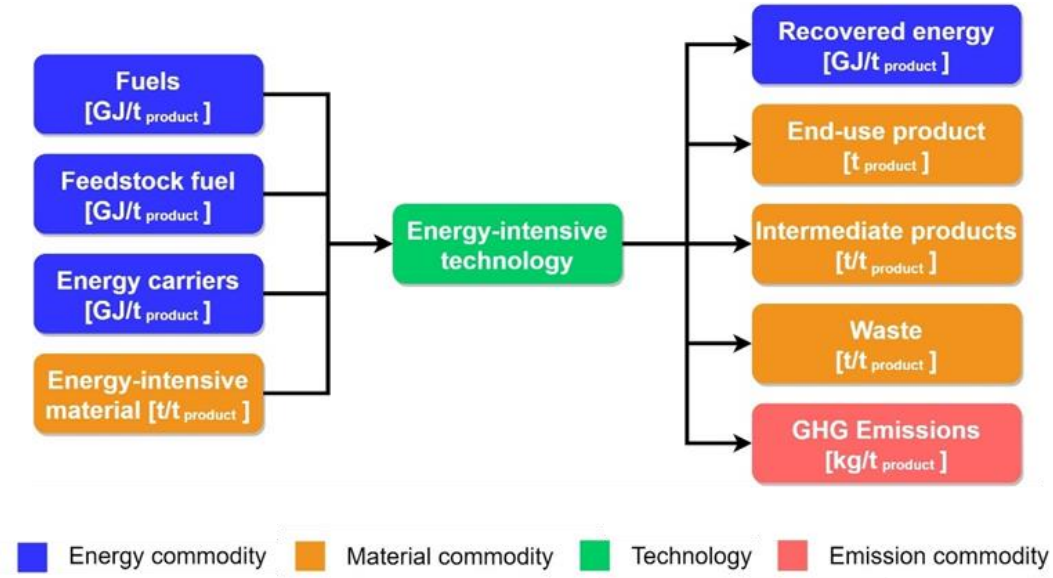

Figure 6. General structure of an energy-intensive industrial technology.

As a clear and unambiguous "key-term definition" is very important for the transparency issue discussed above for energy system modeling [130], the input/output to any technologies in **Figure 6** deserve some explanations. The input of any energy-intensive technology can be constituted by: fuels involved in the transformation process, quantified in $\mathrm{GJ/t_{product}}$, where $\mathrm{t_{product}}$ is the mass of the product in output from the selected technology (can be both an end-use product or an intermediate energy-intensive material needed to produce it): among fuels, coal, natural gas, etc. are considered,; energy carriers involved in the transformation process, quantified in $\mathrm{GJ/t_{product}}$. In this category, we consider process steam and electricity for electrochemical processes and machine drive; Feedstock fuels (only used in the chemical sector), quantified in $\mathrm{GJ/t_{product}}$, which differ from common fuel for the fact that they are not involved in any combustion process; energy-intensive materials involved in the transformation process, quantified in $\mathrm{t/t_{product}}$. the output of any energy-intensive technology can be made of: End-use products, quantified in $\mathrm{t_{product}}$; byproducts to be used in other processes for end-use product manufacturing, quantified in $\mathrm{t/t_{product}}$; recovered energy carriers, e.g. excess steam re-usable in other processes, quantified in $\mathrm{GJ/t_{product}}$; GHG emissions related to the use of fuels and materials, quantified in $\mathrm{kg_{GHG}/t_{final\ product}}$; waste materials, e.g. slag from steel production, quantified in $\mathrm{t/t_{product}}$, even though they cannot represent any valuable element

until circular economy and material flows are not implemented in the ESOM framework.

Each technology is characterized by technical factors, such as its energy input requirements, the starting date for the availability of the technology in the production system, the plant lifetime and the availability factor (i.e., the fraction of time for which the plant can be available for operation to produce the demand commodity over a year), by economic factors, such as investment cost or annual fixed O&M costs, both given in $\$/t_{\text{final product}}$, and an environmental performance factor. Variable O&M costs, related to the utilization of industrial processes, are not taken into account in this analysis due to their large variability.

Manufacturing- and other process-related specific emissions can already be calculated at the stage of the characterization of the different technological process: the fuel input of each technology can be multiplied by the corresponding emission factor among the ones presented in **Table 14** [131]. Emission factors highlight how coal and coke are the most highly emitting fuels (almost double emissions per energy unit with respect to natural gas), while an important remark has to be done on biomass, which is not considered as a zero-emission source, as CO_2 sequestration during vegetable life before combustion of the biomass is not considered [131].

Table 14. Fuels in use in the industrial sector and their CO_2 emission factors, based on their composition in TEMOA-Europe.

Fuel	**Composition**	**Emission factor (kg_{CO_2}/GJ)**
Biomass	Solid biomass 56 %, biogas 12 %, waste 31 %	13.9
Coke	-	96.0
Coal	Hard coal 78 %, brown coal 22 %	104.9
Coke oven gas	-	44.4
Ethane	-	57.9
Gas oil	-	74.1
Heavy fuel oil	Heavy fuel oil 92 %, non-specified oil 8 %	77.1
LPG	-	63.1
Naphtha	-	73.3
Natural gas	-	56.1
Oil	Gas oil 88 %, gasoline 2 %, jet kerosene 2 %, other kerosene 9 %	73.8

For each technology in the industrial energy-intensive subsectors, the level of deployment and the corresponding starting date are reported in **Table 34**-**Table 38** in the **Appendix**, where, on top of 39 traditional technologies (some of them already considered in, e.g. [129]), also 9 innovative technologies at the commercial stage, 15 in their demonstration phase and 2 in R&D phase are taken into account. The reason for considering a broad set of innovative technologies is given by the TEMOA-Europe long-term time scale up to 2100. That would allow to depict an evolution of the energy system including at least some technologies which may largely shape future energy use, also identifying the most critical ones in ambitious decarbonization scenarios across several sectors. A comparison of the general structure and content of each subsector, implemented in this database, with respect to the JRC-EU-TIMES open database and the IEA ETP Model, is also presented in **Table 34**-**Table 38**.

2.3.1 Iron and steel

2.3.1.1 Technical characterization

The blast furnace-basic oxygen furnace (BF-BOF) route is modeled according to the 2014 global average total energy intensity of 18.7 GJ/t_{CS} * [27], out of which 13.3 GJ/t_{CS} are used for iron reduction, provided that 20% of scrap is used [132]. Considering such data, additional 5.4 GJ/t_{CS} should be allocated to the remaining processes. After the reduction of iron ore, the BF needs 2.52 GJ/t_{HM} † (average EU data) [133], whereas the BOF processing only accounts for 1.00 GJ/t_{CS}, distributed among natural gas, coke oven gas, electricity and steam, according to the estimations in [133], also considering that off-gas recovery can save up to 0.70 GJ/t_{CS} and can be recirculated in the steelmaking plant. Since 2.52 GJ/t_{HM} correspond roughly to 4.40 GJ/t_{CS}, the ratio of these two values (1 $t_{CS} \simeq 0.57$ t_{HM}) is used for the conversion of energy quantities in GJ/t_{CS}, to be used in the overall BF-BOF route energy intensity accounting. The BF also produces 175-350 kg/t_{HM} (or equivalently $\simeq$ 100- 200 kg/t_{CS}) of waste slag.

As far as the direct reduced iron-electric arc furnace (DRI-EAF) process is concerned, most of direct-reduced iron is produced by using the low-energy-intensive Midrex technology option, considered as the representative DRI process here. According to [27], the global average energy intensity of the DRI-EAF route

* t_{CS}: tons of crude steel
† t_{HM}: tons of hot metal

is 22.4 GJ/t_{CS} (2014 data). Since such data is not sufficient, the Best Available Technique (BAT) can be taken as baseline for the evaluation of the consumption breakdown in the current DRI-EAF: [134] provides details about the energy consumption breakdown, and will be used to describe the future development of this technology, too. The BAT total consumption of 18.5 GJ/t_{CS} is used to derive energy inputs for the current version of the plant by simply scaling up BAT consumption of natural gas and electricity, to reach a total of 22.4 GJ/t_{CS}.

BAT energy intensity for steel from scrap and electric arc furnace is 4.3 GJ/t_{CS} [134], marking drastic savings in energy consumption compared to other processes. However, this consumption level is considered as future evolution of the process, while the current data is retrieved from [27]: an overall consumption of 6.7 GJ/t_{CS} is used and the energy input breakdown is made coherently with the values reported in [134]. The adoption of this process is limited only by the availability of usable scrap.

While being an interesting technology, the Smelting reduction-BOF process is also quite energy-intensive. In addition, the net energy intensity of the ironmaking phase is quite high, 17.3 GJ/t_{CS} [134], out of which 15.9 GJ/t_{CS} are supplied in form of coal, and the remaining part by oxygen (1.2 GJ/t_{CS}) and electricity for machine drive (0.3 GJ/t_{CS}). The BOF part of the process is characterized as in the BF-BOF process.

For the BF-BOF with CCS, energy consumption (in form of electricity and/or steam) values associated with CCS technologies in the iron and steel sector are reported in **Table 15** [135], where several technological options for CCS in steelmaking plants, with the relative capture yields y, and specific electricity/steam energy consumption per ton of captured CO_2, $\varepsilon_{el,t}$ and $\varepsilon_{st,t}$, respectively, are indicated.

PSA is able to capture 79.7% of the produced CO_2. The electricity contribution needed for CCS is calculated using **Equation 6.**

$$MD_{CCS} = \varepsilon_{el,t} \cdot \sum_{i} k_i \cdot e_i \cdot 10^{-3} \qquad 6$$

where MD_{CCS} represents the electrical input needed for machine drive to perform carbon capture, quantified in GJ/t_{CS}; $\varepsilon_{el,t} = 0.36\ GJ/t_{CO_2}$ in the case of PSA [3]; k_i is the static emission coefficient associated to commodity i, expressed

in kg_{CO_2}/GJ; e_i is the energy intensity associated to the carbon-rich commodity i, expressed in GJ/t_{CS}. In the case of the BF, where CO_2 sources are blast furnace gas, coke oven gas and natural gas, $MD_{CCS} = 0.34\ GJ/t_{CS}$.

Table 15. Overview of technology options for CO_2 separation and capture in the iron and steel sector [135].

Technology	CO_2 yield y $[\%_{vol}]$	Electricity $\varepsilon_{el,t}$ $[GJ/t_{CO_2}]$	Steam $\varepsilon_{st,t}$ $[GJ/t_{CO_2}]$
Pressure swing adsorption (PSA)	79.7	0.36	-
Vacuum PSA (VPSA)	87.2	0.38	-
VPSA + compression & cryogenic flash	96.3	1.05	-
Amines + compression	100.0	3.20	0.61
PSA + cryogenic distillation + compression	100.0	1.12	-

Considering endogenous static emission coefficients for the BF emitting commodities, as customarily done in TIMES models, the quantity of captured CO_2 from such plant is calculated according to **Equation 7** – where $SNKCO2_i$ is the quantity of CO_2 captured from commodity i, expressed in kg_{CO_2}/t_{CS} – and reported in **Figure 7**.

$$SNKCO2_i = y \cdot k_i \cdot e_i \quad (7)$$

Thus, the blast furnace in the BF-BOF with CCS is just characterized as the traditional BF, but considering additional electricity required for the compression phase for CCS.

The BF-TGR-BOF with CCS accounts for beneficial reductions in the energy requirement for the iron reduction phase ($\sim$ 18% in the latest ULCOS developments [4]), with respect to the traditional BF characterized in this work, considering an additional contribution from natural gas (1.40 GJ/t_{CS}), and the electricity need for CCS (performed via PSA), evaluated according to **Equation 6**. The quantity of captured CO_2 from such plant (BF gas, coke oven gas, natural gas and BF reductant are the emitting sources) is calculated according to

Equation 7 and reported in **Figure 7**. Concerning the BOF, the approach used previously is adopted again.

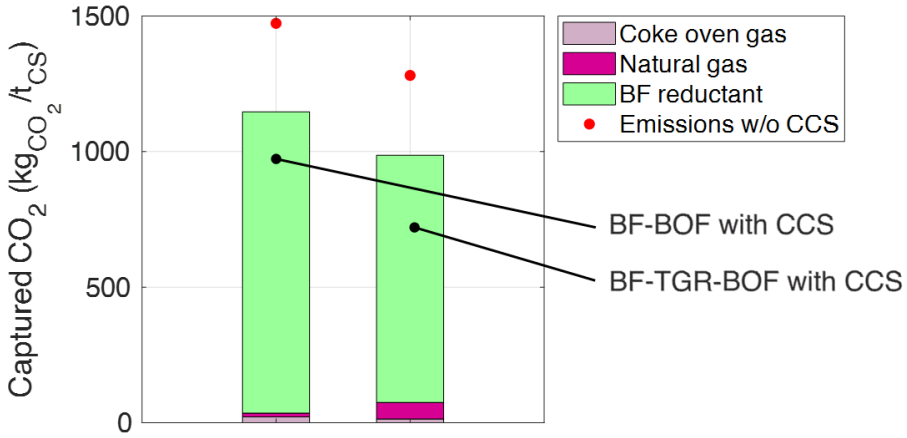

Figure 7. Captured CO_2 (kg_{CO_2}/t_{CS}) in traditional BF plants and BF-TGR plants equipped with CCS.

The CO_2 capture in a DRI-EAF with CCS process can be performed through pre-combustion using PSA, VPSA or chemical absorption [135]. The attempt to model DRI-EAF with CCS in this work will take the best practice DRI-EAF from [134] as baseline, with the application of PSA, and MD_{CCS} calculated according to **Equation 6**, resulting in 0.35 GJ/t_{CS}, given the quantity of captured CO_2, calculated according to **Equation 7**, resulting in 782.5 kg_{CO_2}/t_{CS} (natural gas is the only emitting source).

The total energy consumption of a commercial HIsarna-BOF allows 20% energy saving with respect to the current BF, while assuring the same yearly yield [136]. The carbon-rich source is here only coal, which will then replace blast furnace gas, coke oven gas and BF reductant. The second steelmaking process can be performed either by BOF or EAF (the latter option would require an additional step, namely desulphurization). For this reason, it is difficult to foresee an economically feasible route with EAF [137], even if more interesting from the energy consumption point of view. The BOF is again modeled as before. An estimation of the additional electricity needed for capture in HIsarna-BOF with CCS can be performed by using **Equation 6**, which gives $MD_{CCS} = 0.36\ GJ/t_{CS}$ using the PSA technique. The use of VPSA could be envisaged for a further development of the technology in the model, in order to capture higher CO_2 yields, at the cost of higher electricity consumption.

The amount of hydrogen needed in the hydrogen direct reduction (HDR)-EAF route is 51 $\mathrm{kg/t_{CS}}$ [138], corresponding to 6.12 $\mathrm{GJ/t_{CS}}$ if considering 120 MJ/kg as the hydrogen energy content. The total energy intensity for the HDR process is estimated at 12.53 $\mathrm{GJ/t_{CS}}$ [138], out of which 11.25 $\mathrm{GJ/t_{CS}}$ needed for the production of hydrogen from electrolysis. The difference between the total HDR consumption and energy for hydrogen production is just the electricity consumed for the auxiliary services, 1.28 $\mathrm{GJ/t_{CS}}$. The second part of the process is performed in the EAF, considering best practices values [134], due to the high grade of innovation introduced with this technology and its environmental-friendly footprint.

The Ulcored system with CCS can be modelled as a best practice DRI-EAF process, with an additional electricity consumption, calculated using **Equation 6**: using the VPSA, and considering natural gas as the only emitting source, $\mathrm{MD_{CCS}} = 0.37\ \mathrm{GJ/t_{CS}}$ should be added in the process. Finally, the application of **Equation 7** to natural gas gives 856.1 $\mathrm{kg_{CO_2}/t_{CS}}$ of captured $\mathrm{CO_2}$. Future developments for this technology envisage the possibility of reducing the need of natural gas by 15-20%, and the use of either coal, biomass or waste degasification or pure hydrogen as alternatives to natural gas [135].

Table 39 in **Appendix** reports the detail of the technical features for steel production technologies in the TEMOA-Europe database.

Energy-intensity values for the Ulcolysis and Ulcowin routes are retrieved from [139]; energy is mainly consumed as electricity for the electrochemical process and for the EAF steelmaking phase, with a relevant production of slag as waste (182 $\mathrm{kg/t_{CS}}$ from Ulcowin, 69 $\mathrm{kg/t_{CS}}$ from Ulcolysis). Several products are included among ferroalloys, including a vast category of alloys iron, chromium, silicon, manganese and other elements [140]. The combined production of ferrochromium FeCr, ferromanganese FeMn, ferrosilicon FeSi and silicomanganese SiMn has constituted the largest part of global ferroalloys production during the last 20 years (88% in 2002, 72% in 2011 and 65% in 2015, thus highlighting a constantly decreasing trend [141]), so a single technology is used to aggregate all ferroalloys (since data for energy consumption are only available for the most traditional ferroalloys), and its energy consumption is made up by the weighted average of values related to the production of the mentioned ferroalloys between 2011 and 2015. On the other hand, the JRC-EU-TIMES only considers ferrochromium as representative for the entire production field. Energy intensity values are retrieved considering FeSi of the most common typology,

containing 75% silicon, see **Table 16**. The analysis of energy consumption in [129] considered again historical data, with values from 2002 to 2005. Since the situation in this production field is quite stable, this approach seemed reliable.

Table 16. Share of production for FeCr, FeSi, SiMn and FeMn between 2011 and 2015, and relative energy consumption, elaborated by the authors, based on [141].

	Unit	**FeCr**	**FeSi**	**SiMn**	**FeMn**	**Weighted average**
Normalized production share *	%	30	22	32	16	
Electricity	GJ/t_{Fea} †	11.7	27.0	14.1	9.7	15.6
Coke	GJ/t_{Fea}	14.6	32.4	11.0	11.9	17.0

Lifetime and availability factors of steelmaking plants are based on data present in the JRC-EU-TIMES Model database [63]. While the structure of the subsector in JRC-EU-TIMES provides a detailed interconnected description of iron ore pelletizing/sintering, raw iron production and finally steelmaking, in models like ETM [129] or the ETP Model [27], that "splitting" is not represented, and each technology envisages all the required steps for steelmaking. For this reason, the lowest lifetime among the needed steps in the JRC-EU-TIMES will be taken as representative here and, in particular, 30 years are considered for BOF and 20 years for EAF. For electrowinning steelmaking, which is not present in JRC-EU TIMES, a lifetime of 20 years will be assumed. Regarding the availability factor for steelmaking processes, an 85% yearly availability is considered for all the technologies, as in JRC-EU TIMES. A lifetime of 30 years and an availability factor of 90% is considered for the generic ferroalloys production process, as from [129].

2.3.1.2 Economic characterization

Investment cost figures for commercial steelmaking processes (BF-BOF, DRI-EAF, Steel from scrap-EAF and Smelting reduction-BOF) are retrieved from [142]. Moreover, [143] reports a cost analysis for the HDR-EAF process. CAPEX and OPEX for HIsarna-BOF and HIsarna-BOF with CCS are identified in [137] as

* Contribution to production of the mentioned ferroalloys only.
† t_{Fea}: ton of ferroalloy.

the 75% and 90% of those for the BF-BOF route, respectively. Investment cost for electrowinning steelmaking strongly depends on the economics of the integrated electrolytic plant. In such case, as for CCS-equipped plants, determining the cost is a complex issue, mainly because of little experience in actual operation. Regarding Ulcolysis and Ulcowin, in [139] an estimation of 900-3350 € per ton of processed iron is considered. Since Ulcolysis is expected to require $1.51\ t_{Fe}/t_{CS}$, while Ulcowin $1.59\ t_{Fe}/t_{CS}$, an investment cost for such plants can be estimated at 1360-5070 $€/t_{CS}$ for Ulcolysis, and 1430-5330 $€/t_{CS}$ for Ulcowin. The largest values will be used as soon as the technology is introduced as commercially available in the model (2030), to reach the lowest calculated value in 2050 (as in [64] for chemicals production for electrolysis-based technologies, for which the minimum cost is estimated to be reached in 2050).

Investment cost for CCS-equipped plants are obtained here by summing up the contribution of the original plant they derive from, and the capital cost of the CCS unit, reported, in € per ton of captured CO_2 in [144]. The cost of the CCS unit is retrieved by using the simple correlation in **Equation 8**:

$$\mathrm{INVCOST}_{\mathrm{CCS,t}} = \mathrm{SNKCO2}_{\mathrm{t}} \cdot c_{CCS} \quad (8)$$

where $\mathrm{INVCOST}_{\mathrm{CCS,t}}$ is the capital cost component associated with CCS-equipped technology t, quantified in $€/t_{CS}$, $\mathrm{SNKCO2}_{\mathrm{t}}$ is the amount of captured CO_2 by technology t, quantified in kg_{CO_2}/t_{CS} and c_{CCS} is the unit cost of CCS technology, quantified in $€/kg_{CO_2}$. It should be noted that just the traditional BF, BF-TGR and Corex with CCS are included in [144]. Anyway, since smelting reduction is considered as the natural evolution of DRI processes [145], while HIsarna is an advanced DRI technology, data for Corex will be used as baseline for DRI-EAF, HIsarna and Ulcored with CCS. Further information is reported in **Table 17**.

Fixed O&M costs for BF-BOF, DRI-EAF, BF-TGR, HIsarna (with and without CCS), Ulcored and electrowinning routes are reported in[139]. For the remaining technologies, some assumptions are needed: steel from scrap is associated with a EAF steelmaking phase, thus the same cost of the traditional DRI-EAF will be used; fixed O&M cost for the Smelting reduction-BOF route will be taken the same as for the traditional BF-BOF, and the same happens for the BF-BOF with CCS, while the DRI-EAF with CCS and the HDR-EAF receive the same cost as their traditional correspondent (DRI-EAF). All economic features are finally reported in **Table 18**, and data available in € were converted in $,

according to the 2010 average exchange rate, 0.754 €/$ [146] (this choice was made since the standard monetary unit for the JRC-EU-TIMES is $€_{2010}$).

Table 17. Investment cost for CCS plants in steelmaking technologies

Technology	Captured CO_2 (kg/t_{CS})	CCS technology	CCS unit cost ($\$/kg_{CO_2}$)	CCS investment cost ($\$/t_{CS}$)
DRI-EAF with CCS	782.5	PSA	0.053	42
BF-BOF with CCS (2020)	1146.9	PSA	0.25	287
BF-BOF with CCS (2050)	1011.3	PSA	0.026	27
BF-TGR-BOF with CCS	986.4	PSA	0.08	79
HIsarna-BOF with CCS	1010.6	PSA	0.053	54
Ulcored with CCS	856.1	VPSA	0.053	45

While fixed O&M costs do not present relevant differences, the broad range covered by investments costs reflect the variety of the existing production technologies in the steel market. The scrap-based technology is the cheapest one, making this route the most attractive economically, other than environmentally. Instead, the most innovative processes have, as of today, cost estimations which keep them out of the market. However, both technologies based on CCS and electrolytical processes are expected to contract their costs in the future. A further electrification of the sector could benefit these technologies that base their operation on electricity.

Ferroalloys production is not envisaged in [63], already taken as reference for the estimation of lifetime and availability factor of steelmaking technologies. For this reason, such parameters and also cost figures will be preserved as in [129] with an investment cost of 600 $\$/t_{Fea}$ and a fixed O&M cost of 60 $\$/t_{Fea}/year$ are considered.

Table 18. Costs for steelmaking processes.

Technology	Investment cost ($\$/t_{CS}$)	Fixed O&M cost ($\$/t_{CS}/year$)
BF-BOF	586	14.6
DRI-EAF	549	20.9
Steel from scrap-EAF	244	20.9
Smelting reduction-BOF	521	14.6
DRI-EAF with CCS	590	11.0
BF-BOF with CCS	611-825	14.2
BF-TGR-BOF with CCS	661	14.5
HIsarna-BOF	439	14.9
HIsarna-BOF with CCS	493	20.9
Ulcored with CCS	594	18.3
HDR-EAF	761	26.9
Ulcolysis	1800-6720	20.2
Ulcowin	1900-6940	17.0

2.3.1.3 Environmental performances

Pollutant emissions for each steelmaking technology are strictly related to the nature of the adopted fuels and their consumption in the process. In the case of CO_2, CH_4 and N_2O, endogenous static emission coefficients are typically included in macro-scale models for all fuels. When considering only CO_2, specific emissions from the combustion processes in the analyzed steelmaking technologies are represented in **Figure 8**.

Despite being mostly fueled by natural gas, the DRI-EAF process modeled in this work does not offer impressive improvements with respect to the BF-BOF route, if not considering the contribution of electricity to direct emissions. Instead, the scrap-EAF route can offer ~ 84% direct emission reduction with respect to the traditional primary steel production technologies, even if requiring the double of their electricity consumption. The smelting reduction process is not so impressive in terms of CO_2 direct emissions, with the highest value in the subsector, but the use of coal can be interesting for the reduction in the emissions of other dangerous substances, e.g. sulfur [147], present in coke and blast furnace gas. Among innovative technologies, CCS-equipped plants provide large abatement performances, even with higher energy consumption than traditional technologies, while HDR and electrowinning technologies are linked with the capability of producing clean hydrogen and electricity, respectively.

As far as ferroalloys production are concerned, given the energy-intensity characteristics from the average CO_2 emissions from ferroalloys manufacturing are ~ 1782 kg_{CO_2}/t_{Fea}.

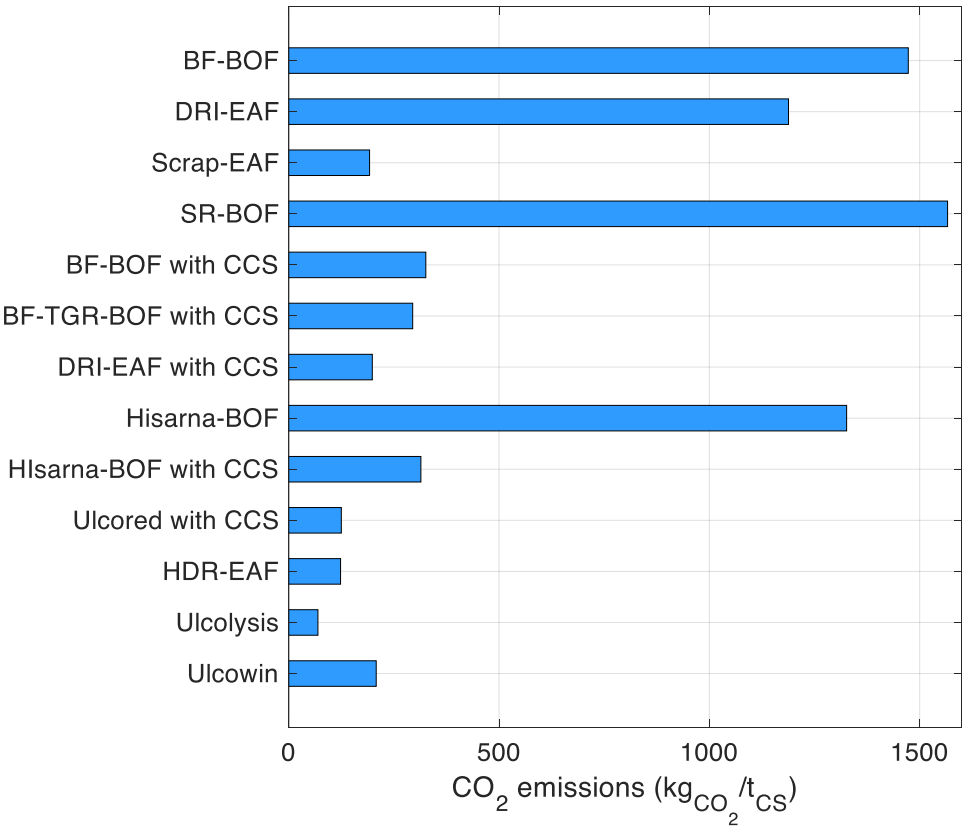

Figure 8. Specific CO_2 emissions of steelmaking technologies. Note that the values for BF-BOF, DRI-EAF, Scrap-EAF and BF-BOF with CCS refer to the basic versions of the processes characterized for the year 2020.

2.3.2 Non-ferrous metals

2.3.2.1 Technical characterization

According to [27], world average energy intensity for Bayer process is 14.7 $GJ/t_{Al_2O_3}$, but the use of BAT (assumed for the year 2050, as in the iron and steel sector) would result in a net decrease, to reach 10.4 $GJ/t_{Al_2O_3}$, with energy breakdown based on [148]. The world average energy consumption for the Hall-Héroult process is 51.48 GJ/t_{Al} [27], very close to the BAT value of 48.96 GJ/t_{Al} [134]. Nearly all the energy consumed is electricity, which is used in the smelting

process. The only other non-negligible fuel source is natural gas involved in the production of anodes, quantified in 2.8 GJ/t_{Al} [149].

An average consumption of 4.3 GJ/t_{Al} is proposed in [150] for secondary aluminum production. More than 86% of the used fuel is natural gas, while the use of heating oils is attested at 3.3%. The remaining part is used as electricity for heating. Recycling is only limited by the availability of scrap: recycled aluminum constituted 33% of world supply in 2012 [151], but it should grow up to 40% by 2030 to meet the IEA SDS targets [152].

The potential energy savings with the use of Hall-Héroult process with inert anodes are estimated at 11 GJ/t_{Al}, assumed proportionally distributed among the different energy sources. The carbothermic reduction of alumina would be able to allow energy savings of 30% compared to a modern Hall-Héroult carbon anode technology, despite a considerable amount of energy expenditure related to the production of alumina [153]. These savings are assumed to be proportionally distributed among the different energy sources. Kaolinite reduction, with an energy consumption mainly in the form of electricity, is promising for its potential 26% energy intensity reduction, with respect to the traditional route starting with alumina [154].

Table 40 in **Appendix** reports the detailed energy-intensity for alumina and aluminum production technologies.

Although theoretical energy requirement for copper production is very low, actual specific energy consumption is much higher, largely depending on copper concentration in the metal ore. Detailed energy consumption figures for copper are available for a Chilean copper factory (Chile is the world's largest producer of copper [155]) and taken as representative plant in [156]. **Figure 9** represents the detailed energy-intensity breakdown for copper production, showing that electricity plays the largest role, both as direct source and as a supply for machine drive. An improvement in energy use during time is not assumed due to the absence of literature.

Around the world, the hydrometallurgical route for zinc consumes on average ~20.3 GJ/t_{Zn}, out of which electricity represents ~77% of total consumption (15.55 GJ/t_{Zn}), in average, while the remaining part is steam (4.73 GJ/t_{Zn}) [149].

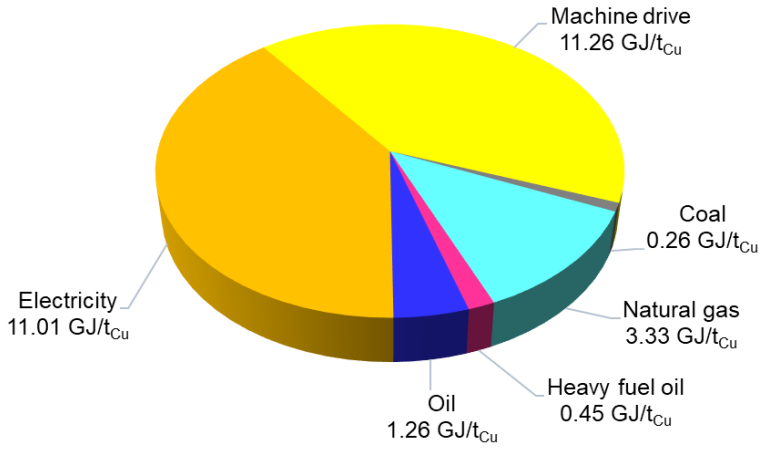

Figure 9. Energy-intensity breakdown for copper production. An improvement in energy use during time is not supposed due to the absence of literature.

Lifetime and availability factors for technologies involved in non-ferrous metals production are taken again from [63]: lifetime of 20 years and an availability factor of 0.95 are considered for all the modelled aluminum technologies. By extension, the mentioned availability factor is also taken for alumina production, while considering a lifetime of 40 years, i.e. the average value provided in [157]. Copper and zinc production are characterized with availability factor of 0.90 and a lifetime of 30 years [129].

2.3.2.2 Economic characterization

The economics of the Bayer process are retrieved from [157]. Regarding aluminum production facilities, an average investment cost from [151] is taken as reference for Hall-Héroult plants. Fixed O&M cost is indicated in [63], but in a process including both alumina reduction and production of aluminum, therefore the fixed O&M cost used for Bayer process is subtracted from that. Secondary aluminum is cheaper than the traditional Hall-Héroult process, in terms of investment cost [63]. On the other hand, fixed O&M cost results far higher than for the primary route [5]. Shifting the focus towards innovative aluminum technologies, Hall-Héroult with inert anodes would require costs estimated as lower than for traditional plants [63]. For carbothermic reduction, an investment cost much lower than for Hall-Héroult is estimated in [153], while fixed O&M cost is the 20% lower than the traditional Hall-Héroult process. Kaolinite reduction has a lower raw material price, and could be competitive on the market, as suggested in [154]. Anyway, in absence of more detailed data, costs for this

particular innovative process have been assumed equal to those of the Bayer process only. **Table 19** reports all investment and fixed O&M costs for alumina and aluminum production technologies, properly converted (when needed) in $ according to the 2010 average exchange rate, 0.754 €/$ [6].

Table 19. Costs for aluminum and alumina production.

Technology	**Investment cost** ($/$t_{NF}$ *)	**Fixed O&M cost** ($/$t_{NF}$/year)
Bayer process	1560	137
Hall-Héroult	4400	68
Secondary aluminum	1260	365
Hall-Héroult with inert anodes	3880	56
Carbothermic reduction	1300	55
Kaolinite reduction	1560	137

Innovative processes have, for aluminum production, the potential to be disruptive and their appeal could be supported by economical attractiveness. On the shorter term, the secondary route is much cheaper than the traditional primary route, the only drawback being the cost of the scrap and its availability.

Copper production was already characterized in [129] with an investment cost of 4400 $/$t_{Cu}$† and a fixed O&M cost of 10 $/$t_{Cu}$/year, with no supposed evolution in time. The same values used for copper have been deemed appropriate for tin, due to the lack of more detailed data and the absence of this material in databases and models. Zinc, on the other hand, while having the same O&M cost as copper (10 $/$t_{Zn}$/year), is characterized by a much lower investment cost: 2000 $/$t_{Zn}$ [129].

2.3.2.3 Environmental performances

The specific emissions from the combustion processes in the analyzed steelmaking technologies are represented in **Figure 10a** for the Bayer process for alumina production, and in **Figure 10b** for aluminum manufacturing, considering only the contribution of direct CO_2 to pollutant emissions.

* t_{NF}: ton of non-ferrous metals
† t_{Cu}: ton of copper

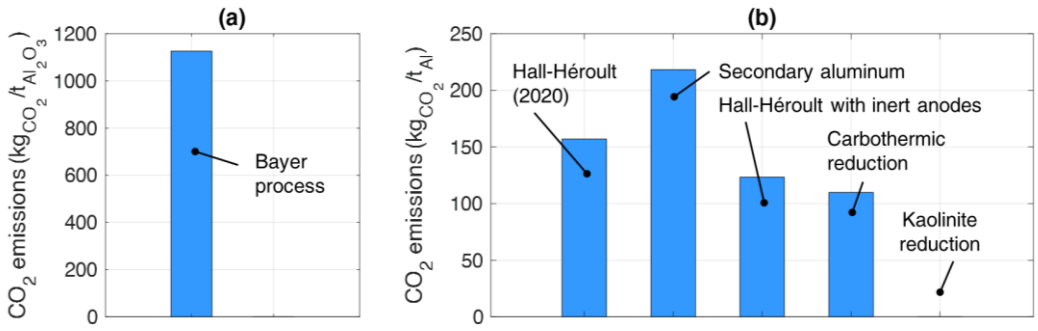

Figure 10. Specific CO_2 emissions of alumina and aluminum production technologies Energy intensity breakdown taken from **Table 40** and emission factors from **Table 14**.

If considering that the traditional Hall-Héroult technology, the one with inert anodes and carbothermic reduction require almost 2 $t_{Al_2O_3}/t_{Al}$, their CO_2 emissions are extremely higher than the secondary aluminum route and, of course, kaolinite reduction, which does not involve any energy-intensive primary material and is completely supplied by electricity. Of course, kaolinite reduction can be a zero-emission process only if using clean electricity sources. On the other hand, secondary aluminum production requires slight electricity contribution, avoiding this issue, but is subject to material availability.

Zinc production as modeled here is fueled by non-emitting commodities, thus it presents no CO_2 emissions. The copper production process emits 246 $kg_{CO_2}/t_{\text{final product}}$.

2.3.3 Non-metallic minerals

2.3.3.1 Technical characterization

The best practice for dry production of clinker establishes a thermal energy intensity of 2.9 GJ_{th}/t_{cl}* [158]. However, the least expensive, least efficient and more widespread commercially available system consumes a total of 4.6 GJ/t_{cl} (including thermal and electrical requirements) [159]. In order to obtain a representative value of the global average energy intensity of the process, the average of the specific energy consumption for the major producer countries (representing over 70% of total world production), weighted on their yearly yield of cement, has been considered, as from **Figure 11**.

* t_{cl}: ton of clinker.

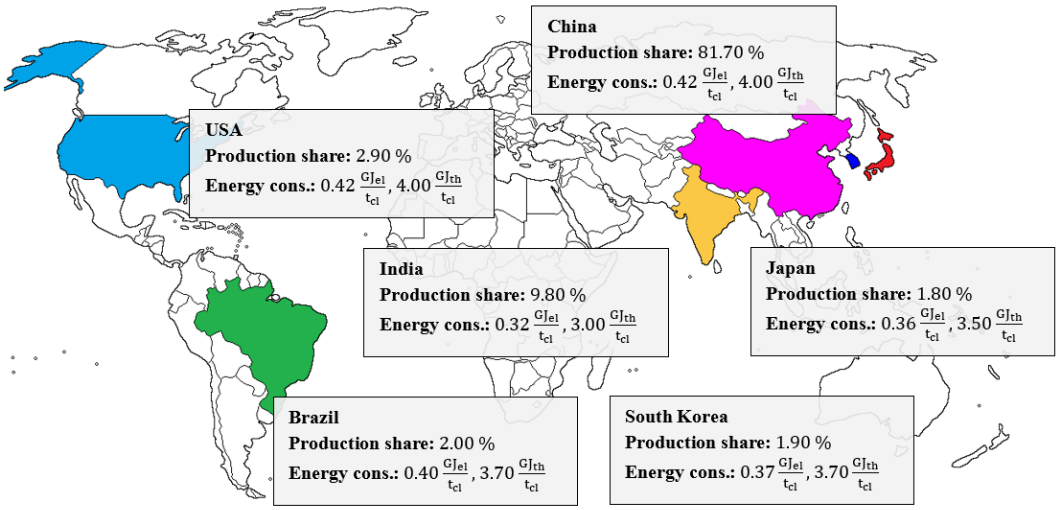

Figure 11. Dry-clinker production statistics and relative energy consumption, elaborated by the authors, based on [159], [160].

The estimation leads to an average total energy intensity 4.31 GJ/t_{cl}, of which the majority (3.90 GJ/t_{cl}) is represented by the thermal component. Since that technology is very versatile in accepting different fuels, coal, oil, natural gas and biomass can be all used to provide the required thermal energy. The repartition of fuels is made according to [158] as reported in **Figure 12a**, while **Table 41** in **Appendix** provides details about the correspondent energy input requirement in GJ/t_{cl}.

As there is no substantial difference between a dry and a wet process plant for clinker production, the energy consumption component related to thermal power is simply rescaled, in relation to the average thermal energy intensity of the wet process, 6.07 GJ_{th}/t_{cl} [159], due to the additional energy requirement for drying the raw materials.

In absence of further information regarding the application of CCS to the cement sector, data from the techniques selected for the iron and steel sector will be used. Electricity and steam consumption for performing post-combustion CCS using the amines absorption technology, see **Table 15**, are summed up to the standard dry process energy need. Since the selected capture technique consumes both electricity for machine drive, $\varepsilon_{el,t} = 0.61\ GJ/t_{CO_2}$, and steam, $\varepsilon_{st,t} = 3.2\ GJ/t_{CO_2}$, the dry process with post-combustion CCS will require additional

energy calculated according to **Equation 6** and **Equation 9**, respectively for electricity and steam:

$$S_{CCS} = \varepsilon_{st,t} \cdot \sum_{i} k_i \cdot e_i \cdot 10^{-3} \quad (9)$$

where S_{CCS} represents the steam input needed for carbon capture, expressed in GJ/t_{cl}; $\varepsilon_{st,t}$ is the specific steam input needed by the CCS technology t. Considering that in this case carbon-rich sources are coal, heavy fuel oil, natural gas, and that additional 505.2 $kg_{CO_2/t_{cl}}$ are produced during calcination, $MD_{CCS} = 2.66\ GJ/t_{cl}$ and $S_{CCS} = 0.51\ GJ/t_{cl}$.

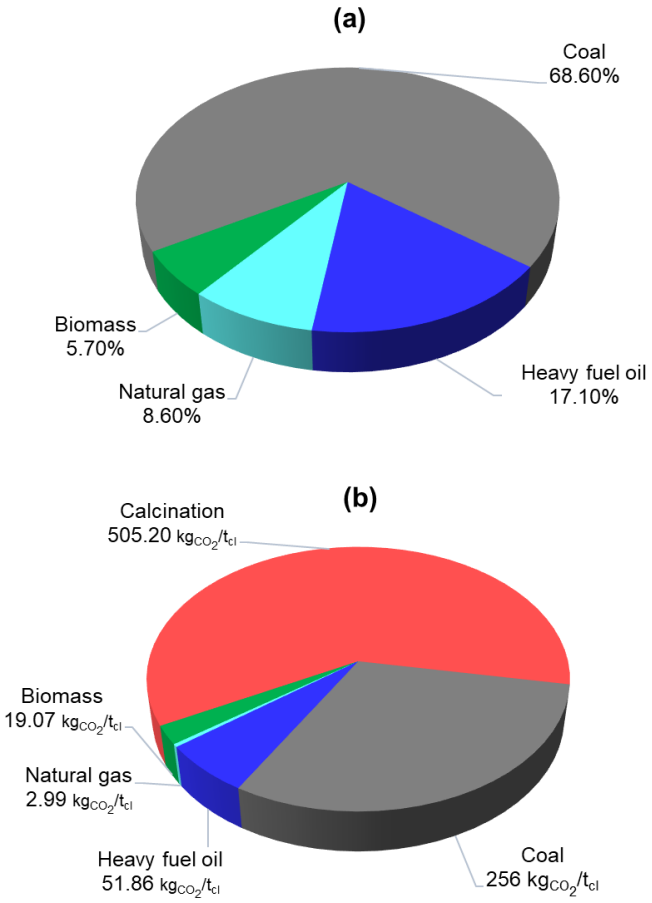

Figure 12. Use of fuels in the dry process for clinker production for the year 2020, elaborated by the authors, based on [158] (a), and CCS features for post-combustion CCS applied to the dry process, in terms of captured CO_2 (b). An improvement in energy use during time is not supposed due to the absence of literature.

For the dry process with oxy-fuel CCS, the thermal energy consumption is in the range of the standard plant. Regarding electricity consumption for oxy-fuel combustion, [161] recommends to consider, as a rule of thumb, twice the consumption of the traditional dry process, for capturing the same amount of CO_2 as with post-combustion CCS.

Energy intensity for the cement blending process itself is negligible. The moderate energy consumption for alkali-activated concrete (AAC) production, together with the absence of calcination emissions makes this route particularly appealing to meet the sustainability targets, in particular, AAC based on high-magnesium nickel slag requires 1.2 GJ/t_{cmt}* [162]. In the absence of additional information, its total energy consumption value has been rescaled by the dry process for clinker production. Belite cement production requires lower energy and produces lower CO_2 emissions from fuel combustion [7]. Specifically, a saving of 10% thermal energy, and an increase of 5% of electricity use due to grinding with respect to ordinary cement blending should be taken into account for commercial belite [163].

Concerning lime, long rotary kilns allow good fuel flexibility: solid biomass waste represents a solid share of fuel for this technology, ~ 14% in the EU-27 in 2008 [158]. The distribution of fuel use in the EU, taken from the same source, is considered as representative for global production. Energy-intensity is, however, significant in this process, on average: 7.6 GJ/t_{lime} of thermal energy and only 0.08 GJ/t_{lime} of electricity. Thermal energy inputs, distributed according to the shares from [158], give the results reported in **Figure 13**. An improvement in energy use during time is not supposed due to the absence of literature.

A detailed energy-intensity breakdown for glass production is reported in **Figure 14**. Fossil fuel furnaces are fueled by a mix of natural gas (53-79%) and fuel oil [164]. Here the mean value of that range (66%) for the natural gas contribution will be considered. Additional energy is required for electricity boosting and electricity for oxygen production (in oxy-fuel combustion furnaces). A critical point in the characterization of this subsector was the high variability of energy requirements, strongly depending on the specificity of the processes, even if usually in the same range of values as for the melting step. Restricting the technologies to container glass, the mean specific total energy use has been

* t_{cmt}: ton of cement

attested at 7.7 GJ/t_{gl}*. Energy required for glass finishing has been then added, according to data from [164]: a range of 5-10 GJ/t_{gl} was indicated, and the mean value of 7.5 GJ/t_{gl} has been considered here as representative value. All-electric glass furnaces show much lower energy intensity, on average 3.3 GJ/t_{gl} [164]. Note that the same energy for finishing as in fossil fuel furnaces is considered here, too.

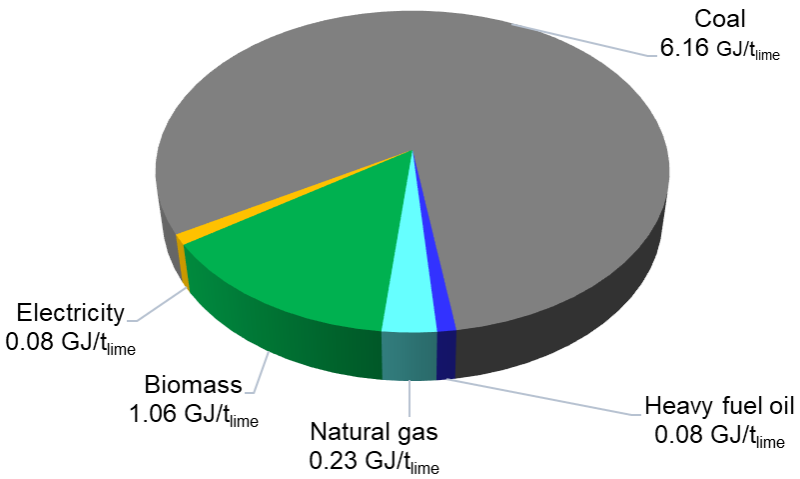

Figure 13. Energy-intensity breakdown for the lime production process for the year 2020.

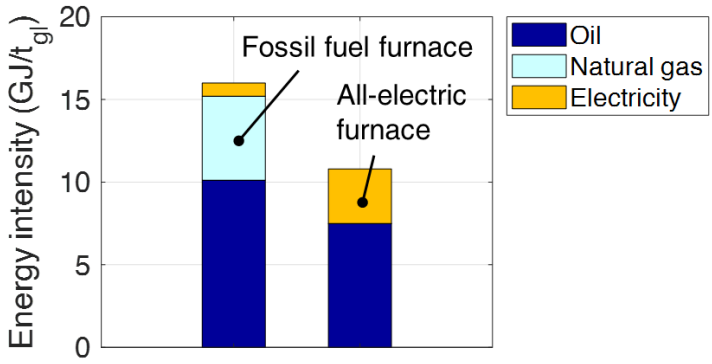

Figure 14. Energy-intensity breakdown for glassmaking technologies.

* t_{gl}: ton of glass

2.3.3.2 Economic characterization

Data regarding costs for the dry process for clinker production (both with and without CCS) are retrieved from [160]. Due to the strong similarities between wet and dry processes, the same cost figures are also assumed for the latter. Costs for cement blending are almost negligible, considering that grinding of clinker, substitutes and additives into cement plays a small role if compared with clinker production [159], [165]. Regarding AAC, the cost of geopolymer cement concrete and the addition of activating chemicals make the geopolymer cement significantly more expensive than ordinary Portland cement, making this route far more expensive than the traditional clinker-cement blending process, even in the absence of clinker production [166], [167]. Finally, since belite cement production is not so different with respect to the production of OPC, cost figures can be assumed equal to the sum of dry process and cement blending. **Table 20** reports all cost information about clinker and cement technologies, properly converted, when needed, in terms of \$, according to the 2010 average exchange rate, 0.754 €/\$ [146].

Table 20. Costs for clinker and cement production.

Technology	**Investment cost ($/t$_{NM}$*)**	**Fixed O&M cost ($/t$_{NM}$/year)**
Dry clinker	349	73
Wet clinker	349	73
Blended cement	12	3
Dry clinker with post-combustion CCS	740	145
Dry clinker with oxyfuel CCS	433	88
AAC	1100	230
Belite cement	361	76

Concerning lime production, [63] reports an investment cost of 300 €/t_{lime} and O&M costs of 15 €/t_{lime}. Taking as reference the same source, container glass furnaces, considered as representative of the sector in this work, have been characterized with an investment cost of 332 \$/t_{glass} and fixed O&M cost of 27 \$/t_{gl}/year. As for ceramics, in absence of more recent reliable data, these

* t_{NM}: ton of non-metallic minerals

parameters have been collected from [129], which in turn reports [62] as source: the investment cost is 125 $\$/t_{cer}$ and the fixed O&M cost 15 $\$/t_{cer}/year$.

2.3.3.3 Environmental performances

Pollutants are emitted both from fuel consumption and from calcination reaction when clinker is made. Specifically clinker production generates 505.2 kg_{CO_2}/t_{cl} from the limestone decomposition process ($CaCO_3$ forming CaO and CO_2) during calcination [8]. This is true for several technologies modeled: dry process (with or without CCS), wet process and belite cement. **Figure 15** reports overall CO_2emissions for technologies involved in cement production: among them, just the coupling of a dry process for clinker production with CCS and cement blending would allow a net zero-emission balance. However, the use of alternative cements like AAC and belite would allow to avoid emissions from the traditional clinker production processes.

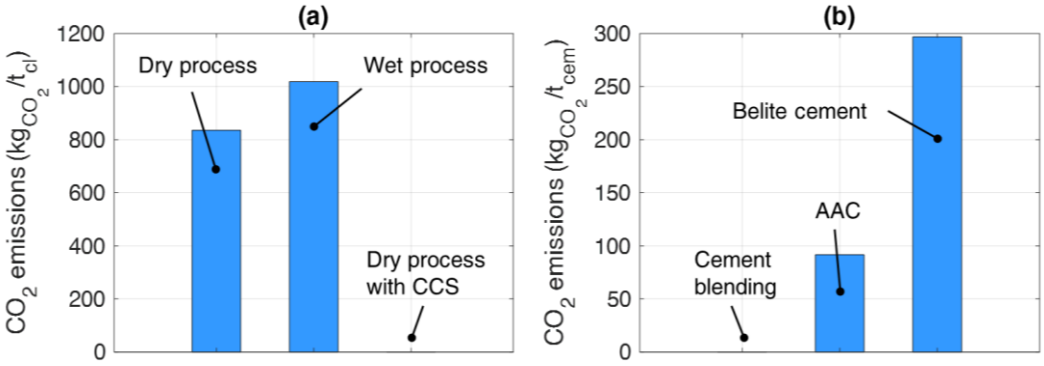

Figure 15. Specific CO_2 emissions of clinker and cement production technologies.

Glassmaking also brings along a considerable amount of emissions. Even the electric furnace-based process implies fossil fuel consumption for refining and, as a consequence, direct emissions as shown in **Figure 16**. Concerning direct emissions for ceramics production, the low natural gas consumption results in just 129 kg_{CO_2}/t_{cer}.

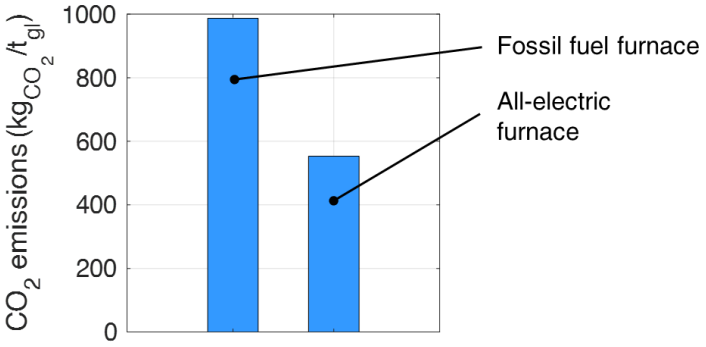

Figure 16. Specific CO_2 emissions of glassmaking processes.

2.3.4 Chemicals

2.3.4.1 Technical characterization

As a general remark, fuels in the chemicals subsector can be consumed in two ways: as energy to drive processes (as in the other industrial subsectors) and as feedstock. The word "feedstock" describes the use of various fuels as material inputs. Differently from iron ore used in the iron and steel sector or from alumina used for aluminum production, chemical feedstock represents the source of primary chemicals (hydrogen and carbon) for generating final products but quantified in energy units because indistinguishable from energy inputs before use. The importance of feedstock is relevant since they represent almost half of total energy use in the chemical sector, as of today [129], [168]. The detailed technical characterization for HVCs, ammonia and methanol is reported in **Table 42**, **Table 43** and **Table 44** in **Appendix**. Data about energy intensity and the related energy breakdown are retrieved according to [64], which is the only publicly available source by IEA providing data for energy modeling.

While all the technological routes for HVC production have comparable consumptions of the particular fuels and feedstock, bioethanol dehydration (BDH) adopts a very large steam input, but the lowest amount of feedstock and fuel among the considered processes. On the other hand, it should be noted that the feasibility of BDH is strongly subject to the availability of biomass [48].

Concerning ammonia production, electrolysis is the only route allowing the absence of directly emitting sources, and the same applies for methanol production.

For chlorine, the energy requirement has been modeled according to the European BATs [169], considering the mercury cell, diaphragm cell and membrane cell technologies. In addition, all these technologies produce hydrogen as byproduct but unfortunately such hydrogen is not so often exploited. Data considered in this analysis for chlorine production are summarized in **Figure 17**, highlighting that the currently most diffuse process – mercury cell – is also the most energy intensive alternative.

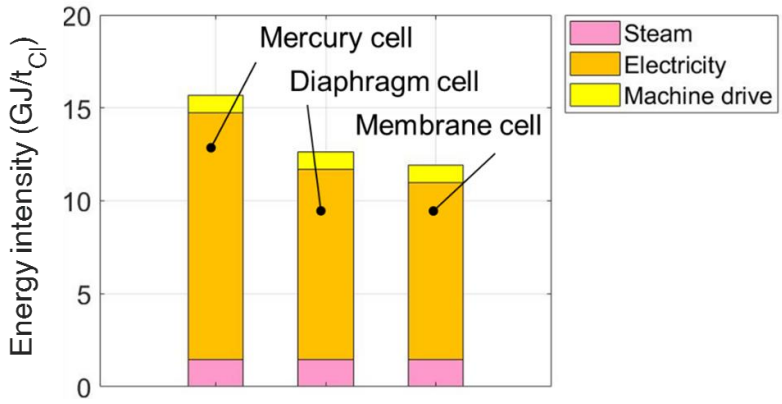

Figure 17. Energy-intensity breakdown for chlorine production technologies.

Lifetime and availability factors for the production of chemicals are found again in [63]. However, there the only distinction is made between ammonia and "other chemicals" production, including both olefins and methanol. The considered lifetime and availability factor for "other chemicals" are 30 years and 85%, respectively, with the only exception for electrochemical processes, which instead are characterized by an availability factor of 95%. On the other hand, ammonia plants are characterized by a lifetime of 25 years and an availability factor of 90%.

2.3.4.2 Economic characterization

Costs for HVC, ammonia and methanol are based on [9] and reported in **Table 21**. Concerning electrolysis processes, the cost of the electrolytic plant is already considered in the model characterization of hydrogen-generation technologies, thus costs for the synthesis unit only are considered. Regarding chlorine, the costs for all the three routes are estimated at 676 $\$/t_{Cl}$, while O&M costs at 7 $\$/t_{Cl}$ [169].

Table 21. Costs for the chemicals sector.

Product	Technology	Investment cost ($\$/t_{ch}$)	Fixed O&M cost ($\$/t_{ch}/year$)
HVC	Naphtha SC	2060	51
	Ethane SC	1490	37
	Gas oil SC	2330	58
	LPG SC	1900	48
	Propane dehydrogenation (PDH)	1690	42
	Naphtha catalytic cracking (NCC)	3000	75
	Methanol-to-olefins (MTO)	1000	25
	BDH	1330	33
Ammonia	NG steam reforming (SR)	860	22
	Naphtha partial oxidation (POX)	1200	30
	Coal gasification (GSF)	2060	52
	Biomass GSF	6000	300
	Synthesis via electrolysis*	110	3
	NG SR with CCS	930	51
Methanol	NG SR	300	22
	Coke oven gas SR	300	22
	LPG POX	300	22
	Coal GSF	710	18
	Synthesis via electrolysis†	44	1
	Biomass GSF	4900	123
Chlorine	Mercury cell	676	7
	Diaphragm cell	676	7
	Membrane cell	676	7

Concerning HVCs, the MTO route has received great attention thanks mainly to its intrinsic competitiveness but also to the price of methanol. Indeed, methanol production is cheap, on average, the only exception being the biomass-based process which has an out-of-scale investment cost because of the low yield

* The reported costs only consider the ammonia synthesis unit.
† The reported costs only consider the methanol synthesis unit.

achievable via that route. Even if the costs of electrolytic processes here presented do not account for energy costs, their attractiveness is undeniable.

2.3.4.3 Environmental performances

Starting from the energy-intensity breakdown by fuels, energy carriers and feedstock for the considered processes, emission factors have been applied to retrieve direct emissions coming from such processes, which are reported in **Figure 18** for HVCs, **Figure 19** for ammonia and **Figure 20** for methanol, respectively.

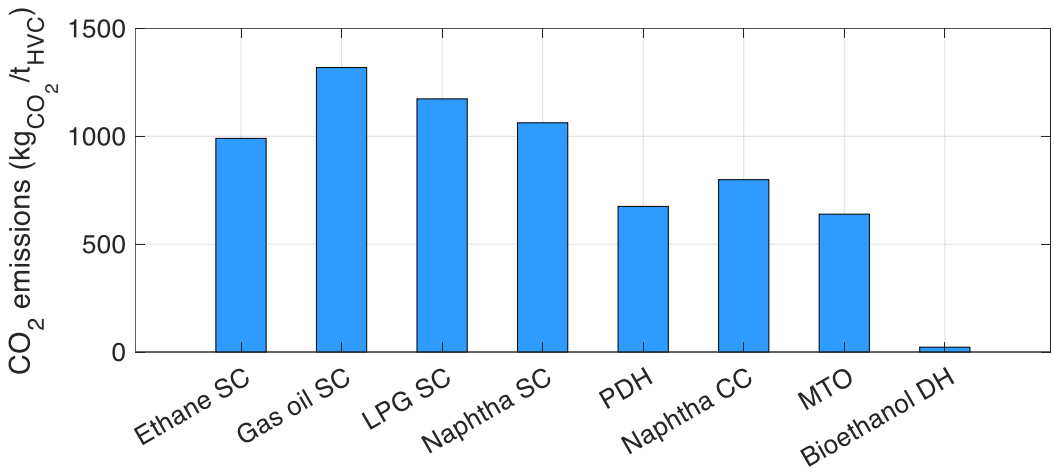

Figure 18. Specific CO_2 emissions of HVC production processes.

Concerning HVCs, bioethanol dehydration is the only route able to reach almost zero direct emissions, due to its use of just biomass and steam, while innovative techniques (PDH, NCC and MTO) also show good capabilities to reduce emissions with respect to the most traditional alternatives. Note that, however, emissions for MTO sum up with the ones from the adopted methanol production route.

Emissions from methanol production are very high just if involving coal in the process, but its substitution with biomass in the gasification process would allow to cut emissions by 85%. For electrolysis, the same observation as for ammonia applies here.

Chlorine production technologies are practically emission-free, if just considering direct emissions from combustion processes, which are absent.

Anyway, the strong reliance on electricity makes the evaluation largely dependent on the adopted electricity production mix.

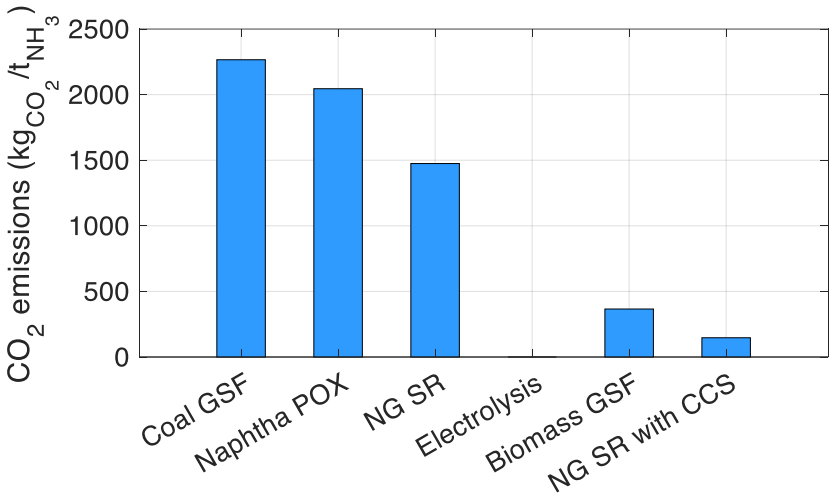

Figure 19. Specific CO_2 emissions of ammonia production processes.

Concerning ammonia, the electrolysis routes shows zero emissions, but it is subject to the generation source for electricity involved in the process, while biomass gasification and NG SR with CCS show extremely better performances with respect to the most traditional processes.

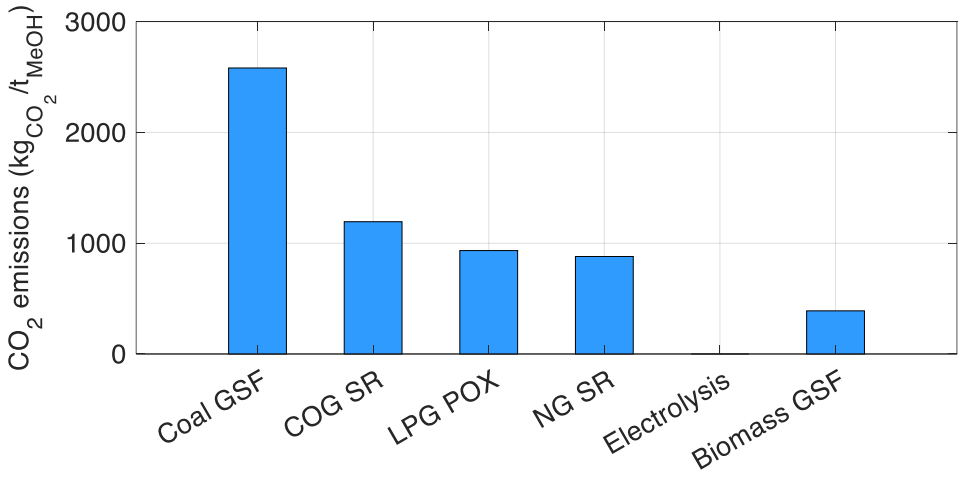

Figure 20. Specific CO_2 emissions of methanol production processes.

2.3.5 Pulp and paper

2.3.5.1 Technical characterization

Pulp and paper mills may exist as integrated or separate systems, but they are in general complex plants incorporating many different process areas (raw material preparation, pulping, pulp processing, chemical recovery, bleaching, stock preparation and papermaking). They are aimed at supplying demand from printed paper, packaging material, household and sanitary paper. The most energy consuming part of the pulp and paper processing is drying of paper products and pulp [170].

For mechanical pulping, semi-chemical pulping, recycled fiber pulping and papermaking energy use is based on [171], while the source about chemical processes is [172]. Energy intensity for recycled fiber pulping is almost negligible with respect to the other routes, even if subject to the availability of usable recycled paper, while chemical processes (Kraft and Sulfite) have both higher energy intensity and wood requirements. Anyway, the type of pulping stage defines the quality and properties of the produced paper, even if this is not a peculiarity that can be directly addressed here, if considering a single end-use commodity for paper. For paper production, $0.58\ t_{pulp}/t_{paper}$ are currently needed [172], apart from energy inputs. Details are reported in **Table 45** in **Appendix**.

Always taking [63] as reference, lifetime for pulp mills is 30 years, with 95% availability factor. A lifetime of 20 years and an availability factor of 95% are reported for papermaking plants.

2.3.5.2 Economic characterization

Concerning the economics of pulping technologies, since mill costs strongly depend on the final product, plant capacity, integration or not of pulp and paper processing, both CAPEX and OPEX, reported in **Table 22**, are retrieved from [63], and properly converted in $, according to the 2010 average exchange rate, $0.754\ €/\$$ [146]. Semi-chemical pulping is not included in the JRC-EU TIMES database, then the mean value between costs for mechanical and chemical pulping will be assumed to represent it. Regarding paper, the mean value between low quality and high quality-papermaking investment and fixed O&M costs are taken from [63].

Data presented in **Table 22** show that the chemical route for pulp production has an investment cost almost not comparable with the other technologies. This is mainly due to the chemicals involved in the process. Nevertheless, the benefits in term of energy efficiency and the possible market of byproducts make this alternative the most widespread.

Table 22. Economic parameters for pulp and paper technologies, based on [5].

	Investment cost ($\$/\mathbf{t_{pulp}}$)	**Fixed O&M cost** ($\$/\mathbf{t_{pulp}/year}$)
Mechanical pulping	399	20
Semi-chemical pulping	1100	37
Recycled fiber pulping	851	40
Chemical pulping*	1800	53
Papermaking	2390	118

2.3.5.3 Environmental performances

Despite being largely energy-intensive processes, pulp and paper production processes do not involve any direct CO_2 emission, making use of just heat, steam and electricity, which in turn are subject to the variability of their production sources, influencing the environmental performances of this subsector. Fossil fuel consumption, and consequently CO_2 emissions, can be related to the auxiliary equipment, e.g. for lighting and heating in the industrial facility, but not directly related to pulp and paper production. For this reason, this additional energy use is considered in the ETP Model [27], as in ETM [129], under "Other industrial energy uses". In the JRC-EU-TIMES [63], instead, direct use of fossil fuels is taken into account for pulp and paper manufacturing, thus implying direct emissions.

2.4 Hydrogen

The hydrogen module included in TEMOA-Europe is mainly based on the JRC-EU-TIMES [63], covering the hydrogen value chain in 4 steps: production, storage, delivery and end-use, as presented in **Table 23**. **Figure 21** reports an

* Includes both Kraft and sulfite pulping.

overview of the TEMOA-Europe hydrogen module; note also that hydrogen can be generated as a by-product by chlorine production technologies.

Table 23. Overview of the hydrogen value chain in TEMOA-Europe.

Value chain step	Classification
Production (17 technologies)	• Centralized production (underground storage) • Centralized production (underground storage) produced from electrolysis • Centralized production (tank storage) • Centralized production (tank storage) produced from electrolysis • Decentralized production (tank storage) • Decentralized production (tank storage) produced from electrolysis
Storage (3 processes)	• Underground • Centralized tank • Decentralized tank
Delivery (12 technologies)	• One or more processes for each end-use sector, including blending with natural gas
Synfuel production (11 technologies)	• Methane production • Diesel production • Kerosene production • Methanol production
Electricity production (1 technology)	• Utility scale fuel cell generation plant
End-use	• Industry (3 technologies) • Transport (5 technologies)

Table 24 lists the commodities and associated codes related to hydrogen production and use.

The description of the hydrogen production technologies listed in **Table 23** and included in TEMOA-Europe retraces the classification of the European Commission for the hydrogen strategy [173] including:

- Grey hydrogen produced using fossil fuels;
- Blue hydrogen produced using fossil fuels processes equipped with carbon capture;

- Water electrolysis-based hydrogen production;
- Renewable energy sources-based hydrogen production;
- Green hydrogen production using renewable-based electricity in electrolytic processes.

Produced hydrogen can be either stored without losses before the delivery or delivered to consumption processes. Storage processes in **Table 23** are used according to the scale of the associated production technology [174]:

- Underground storage: associated to medium- or large-scale production conventional technologies (e.g. SMR).
- Centralized tank storage: associated to unconventional processes (e.g., oxidation of heavy oil) and small-scale production.
- Decentralized tank storage: associated to small-scale production.

The delivery process is again based on [63] and allows considers both pure hydrogen and methane-hydrogen blending. Hydrogen may undergo several steps in the JRC-EU-TIMES [63] as in the list below:

- Compression;
- Underground storage;
- Transmission;
- Distribution;
- Liquefaction;
- Storage bulk;
- Road transport;
- Refueling.

The additional possibly needed commodities (electricity and gasoline) are taken into account for the delivery process assigned to the specific hydrogen commodity. The delivery process associated to each centralized or decentralized production technology are listed in **Table 25** and **Table 26**, respectively, and generate commodities to be consumed in different end-use sectors.

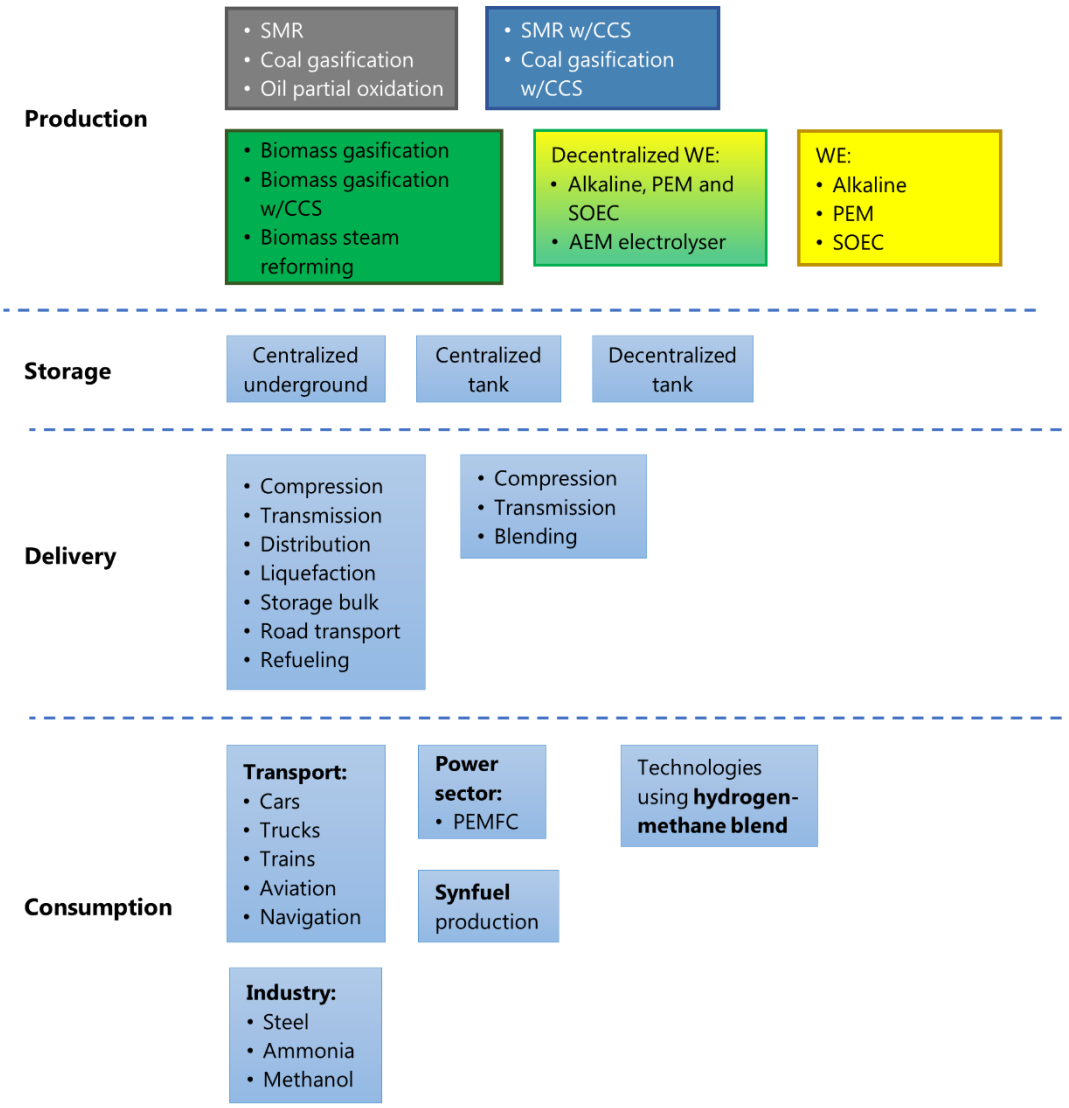

Figure 21. Overview of the TEMOA-Europe hydrogen module [175].

The delivery of the methane-hydrogen blend involves compression, underground storage, transmission and blending, and produces a fuel that can be used in substitution of natural gas in all sectors. While the economic parameters of this steps retrace again the characterization in [63]. The hydrogen share in the methane-hydrogen blend is fixed to 5% in [63], while a maximum allowable share is taken into account in TEMOA-Europe that can vary along the decades: based on [176] and [177], a maximum 5% volume fraction is allowed in 2020, while a maximum 20% volume fraction is possible from 2050 on.

Table 24. Commodities envisaged in the production and end-use steps of the TEMOA-Europe hydrogen value chain.

Value chain step	Commodity	Code
Production	Hydrogen, centralized production, underground storage	UPS_HH2_CU
	Hydrogen, centralized production, tank storage	UPS_HH2_CT
	Hydrogen, decentralized production, tank storage	UPS_HH2_DT
	Hydrogen from water electrolysis (WE), centralized production, underground storage	UPS_HH2_WE_CU
	Hydrogen from WE, centralized production, underground storage	UPS_HH2_WE_DT
End-use	Liquid hydrogen (transport)	TRA_L2H
	Gaseous hydrogen (transport)	TRA_GH2
	Hydrogen (industry)	IND_HH2
	Hydrogen from WE (industry)	IND_HH2_WE

While details about end-use demand technologies consuming hydrogen as fuel are described in **Sections 2.1**, **2.2** and **2.3**, both pure and blended hydrogen can be also used in the power sector for utility scale proton exchange membrane fuel cell (PEMFC)-based electricity generation plants, as in [63], and especially for synfuel production.

Technologies for synfuel production are characterized as in [63]. Synfuel production includes:

- Synfuels produced through methanation, hydrogenation or co-electrolysis of hydrogen and CO_2: synthetic methane, synthetic diesel, synthetic kerosene and synthetic methanol. The CO_2 flow can be derived either as CO_2 stored in plants equipped with CCS or CO_2 in atmosphere directly captured in air.
- e-ammonia produced using WE-based hydrogen. e-ammonia is defined as an electro-fuel, since it is produced hydrogen produced through electrolysis.

Note that CO_2-synfuels are identical to the corresponding fossil fuels from a chemical point of view in terms of specific CO_2 emissions. Hence, technologies

that already consume fossil fuels can now consume the corresponding synfuel without any modifications in their characterization.

Table 25. Delivery processes for pure hydrogen from centralized production modeled in TEMOA-Europe. For each process, the steps included in the delivery chain are indicated with "×".

Input	Delivery process	Compression	Underground storage	Transmission	Distribution	Liquefaction	Storage bulk	Road transport	Refueling *	Output
UPS_HH2_CU Electricity Gasoline	1	×	×	×		×	Liquid	×	L2L	TRALH2
	2	×	×	×		×	Liquid	×	L2G	TRAGH2
	3	×	×	×			Gas	×	G2G	TRAGH2
UPS_HH2_CU Electricity	4	×	×	×	×				G2G	TRAGH2
UPS_HH2_CT Electricity Gasoline	5	×		×		×	Liquid	×	L2L	TRA_LH2
	6	×		×		×	Liquid	×	L2G	TRA_GH2
UPS_HH2_CT Electricity	7	×		×	×				G2G	TRAGH2
	8	×		×	×					IND_HH2
	9	×		×	×					IND_HH2_WE

** Refueling can be liquid-to-liquid (L2L), liquid-to-gas (L2G) and gas-to-gas (GTG).*

Table 26. Delivery processes for pure hydrogen from decentralized production modeled in TEMOA-Europe. For each process, the steps included in the delivery chain are indicated with "×".

Input	Delivery process	Local gas storage bulk	Distribution	On-site liquefaction	Refueling	Output
UPS_HH2_DT	10	×		×	L2L	TRA_LH2
Electricity	11	×			G2G	TRA_GH2
UPS_HH2_WE_DT Electricity	12	×	×			IND_HH2_WE

2.5 Nuclear fusion

In the framework of the consideration of nuclear fusion technologies among the available alternatives in the electricity generation sector, its main technical and economic features are lumped in the following parameters for the characterization in TEMOA-Europe, see also **Table 27**:

- Lithium consumption
- Yearly operation time (annual availability)
- Lifetime
- Investment, fixed O&M and variable O&M costs

Being the optimization process performed with ESOMs generally driven by an economic paradigm (aiming at producing the minimum-cost energy system in the examined scenario), the economic parameters (costs) play a crucial role to establish the optimal technology mix. The work in [45] does not show any data used for the characterization of nuclear fusion power plants in the PLANELEC-Pro, while in [46] and [48] some detailed information about the adopted data for the Asian-DEMO reactor encompassing the features of both CREST and SlimCS reactors are reported. Specifically, the starting availability dates, lifetimes and investment costs show good agreement in [46] and [48], even though the two works were developed 12 years apart. In particular, nuclear fusion availability starts in 2048 in the World-TIMES [46] and in 2050 in ITER-participating countries in the DNE 21+ [48]. The assumed lifetime is 40 years in both models, while investment costs range from 8820 $/kW in [46] to 8500 $/kW in [48]. Such data is considered for the first year of availability of the plants, while a

physiological cost decrease driven by technology learning is progressively taken into account in both World-TIMES and DNE 21+. In addition, DNE 21+ considers one basic and one advanced versions of the technology based on the Asian tokamak concepts, accounting for a 22% cost reduction between the two types of plants. Concerning the fixed and variable operation and maintenance costs, the study in [46] is the only document reporting data adopted in the World-TIMES model, which considers 77 $/kW and 0.36 $/GJ for them, respectively. On the other hand, the annual capacity factor is only quoted in [48] to be 90 %, as adopted in the DNE 21+.

Two technologies were already included in ETM [178] to represent two different stages of development of a reactor based on the EU-DEMO concept, the first available starting from 2050 (Basic EU-DEMO-based concept), the second available starting from 2070 (Advanced EU-DEMO-based concept) [179]. The costs for those fusion technologies are computed according to the fusion reactor cost estimation performed by means of the PROCESS code [180], which aims to minimize the cost of electricity, accounting for constraints on engineering, physics and materials of the nuclear fusion power plant (NFPP) [181] and arbitrarily increased by 30 %. In this work, a single technology is considered for the EU-DEMO-based commercial NFPP accounting for a shift in the starting date for the availability of the technology due to the most recent adjustments to the EUROfusion Roadmap towards commercial NFPPs [32] placing commercial fusion starting from 2060. Specific lithium consumption and cost reductions are prescribed starting from 2080 (instead of 2070 as in the previous ETM-based analyses).

Concerning ARC, it was added to ETM and made available starting from 2035, as expected in [36], despite the several technical and economic criticalities concerning nuclear fusion for electricity production. The techno-economic parameters representing the EU-DEMO-like plant included in ETM are reported in **Table 27** and compared with those assumed for an ARC-like plant. In particular, it is highlighted how the compact nature of ARC allows to consider a shorter construction time (5 years) than the EU-DEMO-based reactor concepts (10 years). Nonetheless, construction times have no role in the TEMOA optimization algorithm [56], while they represent a decision parameter in TIMES when run in myopic (partial look-ahead) mode [55].

Also the Asian-DEMO-based reactor, in the wake of the approach adopted in [48] was added to the TEMOA-Europe technological database as representative of a family of NFPP developed in Asia, considering a single technology available

starting from 2060. The same investment cost as in [48] is taken into account for the Asian-DEMO (more than 40% higher than for the 2060 version of the EU-DEMO-based reactor), while fixed and variable operation and maintenance costs are assumed as comparable to those of the EU-DEMO-based NFPP.

Lithium consumption is taken into account as a parameter contributing to the economic optimization in ETM [16]. However, while its cumulative availability, attested at 12 Mt [182] makes it essentially inexhaustible, the extraction process contributes to the total cost of the system with a contribution of 93 k$/t [182], which remains small when compared to the total NFPP cost, for all the technologies considered here. All in all, such a parameter is expected not to have a considerable influence on the choices made by the model.

The lithium consumption is estimated on the basis of the expected declared tritium consumption for all the reactors considered here and reported in **Table 27**. The tritium consumption for the EU-DEMO is estimated at 0.38 – 0.76 kg/day for 1.5 GW_e, corresponding to 92.4 – 184.9 kg/year for 1 GW_e full power year (fpy) and, approximately, to 14 – 7 kg of $^6Li/PJ_e$ [183]. For the Asian-DEMO-based reactor, the estimation of 123 kg of tritium per GWy_e performed in [35] for the K-DEMO is considered to be applied, corresponding to ~ 9 kg of $^6Li/PJ_e$.

As no data concerning tritium consumption for ARC could be found in the literature, the 14.1 MeV neutrons being stopped in the blanket were taken as starting point to estimate the tritium (thus lithium) requirement. Considering the ARC fusion power (525 MW) [184], a fusion frequency of $2.32 \cdot 10^{20}$ 1/s and the tritium mass, the tritium consumption can be estimated. The obtained requirement is 0.10 kg/day, equivalent to 36.5 kg/year for the rated net electric power to the grid at a first development stage of 190 MW_e (set at 2035 in this work) [184], returning 192.1 kg/GW_e. The final estimations for ^6Li consumption per PJ_e for ARC are reported in **Table 27**. A further development is taken into account for the ARC-based reactor technology in 2050, with a shift to a higher electrical power output of 250 MW_e, expected in [36] and to a lower specific lithium consumption (starting from the same fusion power of 525 MW).

Table 27 also highlights how ARC would represent the least expensive NFPP concept, in terms of single plant costs (construction, operation and maintenance) and investment requirement per MW installed power. On the other hand, the costs for the EU-DEMO and the Asian-DEMO are computed on the basis of a reactor expected to provide 500 MW_e to the grid, and that would make ARC's investment

cost per MW_e (2035) just the 10% lower than EU-DEMO (2060), while the economic advantage of ARC for this analysis is visible when, in 2050, it would provide 250 MW_e electricity to the grid with a cost per MW_e more than 50% lower than EU-DEMO (2060).

Nevertheless, costs reported in **Table 27** may be highly disputable due to the strong uncertainties related to the development of fusion technologies. For instance, costs for the ITER project have been already significantly revised upwards [43] and research and development costs for fusion (as in all the other sectors of the whole economy) may be affected by the current framework of generally high inflation and issues to the [185] supply chain. The availability factor considered here for fusion technologies, close to 70% (considering a operation time around 6000 hours per year) is adopted to account for the periodical replacement of main components, such as the blanket and the divertor [186].

Note that in TEMOA-Europe, presented in **Chapter 3**, both the European-DEMO, the Asian-DEMO and ARC are modeled as a single technology each encompassing both efficiency and cost improvements envisaged between the basic and advanced technologies in ETM (actually only for EU-DEMO). That is done in order to avoid entering in function of the advanced technology without any installation of the base reactor in the preceding time periods.

Table 27. Comparison of techno-economic description of the EU-DEMO, the Asian-DEMO and ARC-based nuclear fusion reactors.

Parameter		**EU-DEMO**	**Asian-DEMO**	**ARC**
Lithium consumption (kg of $^{6}Li/PJ_{e)}$		14 (2060) 7 (2080)	9	14 (2035) 11 (2050)
Yearly operation time (h/year)		~ 6000	~ 6000	~ 6000
First year of availability		2060	2060	2035
Lifetime (years)		40	40	40
Construction time (years)		10	10	5
Investment cost (B$/plant)		3.0 (in 2060) 2.2 (in 2080)	4.3	1.0 (in 2035) 0.7 (in 2050)
O&M cost (M$/plant/year)	Fixed	~ 33	~ 33	~ 20* (in 2035) ~ 14 (in 2050)
	Variable	~ 23 (in 2060) ~ 17 (in 2080)	~ 23	

* Preliminary rough estimation, starting from the estimation considering that the O&M cost for an European Pressurized Reactor (EPR) corresponds to 3.3% of the investment cost [234] and reducing that value to the 2% of the investment cost for ARC, as nuclear fission fuel requires more complex management than in a fusion plant.

Chapter 3

TEMOA-Europe: main features and results

This section present the development of the first version of TEMOA-Europe. TEMOA-Europe is the first-of-a-kind open-source and open-data energy system optimization model for the analysis of the European energy mix, particularly suited for studies concerning penetration of nuclear fusion technologies. TEMOA-Europe is based on the energy balance for the European region as structured in the EUROfusion TIMES Model. While ETM is a model of the global energy system in 17 regions connected via trade processes [187], TEMOA-Europe takes into account a closed system representing Europe alone. TEMOA-Europe adopts an optimization strategy aiming to supply energy services at the minimum global cost (more precisely, at the minimum loss of total surplus) [16] starting from 2005 (the so-called "base year") up to 2100, in order to effectively observe the possible effects of the integration of nuclear fusion in the electricity production sector once it would be commercially available. In general, TEMOA-Europe is suited for the exploration of future energy scenarios according to a set of either technical constraints or policy-driven strategies.

Therefore, the TEMOA-Europe dataset includes a detailed techno-economic characterization for the construction of the existing RES in the base year and for its future development, socio-economic trends, constraints for the availability of resources (including limits for both extraction and import) and user-defined constraints for the generation of alternative scenarios, e.g., CO_2 emission

trajectories. Taking advantage of the involvement in the EUROfusion WPSES for the maintenance and development of ETM, which is not fully accessible to the general public for the time being, TEMOA-Europe and ETM present a similar structure.

This section presents the general structure of TEMOA-Europe, along with the novelties purposedly developed to enhance the TEMOA framework and adopted in the model itself. Indeed, the original TEMOA source code already included a large set of parameters and constraints, but they have been enhanced or integrated with additional features within the MAHTEP Group at Politecnico di Torino [188]. The full TEMOA-Europe database in the version produced for this work is available at [189], along with a preprocessing file to reduce the manual compilation of the database.

3.1 Spatial scale, time scale and treatment of time

The spatial scale under consideration in TEMOA-Europe includes 26 out of the 27 EU Member States (excluding Croatia), the EFTA countries (Iceland, Liechtenstein, Norway and Switzerland) and the United Kingdom, as visible in **Figure 22**. The mentioned countries are gathered into a single region, therefore sharing a single set of socio-economic drivers and the same features for all the technologies included in the database. For that reason, results cannot be analyzed for individual countries, as it happens instead in the JRC-EU-TIMES [63] including a different characterization for all the EU countries.

In order to perform future projections, the long-term TEMOA-Europe time scale (from 2005 to 2100) is articulated over several time steps: 2005, 2010, 2015, 2020, 2025, 2030, 2035, 2040, 2050, 2060, 2070, 2080 and 2100. The time periods resolution is chosen to be less refined by the end of the time horizon because of the higher degree of uncertainty about driver projection.

While the annual value of each final service demand of the model is known at the base year and projected using exogenous drivers and elasticities, the intra-annual distribution of the demand is also important to consider seasonal and daily variations of environmental conditions that affect the energy demands. The subdivision of each milestone year into more refined time slices is performed in TEMOA-Europe considering three seasons (intermediate, summer, winter) and three times of day (day, night and peak), leading to 9 time slices per year. A percentage of the total time of the year is assigned to each time-slice, as reported

in **Table 28**. The time repartition among the seasons is uniform (25% of the total time of year per season), while it reflects the different duration of day and night in summer and winter.

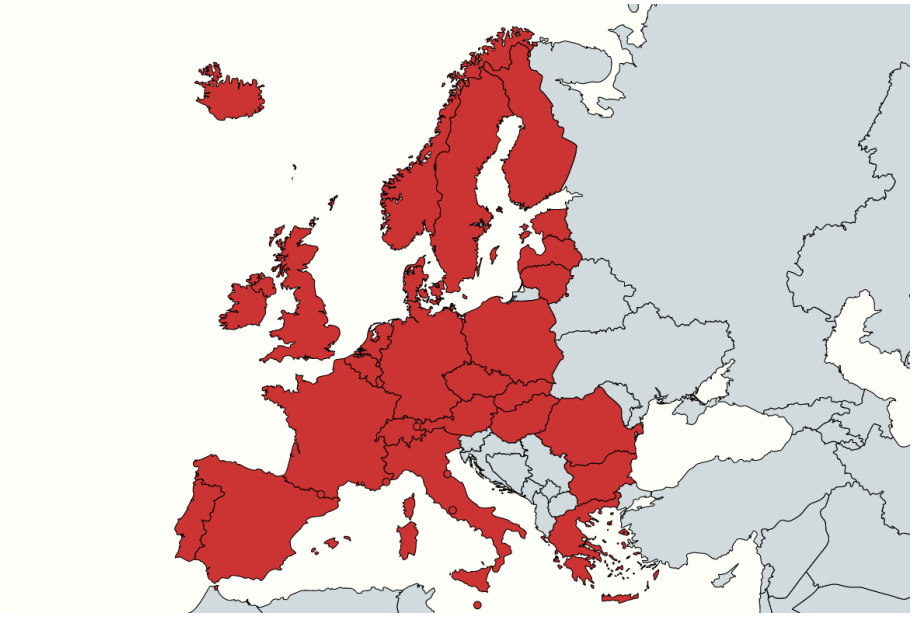

Figure 22. Countries included in the TEMOA-Europe energy statistics.

Table 28. Subdivision of the time scale of each milestone year among seasonal and daily time slices in TEMOA-Europe.

Season / Time of Day	Intermediate	Spring	Summer
Day	19.0%	19.0%	18.8%
Night	9.4%	9.4%	9.4%
Peak	5.0%	5.0%	5.0%

Final service demands could be distributed among the time-slices according to different proportions with respect to those shown in **Table 28** to consider their possible significant dependence on environmental conditions. For instance, that is crucial for lighting and thermal energy in buildings, being lighting demand influenced by the time of day and space heating and cooling strongly dependent

on the season of the year. Such an unbalanced time distribution of demands among the time-slices implies that an overcapacity of technologies producing them is installed, since the energy system must be able to satisfy the demands in all the time-slices (due to the application of inelastic demands, thus not affected by price variations). At the current state of development of TEMOA-Europe all the demands are considered simply on an annual basis, due to their effect on the computational cost. Therefore, intra-annual optimization is now limited to power production, e.g. from renewable energy sources considering their different availability in the different time slices, using a variable capacity factor. To examine in detail also the role of, e.g., storage technologies coupled with renewable energy plants, additional developments of TEMOA-Europe would consider more refined time representation.

3.2 Reference Energy System

The TEMOA-Europe RES is represented in a schematic version in **Figure 23**. It encompasses all the steps between primary commodity production and import and the satisfaction of energy service demands. **Figure 23** also reports the number of both existing (base year) and new technologies included in the TEMOA-Europe RES.

The upstream sector considers the extraction from reserves of fossil fuels (heavy oil, oil sands, natural gas, brown coal, hard coal), uranium and lithium and the availability of primary renewable potential from hydroelectric, geothermal, solar, tide, wave, wind and biomass (including ethanol production from crop, solid biomass, industrial biowaste, municipal wase, renewable biogas and liquid biofuels) sources. Extracted fossil resources are then processed and transformed for use in energy technologies. The upstream sector also includes the hydrogen value chain characterized in **Section 2.4**. In parallel, fossil fuel commodities – oil, gas, liquified natural gas (LNG) and hard coal – can also be imported from abroad.

Fossil fuels, renewable commodities and hydrogen in output from the upstream sector can be either used for power generation or directly adopted in end-use sectors. The power sector considers heat and electricity production plants (including cogeneration) and electricity imports. Also heat and electricity (from centralized and decentralized plants) can be used in end-use sectors (agriculture, commercial, residential, transport and industry). End-use sectors serve a set of end-use demands specified along the entire model time horizon (from 2005 to

2100), as described afterwards in **Section 3.5**. In particular, agriculture is modeled through a single technology aggregating agricultural energy uses. The commercial sector satisfies space heating, space cooling, water heating, refrigeration, cooking, lighting, other non-specified energy uses and electric office equipment demands. Similarly, the residential sector accounts for the satisfaction of space heating, space cooling, water heating, dish washing, clothes washing, clothes drying, refrigeration, cooking, lighting and other electricity use demands. As shown in **Section 2.1** and **Section 2.2**, the transport sector includes road (cars, light commercial vehicles. light trucks, medium trucks, heavy trucks, buses two-wheelers and three-wheelers) and non-road (aviation, trains and navigation) transportation technologies satisfying demands in terms of driven distance, besides non-energy uses, modeled according to a single technology consuming oil-derived lubricant. Also industrial technologies include energy services (steam boiler, process heat, machine drive, electro-chemical processes, feedstock for the chemical sector and other energy uses) production to feed the energy-intensive industrial subsectors described in **Section 2.3**, which satisfy demands in terms of production of industrial materials, and namely steel and ferroalloys in the iron and steel subsector; alumina, aluminum, copper and zinc in the non-ferrous metals subsector; HVCs, ammonia, methanol, chlorine and other minor chemical products in the chemical subsector; paper in the pulp and paper subsector; cement, glass and ceramics in the non-metallic minerals subsector. Also other industries, non-specified industrial energy use and non-energy uses are modeled according to a single aggregated process (as in the case of the agriculture sector), each satisfying a single demand.

Moreover, a sequestration module on the example of that modeled in ETM is present to take into account the possibility to store and utilize CO_2 instead of just venting it. Indeed, some technologies characterized for the power and the industrial sector are able to capture CO_2. Then, that can either contribute to the total levels of CO_2 emissions computed by the tool or be stored/absorbed, considering afforestation and reservoirs (onshore/offshore enhanced oil recovery, onshore/offshore depleted oil fields, offshore gas fields, enhanced coalbed methane recovery, onshore/offshore deep saline aquifers, mineralization and storage in the deep ocean). While details about this section of the model are visible in the TEMOA-Europe database, the presence of a sequestration module eases the realization of low-carbon scenarios providing alternatives for the decarbonization process (instead of the use of low- or zero-emission technologies alone), as long as CCS is considered available in the represented scenario.

All in all, more than 1200 technologies (including ~150 fictitious technologies to group commodities in output from the upstream and the power sector and ease the allocation to the different end-use sectors and the electricity generation sector, too) and ~360 commodities (300 physical commodities representing energy carriers, energy services, materials and 44 demand commodities, besides emission commodities used to represent CO_2 and CH_4 outputs in the different sectors of the RES) are included in TEMOA-Europe.

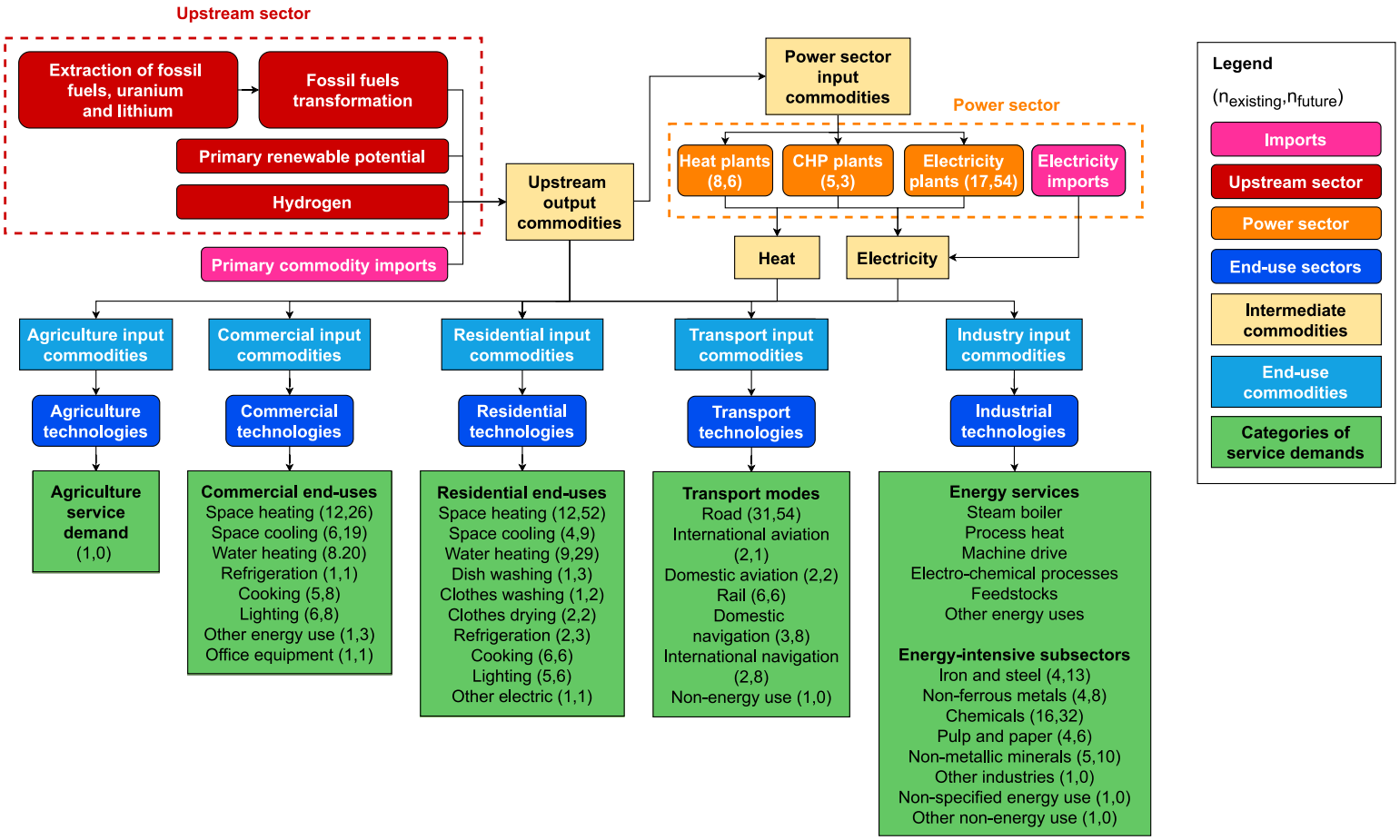

Figure 23. TEMOA-Europe Reference Energy System.

3.3 The optimization problem

The optimization problem solved by TEMOA is comparable to the primal model solved by TIMES [190] and is able to compute the optimal values for the decision variables of the linear programming (LP) problem (e.g. activity level of technologies or new capacity additions), while the dual solution of a TIMES model computes marginal costs assigned to each constraint of the primal problem. Therefore, TEMOA-Europe is based on the minimization of the objective function, which expresses the total cost of total discounted cost of the energy system C_{tot}. The total cost of the system is computed through **Equation 10** according to the discounted sum (through the parameter GlobalDiscountRate [56]) of the cost values – investment cost (M€/cap), fixed (M€/cap) and variable (M€/act) O&M costs – of each technology t selected in the optimal technology mix for the whole considered time scale (considering costs encountered in all periods p, vintages v, seasons s and times of day d). It has to be highlighted that base year technologies are considered as already completely paid off, thus investment costs can be just associated to new technologies. While the investment cost and the fixed O&M cost are proportional to the installed capacity ($Cap_{t,v}$) of a technology, the variable O&M cost is proportional to the total flow of output commodities ($FO_{p,s,d,i,t,v,o}$, where the index i represents input commodities and o represents output commodities). DiscountRate is the technology-specific discount rate (or hurdle rate).

$$\begin{aligned} C_{tot} = \text{GlobalDiscountRate} \cdot & \sum_{t,v} \left(\text{CostInvest}_{t,v} \cdot \text{DiscountRate}_{t,v} \cdot \text{Cap}_{t,v} \right) \\ & + \sum_{p,t,v} \left(\text{CostFixed}_{p,t,v} \cdot \text{DiscountRate}_{t,v} \cdot \text{Cap}_{t,v} \right) \\ & + \sum_{p,t,v} \left(\text{CostVariable}_{p,t,v} \cdot \text{DiscountRate}_{t,v} \cdot \sum_{s,d,i,o} FO_{p,s,d,i,t,v,o} \right) \end{aligned} \quad 10$$

3.4 Techno-economic parameters

A list of the main parameters involved in the construction of the database containing the techno-economic characterization of the RES in TEMOA-Europe is provided in **Table 29**, reporting the parameters description and their names in

TEMOA. In particular, 3 categories of parameters are included in the TEMOA formulation:

- Labels used for internal database processing identify the different kinds of commodities (physical, demand, emissions) and technologies ("supply-side" or "demand-side" sectors), and the belonging of each time period to the set of "existing" or "future" years. More in detail, existing (historical) periods represent a base for the model where the energy system configuration at a certain point in time can be defined and has no freedom neither associated investment costs as the existing technologies are already present in the energy system when the analysis begins. Existing periods are also used to calibrate the energy-use features of the technologies included in the model, based on energy statistics. Future periods, on the other hand, represent the optimization horizon in which the total cost of the system has to be minimized. In the case of TEMOA-Europe, the base year is the only existing year.
- Sets associate definite entities to the labels mentioned above. In TEMOA there are mainly four kinds of sets: periods, sub-annual "time slices", technologies, and energy commodities. Periods require to assign the definition of the milestone years considered as representative of each period. Then, sub-annual time slices subdivide each period into portions of the day (day, night, and peak) and seasons of the year in order to better tune the model of the supply part of the RES under exam. Indeed, production features of some technologies (e.g., renewable plants) can strongly vary according to the seasonal or daily time slices in which they operate. The technologies set contains the definition of all the possible energy technologies that the model can build, and the commodity set contains the definition of all the input and output forms of energy that the different technologies consume and produce.
- Parameters can be used to define processes or constraints, thus, to assign techno-economic features, or to assign upper or lower bounds for the evolution of technologies.

Besides the standard parameters and equations implemented in the TEMOA framework and accurately treated in [56], the development of TEMOA-Italy [92] and TEMOA-Europe within the MAHTEP Group at Politecnico di Torino required the expansion of the model capabilities, including thus new parameters and features to enhance the accuracy in the techno-economic description of the technologies belonging to the RES.

Table 29. Main items included in TEMOA. The new/modified parameters are in bold.

Category	Description	TEMOA name
Labels used for internal database processing	Commodity category	commodity_labels
	Technology category	technology_labels
	Time period labels	time_periods_labels
Sets	Commodity names	commodities
	Technology names	technologies
	Milestone years	time_periods
	Seasons of the year	time_season
	Time periods of the day	time_of_day
Parameters used to define processes	Discount rate	GlobalDiscountRate
	Demands	**Demand**
	Efficiency	Efficiency
	Existing capacity	ExistingCapacity
	Capacity factors	CapacityFactor CapacityFactorTech CapacityFactorProcess
	Capacity to activity	Capacity2Activity
	Fixed O&M cost	CostFixed
	Investment cost	CostInvest
	Variable O&M cost	CostVariable
	Emission factors	**CommodityEmissionFactor** **EmissionActivity**
	Economic lifetime	LifetimeLoanTech
	Technical lifetime	LifetimeTech LifetimeProcess
Parameters used to define constraints	Minimum capacity constraint	MinCapacity
	Maximum capacity constraint	MaxCapacity
	Minimum activity constraint	MinActivity
	Maximum activity constraints	MaxActivity
	Minimum activity for technology groups	MinGenGroupTarget
	Maximum activity for technology groups	**MaxActivityGroup**
	Minimum capacity for technology groups	**MinCapacityGroup**
	Maximum capacity for technology groups	**MaxCapacityGroup**
	Maximum production across time periods	**MaxResource**
	Share of input commodity	TechInputSplit
	Minimum commodity input share for technology groups	**MinInputGroup**
	Maximum commodity input share for technology groups	**MaxInputGroup**
	Share of output commodity	TechOutputSplit
	Maximum commodity output share for technology groups	**MaxOutputGroup**

The first new parameter and the associated equation implemented in the TEMOA model formulation is the annual capacity factor, used to connect the technology capacity (Cap) to its activity (Act), according to **Equation 11**. The capacity-to-activity (Capacity2Activity) factor, representing a conversion factor from capacity to activity unit of measurement and especially useful for electricity production technologies, is also included in the evaluation.

$$(\text{CapacityFactor} \cdot \text{Capacity2Activity}) \cdot \text{Cap} \geq \text{Act} \qquad 11$$

While the activity represents the total flow of output commodities from a technology (e.g., the activity of a power plant is the energy produced during the year in PJ, the activity of industrial facilities is the total periodical production in terms of demand commodity and by-products in Mt, etc.), the capacity of a technology can be defined as its nominal production capability as if it was continuously operated at full load. The capacity of a power plant is for instance its nominal installed power in GW while the activity corresponds to the actual electricity output in PJ; on the other hand, the capacity of industrial facilities is the maximum production capability in Mt, while the activity is the actual production output, always accounted for in Mt. The capacity factor is used to account for the unavailability periods of technology, due to unavailability of its input energy resources or to maintenance. Capacity2Activity represents the maximum annual energy producible if the plant was constantly operated at its nominal power, and it is evaluated according to **Equation 12** for electricity generation technologies, while is usually equal to 1 for all the other technologies sharing the same capacity and activity units.

$$\text{Capacity2Activity} = 8760\left(\frac{\text{h}}{\text{y}}\right) \cdot 3600\left(\frac{\text{s}}{\text{h}}\right) \cdot 10^{-6}\left(\frac{\text{PJ}}{\text{GJ}}\right) = 31.536\left(\frac{\text{PJ}_\text{a}}{\text{GW}}\right) \qquad 12$$

The LifetimeTech (assigned to technologies with constant lifetime along the time scale) and the LifetimeProcess (indexed by time period, so possibly different according to the time period in which the technology is installed) parameters are used to define the technical lifetime of a technology.

Moreover, some operations can be automated to guarantee a manageable database compilation, like the data interpolation/extrapolation and the computation of technology-specific emission factors. An automatic algorithm was developed [191] to perform a preprocessing on the database file (manually

compiled), including all the descriptive parameters of the RES. The new functions implemented to automatically preprocess the data to obtain the desired RES description consist of:

An automatic interpolation and extrapolation process (totally missing in the original TEMOA version [192], that requires the manual specification of the parameters for all the time periods included in the optimization process), performing the same operations encompassed in, e.g., the TIMES framework. This feature, including the option of setting different interpolation and extrapolation rules for different parameters in the Excel files, is automatically executed by the software. In particular, it is possible to assign interpolation/extrapolation options to the parameters included in the TEMOA database to set: 1) the interpolation type (linear or log-linear); 2) whether interpolation only or also extrapolation should be operated; and 3) whether extrapolation should be performed backward or forward. **Table 30** lists the parameters for which interpolation and extrapolation are required, specifying the applied rule. For the technology lifetime, a piecewise constant interpolation curve has been chosen, to maintain an integer value for the parameter. Note that the constraints applied to technology groups (rather than to single technologies) – and namely MaxGenGroupLimit, MinGenGroupTarget, MinInputGroup, MaxInputGroup and MaxCapGroupLimit are only linearly interpolated, but not forward extrapolated, as it happens for the other parameters. These integrations strongly simplify the database construction and its modification, allowing to build larger and more complex RESs.

The automatic evaluation of the technology-specific emission factors, which are implemented in TEMOA through the dedicated parameter EmissionActivity, proportional to the technology activity. A parameter representing the emission factors per unit of commodity consumed (CommodityEmissionFactor) has been added to the database, and the operation performed in the preprocessing script (reported in **Equation 13**) is the sum of the contribution of the Commodity-based Emission Factor CEF, divided by the efficiency of the technology to obtain the correspondent emission factor per unit of output, plus additional process-related emission factor TEF possibly associated to a technology.

$$\text{EmissionActivity}\left(\frac{\text{kt}}{\text{act}}\right) = \frac{1}{\text{Efficiency}\left(\frac{\text{act}}{\text{PJ}}\right)} \cdot \text{CEF}\left(\frac{\text{kt}}{\text{PJ}}\right) + \text{TEF}\left(\frac{\text{kt}}{\text{act}}\right) \qquad 13$$

Table 30. Interpolation/extrapolation rules implemented in the preprocessing Python script.

Parameter	Interpolation/Extrapolation Rule		
	Piecewise Constant Interpolation	**Piecewise Linear Interpolation**	**Forward Constant Extrapolation**
LifetimeProcess	×		×
Efficiency		×	×
TechInputSplit		×	×
TechOutputSplit		×	×
EmissionActivity		×	×
CostInvest		×	×
CostFixed		×	×
CostVariable		×	×
MaxActivity		×	×
MaxGenGroupLimit		×	
MaxCapacity		×	×
MinActivity		×	×
MinGenGroupTarget		×	
MinCapacity		×	×
MaxInputGroup		×	
MaxOutputGroup		×	
MinInputGroup		×	
MaxCapGroupLimit		×	
CapacityFactor		×	×
CapacityFactorProcess		×	×
CapacityCredit		×	×

3.5 Demand projection

In TEMOA-Europe, the expected levels of energy service demands are projected along the analyzed time horizon according to socio-economic drivers. The future projection of energy service demands is performed according to **Equation 14**, where Demand_t and Demand_{t-1} and the service demand levels at time step t and $t-1$, respectively, δ_t and δ_{t-1} are the driver values at time step t and $t-1$, respectively, while e_t is the elasticity of the driver to the demand, associated to the time step.

$$\mathrm{Demand}_t = \mathrm{Demand}_{t-1} \cdot \left[1 + \left(\frac{\delta_t}{\delta_{t-1}} - 1\right) \cdot e_t\right] \qquad 14$$

Elasticities of such kind are usually adopted to correct demand projections in order to capture changing patterns in energy service demands in relation to socio-economic growth, such as a saturation in some energy end-use demands, increased urbanization, or changes in consumption patterns once the basic needs are satisfied [16]. Driver projections along the whole time horizon taken from the International Energy Outlook 2021 [193] are implemented in the TEMOA formulation and included in the TEMOA-Europe database preprocessing script, also available at [189]. In the ESOM context, other elasticities may be used to adapt demand for energy services to the computed price of the commodities involved in the energy system under analysis. Such parameters, either called "price elasticities" or "elasticities of substitutions", can be implemented in TIMES [16] and have also been tested in TEMOA [194]. However, they are not adopted in TEMOA-Europe for the time being. The demand constraint is the most important TEMOA equation as demands for all the energy services included in the model must be exactly met (no overproduction) at each time step. All the categories of service demands that must be satisfied in TEMOA-Europe, along with the drivers to be used in **Equation 14** throughout the time scale, are listed in **Table 31**. The specific driver and elasticity values for each time period, as well as the base year demand level, instead, are reported in detail in the TEMOA-Europe database at [189].

3.6 Constraints

Constraints are used in TEMOA-Europe to 1) define existing capacity for technologies already present in the model base year and their progressive disposal along the time scale and 2) to implement technical, economic and environmental constraints for the future evolution of the energy system.

Besides constraints already implemented in TEMOA to limit the adoption of single technologies either based on their installed capacity or their activity (MaxCapacity and MaxActivity, respectively), some new features have been developed in [92] to enhance the representation of the energy system. As far as the residual capacity of an existing technology (already installed in the base year) is concerned, the existing capacity of a certain technology at the base year should be set, together with its residual capacity evolution in time. The evolution in time of that capacity is generally linear starting from the base year value and goes to

zero after a certain time interval to model the disposal of the existing technology in time (according to their lifetime) and to allow the substitution by new technologies. A constraint for a progressively decreasing maximum activity MaxActivity (linearly decreasing along time) is assigned to all the existing technologies forecasting substitution with new technologies contributing to the generation of the same output and therefore calling for investments in new capacity, i.e. all end-use base year technologies and those belonging to the power sector.

Table 31. Categories of service demands and associated drivers in TEMOA-Europe.

Sector	Service demand	Driver
Agriculture	Agriculture service demand (PJ)	Value added agriculture sector
Commercial	Space heating (PJ)	Value added services
	Space cooling (PJ)	Value added services
	Water heating (PJ)	Value added services
	Refrigeration (PJ)	Value added services
	Cooking (PJ)	Value added services
	Lighting (PJ)	Value added services
	Other energy use (PJ)	Value added services
	Office equipment (PJ)	Value added services
Residential	Space heating (PJ)	Average number of households
	Space cooling (PJ)	GDP per household
	Water heating (PJ)	Population
	Dish washing (PJ)	GDP per household
	Clothes washing (PJ)	GDP per household
	Clothes drying (PJ)	GDP per household
	Refrigeration (PJ)	GDP per household
	Cooking (PJ)	Population
	Lighting (PJ)	GDP per capita
	Other electric (PJ)	GDP per household
Transport	Cars (Bvkm)	GDP per capita
	Light commercial vehicles (Bvkm)	GDP
	Light trucks (Bvkm)	GDP
	Medium trucks (Bvkm)	GDP
	Heavy trucks (Bvkm)	GDP
	Buses (Bvkm)	Population
	Two-wheelers (Bvkm)	GDP
	Three-wheelers (Bvkm)	GDP
	Passenger trains (Bpkm)	Population

	Freight trains (Bfkm)	GDP
	Domestic aviation (Bvkm)	GDP
	International aviation (Bvkm)	GDP
	Domestic navigation (Bvkm)	GDP
	International navigation (Bvkm)	GDP
	Non-energy use (PJ)	GDP
Industry	Iron and steel (Mt)	Value added metals production
	Non-ferrous metals (Mt)	Value added metals production
	Chemicals (Mt)	Value added chemical sector
	Pulp and paper (Mt)	Value added other energy-intensive sectors
	Non-metallic minerals (Mt)	Value added other energy-intensive sectors
	Other industries (PJ)	Value added other industries
	Non-specified energy use (PJ)	GDP
	Other non-energy use (PJ)	GDP

To allow the definition of the maximum available resource potential for fossil fuels, uranium and CO_2 sinking in the region under investigation, the MaxResource parameter is defined in [188]. With respect to the original formulation of the parameter [192] which imposed an upper bound to the summation of the resulting activity of a technology for each time period, the multiplication by the length of each time period is now added in the sum operator to correctly account for the relative weight of each milestone year to the total cumulative activity (see **Equation 15**).

$$\sum_{i=t_{first}}^{t_{last}} Act_i \cdot \Delta t_i \leq MaxResource \qquad 15$$

New constraints on technology groups have also been implemented in the TEMOA framework [92]. The maximum total activity is used to set an upper bound to the total activity of a group of technologies (see **Equation 16**) in the new constraint is MaxActivityGroup, developed similarly to the analogous constraint for the minimum activity of a group of technologies MinGenGroupTarget, already included in TEMOA and redefined as MinActivityGroup for this work. Following the same principle, two new constraints were developed to impose limits on the capacity development for

groups of technologies. That was needed to allow the applications of the capacity curves for electricity generation technologies designed in Section 3.6.1 below. Therefore, MaxCapacityGroup and MinCapacityGroup were developed according to Equations 17 and 18. Moreover, new constraints on commodity shares have been developed to set the minimum (MinInputGroup, see **Equation 19**) or maximum (MaxInputGroup, see **Equation 20**) percentage that can be assigned to a certain commodity in input to a technology group ($\mathrm{commodity}_{\mathrm{in,group}}$) or the maximum (MaxOutputGroup, see **Equation 21**) in output from a technology group ($\mathrm{commodity}_{\mathrm{out,group}}$). Those constraints are very similar to the already implemented TechInputSplit and TechOutputSplit constraints, with the difference that they are applied to technology groups, while TechInputSplit and TechOutputSplit are applied to single technologies, imposing a minimum share to their input and output commodities.

$$\sum_{\text{tech in group}} \mathrm{Act}_{\mathrm{tech}} \leq \mathrm{MaxActivityGroup} \tag{16}$$

$$\sum_{\text{tech in group}} \mathrm{CapacityAvailableByPeriod}_{\mathrm{tech}} \leq \mathrm{MaxCapacityGroup} \tag{17}$$

$$\sum_{\text{tech in group}} \mathrm{CapacityAvailableByPeriod}_{\mathrm{tech}} \geq \mathrm{MinCapacityGroup} \tag{18}$$

$$\frac{\mathrm{commodity}_{\mathrm{in,group}}}{\sum_{\mathrm{i}} \mathrm{commodity}^{\mathrm{i}}_{\mathrm{in,group}}} \geq \mathrm{MinInputGroup} \tag{19}$$

$$\frac{\mathrm{commodity}_{\mathrm{IN,group}}}{\sum_{\mathrm{i}} \mathrm{commodity}^{\mathrm{i}}_{\mathrm{in,group}}} \leq \mathrm{MaxInputGroup} \tag{20}$$

$$\frac{\mathrm{commodity}_{\mathrm{OUT,group}}}{\sum_{\mathrm{i}} \mathrm{commodity}^{\mathrm{i}}_{\mathrm{out,group}}} \leq \mathrm{MaxOutputGroup} \tag{21}$$

3.6.1 Maximum capacity curves for electricity generation technologies

The formulation of educated constraints for TEMOA-Europe concerning the electricity generation sector is necessary due to the special focus dedicated to nuclear fusion. Moreover, Europe represented one of the largest electricity producers in the world (more than 4 PWh in 2021, behind North America and the Asia Pacific area) generating more than 1 Gt CO_2 in 2021 [26]. Electricity generation represented the 16% of the total energy supply (TES) worldwide in 2019 [195], with a 30% reduction with respect to 2010 levels. The increasing electrification shares of end-use sectors to address climate change issues and fulfil decarbonization targets worldwide are driving a massive boost in electricity production [196], with a total generation more than doubled between 1990 and 2019 [195]. However, this growing tendency is not visible in Europe: whereas a continuous growth in electricity generation was experienced starting from the second half of the 1990s until the outbreak of the 2008 financial crisis [197], the subsequent retirement of traditional fossil plants and the simultaneous growing investments in renewable energy started modifying the generation matrix, keeping however electricity production levels quite stable in the last ten years [195], as also visible from **Figure 24**. Nonetheless, electricity generation levels are expected to increase in the near future, and at least a shift towards non-fossil sources for end-use energy services can be expect for the next decades [198]. In this framework, it is important to understand whether this change would be coupled to an adequate structure of the current electricity sector assessing, for instance, possible gaps in the future electricity generation.

The approach using "S-curves" to describe technology adoption is the most widely used in the literature, spreading in the more diverse disciplinary fields and validated against technology diffusion pathways in a variety of sectors, from domestic appliances to computers, cell phones and the internet [199] over the last century. In [200], innovation is compared to the spreading of epidemics, in which the limit to the speed of adoption is the lack of information about anything new. Concerning the electricity generation sector, the S-curve approach is adopted in [201] to fit growth models of wind onshore and solar photovoltaic (PV) technologies in different countries. The methodology is based on the Logistic model [202] and the Gompertz model [203], and the evolution of wind and solar production is modeled according to 4 phases (pre-take-off, take-off, stalling and stability). The fitting parameters are established according to statistical variables representing drivers for the take-off and

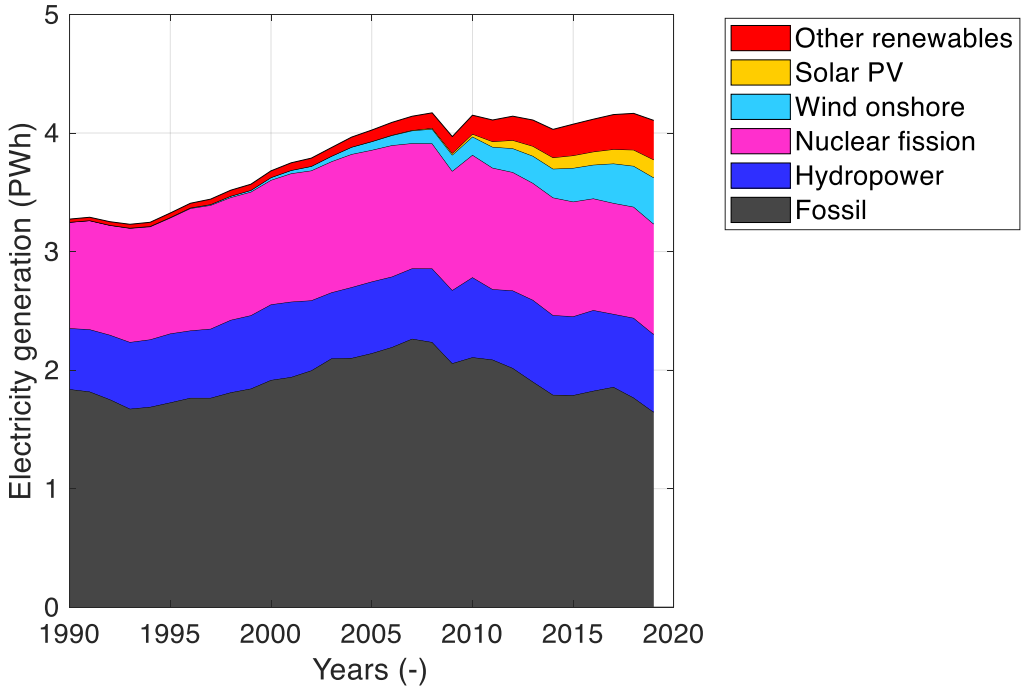

Figure 24. Historical trend for European electricity generation by source.

the maximum achievable growth in a certain region like, e.g., the share of nuclear power, being member of the European Union, the electricity demand growth rate, etc.. Historical data are often used as basis to adopt S-curve forecasting approaches, like in the case of [204] to compute the evolution of electric vehicle uptake across countries in England: an exponential model depending on time and parameters based on speed and shape of the transition towards a full electric vehicle fleet is presented. The typical technological S-curve, sketched in **Figure 25**, usually reports time on the x-axis and quantity on the y-axis. However, elapsed time is sometimes replaced as the relevant parameter by the amount of economic effort put into development [205] or the engineering effort (e.g. number of working hours, allocated budged, employed researchers, etc.) needed for the improvement of technological performances [206]. Whereas the use of time as independent variable is claimed to be erroneous in [207], it is often used in empirical models as data for establishing investment levels are difficult to be retrieved [206]. In general, three phases are identified in technological development: 1) embryonic, 2) growth and 3) maturity (and ageing) [205], supporting the validity of the three-phase sketched model in **Figure 25**. Indeed, the embryonic phase cannot be skipped as time and

experience are needed to develop and enhance technologies, and to deploy sufficient industrial capacity to support a growth phase [208]. In this work, the embryonic phase is associated to a "revolutionary" development phase characterized by fast (exponential) growth, the growth phase to an "evolutionary" phase of linear capacity deployment, while "maturity" to a phase of slow or null growth. The nomenclature "revolutionary", "evolutionary" and "mature" adopted here is borrowed from the experience curve model adopted in the National Energy Modeling System (NEMS) by the U.S. Energy Information Administration [209].

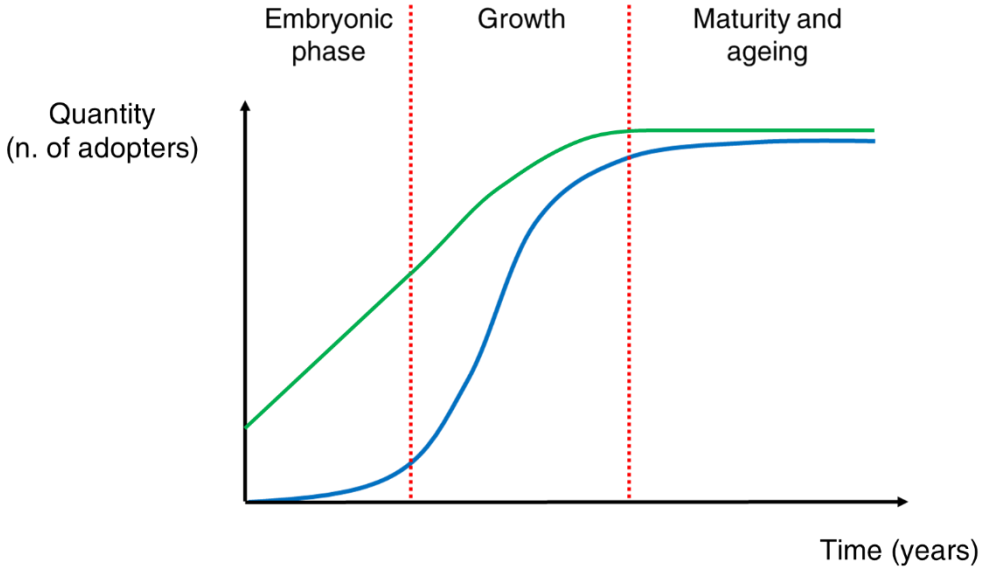

Figure 25. Typical shape of the S-curve for technology adoption, represented both in linear and logarithmic scale on the y-axis.

In [208], these observations were used to formulate a mathematical growth model in three phases:

- exponential growth with doubling of installed capacity every 2 – 4 years. In this phase, described by **Equation** 22, the technology is taken from laboratory scale to a level of visibility in the global energy mix (identified as "materiality" state [210]), supposed to be reached at 0.1-1% of the contribution to total energy supply;

$$P_t = P_{sat} \cdot \frac{\tau_{exp}}{\tau_{life}} \cdot \left[\exp\left(\frac{t - t_{trans}}{\tau_{exp}}\right) - \exp\left(\frac{t - t_{trans} - \tau_{life}}{\tau_{exp}}\right) \right] \qquad 22$$

$$\text{for } t < t_{trans}$$

where P_t is the capacity at time t, P_{sat} is the asymptotic capacity level in the saturated state, τ_{exp} is the characteristic time of exponential growth, computed according to **Equation** 23, τ_{life} is the characteristic lifetime of the electricity generation plants and computed again according to **Equation** 23, t_{trans} is the time at which the transition from the exponential to the linear phase occurs.

$$\frac{\tau_{exp}}{\text{doubling time}} = \frac{\tau_{life}}{\text{technology lifetime}} = (1 + 1/e) \qquad 23$$

- linear growth, described by **Equation** 24.

$$P_t = P_{sat} \cdot \frac{\tau_{exp}}{\tau_{life}} \cdot \left[1 + \frac{t - t_{trans}}{\tau_{exp}} - \exp\left(\frac{t - t_{trans} - \tau_{life}}{\tau_{exp}}\right)\right] \qquad 24$$

$$\text{for } t_{trans} \leq t \leq t_{sat}$$

Note that, despite the definition of "linear" phase provided in [208], **Equation 24** actually includes also non-linear terms.

- saturation phase when the growth is stopped and the level of installed capacity remains fixed, as described by **Equation** 25.

$$P_t = P_{sat} \qquad \text{for } t > t_{sat} \qquad 25$$

The model is based on the fundamental that the rate of deployment, i.e. the number of plants installed each year, is equivalent to the industrial capacity, i.e. the capacity of the industry to produce plant components, to transport and install them, so that this includes workforce, logistics and the factories to produce plant components.

Based on the observations made in [208], the aim of the methodology developed in [52] is to present a method based on the three phases of the S-curve in **Figure 25** and on the available historical data to forecast the deployment of electricity generation technologies. Through the forecast of future developments of the electricity sector technology capacities based on current trends, the work in [52] allows to identify possible gaps in future electricity generation until 2050 to be filled up by new technologies not yet visible on the radars of the electricity market (e.g.

nuclear fusion) or to raise awareness on the inadequacy of either the current installation rates of particular technologies or policies related to their development. The results of the projections are also validated against four IEA scenario results coming from the latest *World Energy Outlook* (WEO) *2021* [2] and the International Renewable Energy Agency (IRENA) *Transforming Energy Scenario* (TRES), examined in [19]. Here, instead, that method is replicated and extended to compute constraints for the maximum capacity development in TEMOA-Europe until 2100.

The method presented in [52] envisages three cases for the future development of the analyzed technologies: 1) extrapolation of historical data is performed in case maturity has been reached in the examined time frame; 2) a S-curve is depicted in case the technology has either shown the roll-over out of the embryonic phase or is still in its initial development stage and shows considerable growth; 3) in the last case, the technology shows not considerable growth despite being far from maturity, and a stagnation of the current capacity is taken into account. Please note that the analysis in [52] is based on a global scale and adapted here to the European context under exam.

3.6.2 Analysis of the historical installed capacity trends in the electricity generation sector

Figure 26 collects the behavior of installed capacity for ten categories of electricity generation plants over the last four decades at the European level. The considered categories include fossil, biomass, hydropower, nuclear fission, geothermal, wind onshore, wind offshore, solar PV, concentrated solar power (CSP) and marine plants. Note that, considering the validity of the S-curve model applied to electricity generation technologies**,** the different technological classes are clearly in different phases of their development throughout the analyzed time frame. In particular, looking at the trends for the categories fossil (including coal, oil and gas power plants), hydropower and nuclear fission in **Figure 26**, they should be associated to. Indeed, global capacity for those technologies is the highest among all sources and shows stable levels always well above 100 GW all over the most part of the last 40 years.

In particular, **Figure 26** shows how nuclear fission was experiencing a considerable growth in the first half of the 1980s; that trend was evidently interrupted in correspondence with the Chernobyl accident in 1986 [211] slightly above 100 GW. On the other hand, the Fukushima accident [212] in 2011 triggered a decreasing installed capacity trend also supported by political choices envisaging,

e.g., the planned nuclear phase-out in Germany [213].

On the other hand, a constantly growing trend is visible for biomass capacity, which has more than quadrupled in the last 20 years, with an average 8% yearly growth rate, corresponding to a doubling time slightly lower than 9 years. Also wind onshore and solar PV have been experiencing a clear growth trend, with far larger rates than the abovementioned biomass technological class. While wind onshore capacity increased by 15 times between 2000 and 2020, it showed a clearly slower growth in the last ten years, with a yearly growth rate well below 10%. Solar PV capacity increased by almost 800 times between 2000 and 2020, as visible in **Figure 26**, with a doubling time even lower than 2 years in the first decade of this century. It has also to be observed that a clear decline of this growth rate has happened after that, with a yearly growth rate that is constantly decreasing and is now around 10%. Other renewable technologies like solar CSP and marine are clearly in their initial development stage with stagnating capacity for the most part of the last two decades; on the other hand, geothermal capacity shows a trend of constant growth since the beginning of the century, but stays well below 10 GW installed capacity, with a doubling time close to 10 years; wind offshore is the only technology showing the clear increasing trend typical of a revolutionary/exponential growth among them, retracing a similar path as that observed for wind onshore.

3.6.3 Modeling future installed capacity trends for electricity generation technologies

The overall methodology for the definition of future maximum capacity trends adopted in TEMOA-Europe is based on **Figure 27** and articulated as described in the following bulleted list.

- Case 1: for technologies that are already in their maturity phase according to historical data for installed capacity (see **Figure 26**), showing a slow growth in the last 40 years and installed capacity above 100 GW in such time frame: the increasing trends for fossil and hydropower technologies over the last two decades suggest that the current industrial capacity is sufficient to support constantly growing capacity additions. However, policy commitments to phase out fossil fuels [7] or nuclear fission plants [214] cannot be recognized by this approach. Since historical data for the development in maturity phase are available here, that is modeled extrapolating the line of best fit of historical data to comply with the actual developments of the energy system (either according to an exponential trend

as in **Equation 26**, where the coefficients b and m are computed according to the Microsoft Excel function `LOGEST` [215], or to a linear trend as in **Equation 27**, where the coefficients m and q are computed according to the Excel function `LINEST` [216]), corresponding to the trend with the maximum coefficient of determination R^2 [217]. Nonetheless, trends for fossil and nuclear installed capacities would be dictated by policy choices more than either actual technological development or capability of the industry to support technological advancement.

$$P_t = b \cdot a^t \quad (26)$$

$$P_t = m \cdot t + q \quad (27)$$

- Case 2: for technologies showing exponential growth in **Figure 26** at the beginning of the available data set, with doubling times below 4 years for at least one decade and a roll-over between revolutionary and evolutionary phase, retracing the typical shape of a S-curve as from **Figure 25**. In this case, an exponential regression is generated in the revolutionary phase, which is identified in the period presenting the best fit of historical data with an exponential curve [217], using **Equation 26**. Then, the evolutionary phase of capacity growth according to a linear trend is modeled according to the linear interpolation between the YOY capacity growth rate at the end of the revolutionary phase and 0, which is the growth rate associated to the end of the evolutionary phase (with a duration computed using **Equation 23**). In the transition between the revolutionary and the evolutionary phase, the derivative of the installed capacity, i.e. the industrial capacity, is continuous, while the duration of the linear growth is limited by the maturity capacity level, as the duration of the evolutionary phase is limited by the assumption that it lasts for one characteristic lifetime of the technology. Case 2 responds to the representation in **Figure 27a**.
- Case 3: for technologies showing considerable growth in **Figure 26** at the beginning of the available data set, with doubling times below 4 years for at least one decade but no evident roll-over between revolutionary and evolutionary phase. In this case, an exponential regression is generated in the revolutionary phase using **Equation 26**, as in case 2. The end of the revolutionary phase is computed backwards considering the assumption that the evolutionary phase would end in 2050 (that means maturity is reached at that point), as no data show evidence for that. Therefore, the projection in

the evolutionary phase is already carried out as in case 2, corresponding again to the representation in **Figure 27b**.

- Case 4: for technologies showing slow growth over the most part of the time scale analyzed in **Figure 26**. In this case, a clear revolutionary phase cannot be identified at any point of the considered time frame as doubling times well above 4 years are computed from the whole set of historical data, therefore stagnation is taken into account for the whole time scale analyzed here. The best fit of historical data (according to a linear fashion as in **Figure 27c**) is used to extrapolate future capacity trends, as the typical shape of a S-curve cannot be retraced.

Figure 28 reports the flowchart for the application of the abovementioned method to forecast curves for the installed capacity of electricity generation curves.

The characteristic parameters used to perform installed capacity projections for Europe according to the abovementioned cases for the different technologies are listed in **Table 32**, while results of the application of the method to European data are shown in **Figure 29**.

Maximum fossil fuel capacity (see **Figure 29a**) is anticipated to increase by 25% in 2050 with respect to 2020 levels, reaching 650 GW. In 2100, instead, it would be increased by 67% with respect to 2020 getting to almost 900 GW. The same trend is observed for hydropower capacity (see **Figure 29a**), reaching almost 300 GW installed capacity by 2100. Eventually, nuclear fission capacity (see **Figure 29b**) shows a decreasing trend in line with the evolution in the last two decades, reaching less than 30 GW by 2100, even well below pre-Chernobyl levels. Although such result is in line with the recent policies considering phase-out or limits to nuclear fission capacity installations (even in countries leaders in the use of nuclear energy like France, that established a limit to bound nuclear contribution in the electricity mix to 50% and capacity to 63.2 GWe [221] by 2035), a decreasing growth trend imposed to a zero-emission technology category would represent a relevant factor for the decisions taken by the ESOM in the construction of the future electricity sector.

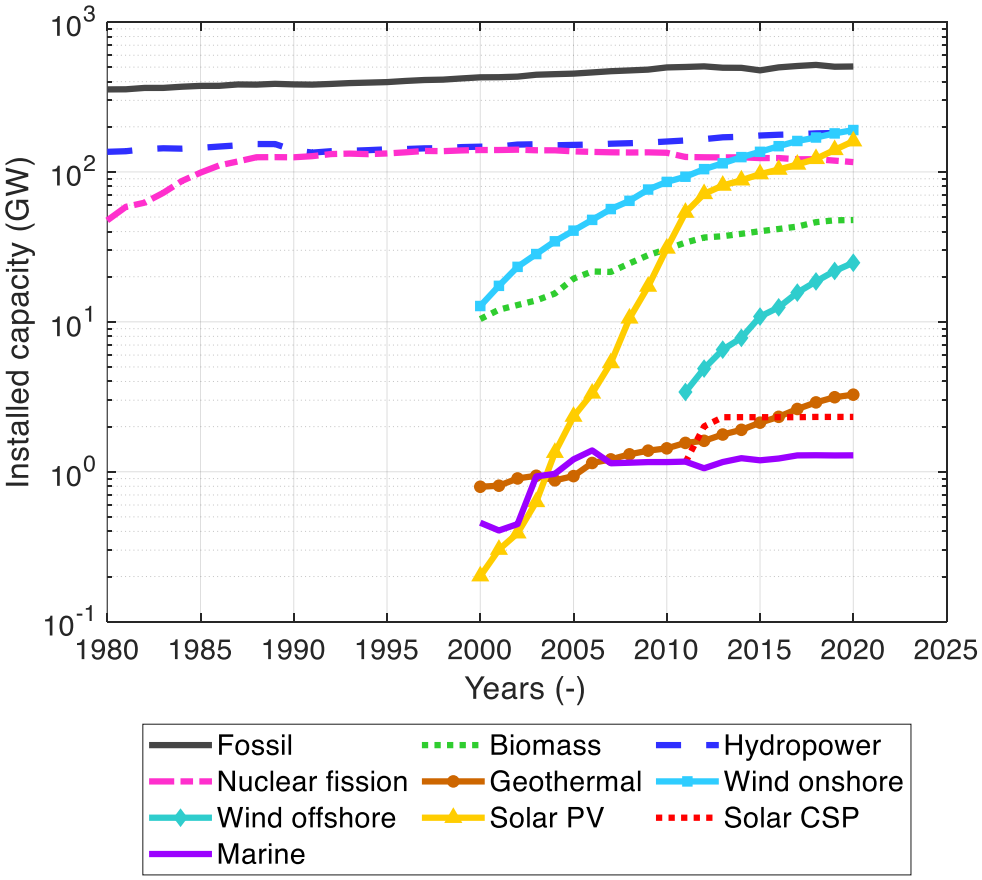

Figure 26. European trends for the installed electricity capacity 1980-2021 (according to data availability) for electricity generation technologies. Elaborated by the author based on [218], [219], [220].

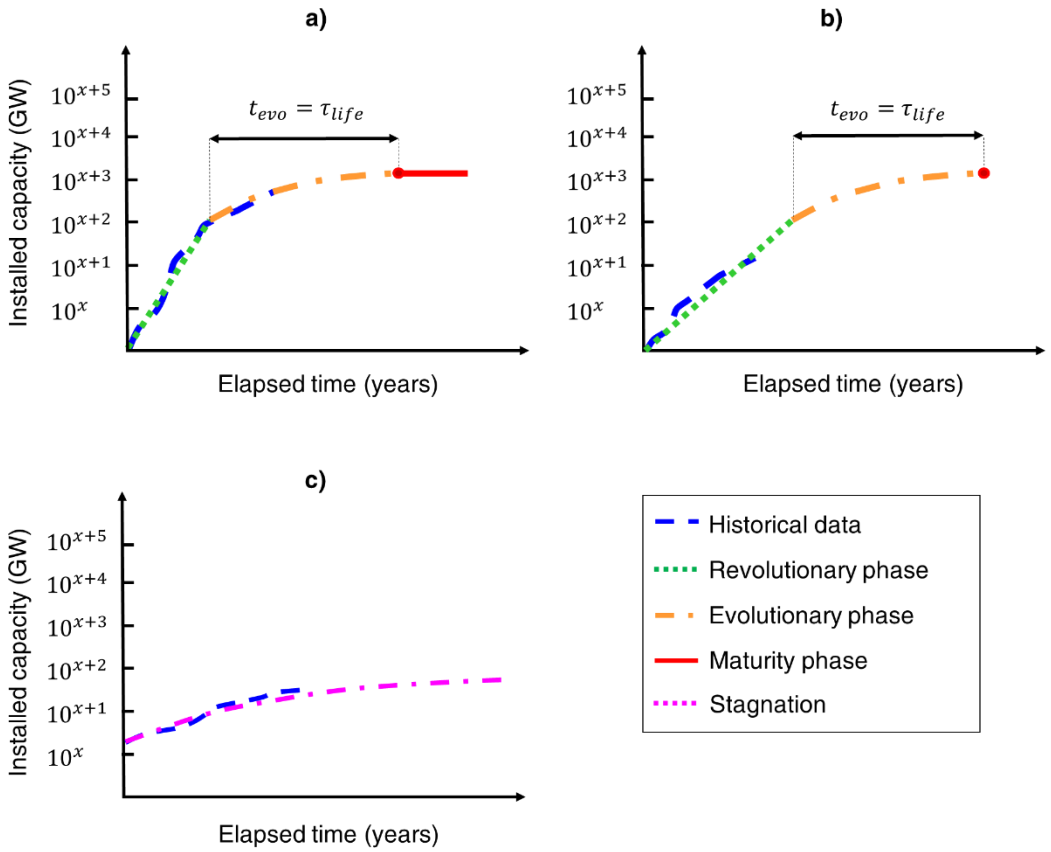

Figure 27. Technology development model to forecast capacity curve trends for electricity generation technologies.

Table 32. Characteristic parameters for technology capacity projections.

Technology	Case	R^2 (%)	b (GW)	a (-)	m (GW/year)	q (GW)
Fossil	1 (Equation 27)	96.2			4.32	341.5
Hydropower	1 (Equation 26)	76.6	133.5	1.006		
Nuclear fission	1 (Equation 27)	90.5			-1.12	144.5
Biomass	4 (Equation 27)	98.9			2.04	7.24
Geothermal	4 (Equation 26)	98.7	0.670	1.076		
Wind onshore	2	98.5	13.89	1.176		
Wind offshore	3	95.9	3.385	1.226		
Solar PV	3	90.7	26.49	1.179		
Solar CSP	4 (Equation 27)	78.0			0.0016	2.308
Marine energy	4 (Equation 27)	76.8			0.0251	1.098

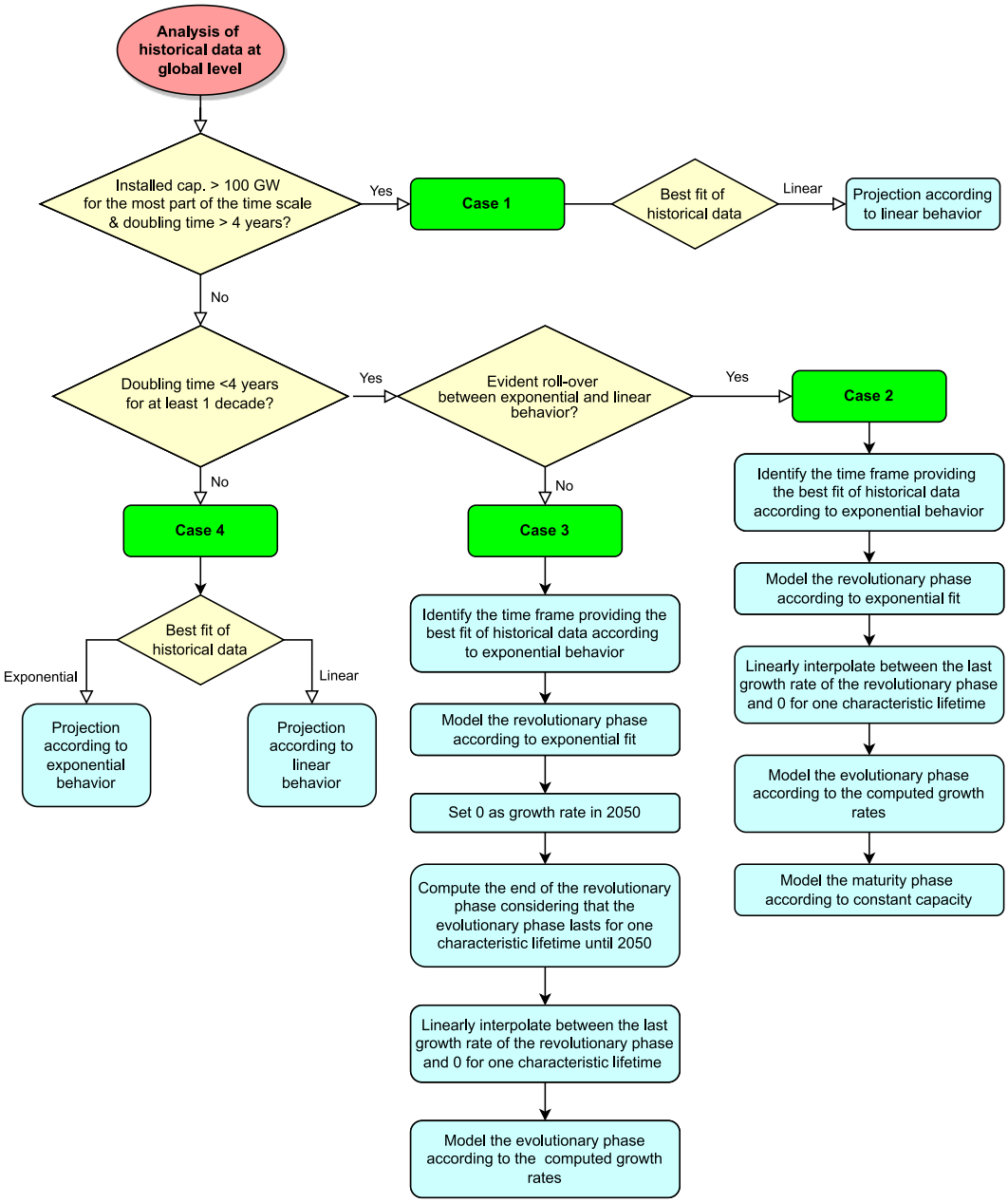

Figure 28. Flowchart for the application of the method to forecast installed capacity curves for electricity generation technologies.

Biomass and geothermal technologies (see **Figure 29b**) are modeled considering stagnation of installed capacity according to a linear trend using the parameters in **Table 32**. This leads to doubling of installed capacity by 2050 with

respect to 2100, while reaching more than 200 GW (biomass) and 12 GW (geothermal) by 2100, corresponding to more than four times the installed capacity in 2020.

Concerning wind technologies, they follow almost the same trend but delayed by a decade. Both onshore and offshore technologies experienced a dramatic increase retracing an exponential behavior in the first decade of their development. On the other hand, wind onshore shows a clear bend towards linear development in the last part the first decade of this century (see **Figure 29c**). Then, according to case 2 described above, an evolutionary phase is modeled in a linear fashion for a technology lifetime of 20 years [222]. That leads to maturity by the early 2030s, at a level slightly below 400 GW installed capacity. In the case of wind offshore, the historical data in **Figure 26** show large growth with a 3 years-doubling time. A roll-over between revolutionary and evolutionary phase is not evident here, as it happened for wind onshore. Therefore, case 3 is used for the projection with parameters listed in **Table 32**. In order to guarantee that maturity is reached by 2050, the revolutionary phase would last until 2022, while maturity would be then reached at 170 GW, as visible in **Figure 29c**.

The historical data for installed solar PV capacity show the fastest growth among the technologies in **Figure 26** in the last decade, with a doubling time lower than 2.5 years, thus sufficient to identify a revolutionary phase. As the roll-over to the evolutionary phase is not evident – despite a clear brake of the growth rate since 2013 – the projection is performed according to case 3 guaranteeing that maturity is reached by 2050. Therefore, the revolutionary phase to model the evolution of solar PV technologies would last until 2022 and is characterized by the parameters in **Table 32**. Maturity would be reached at 2.6 TW, as visible in **Figure 29d**.

The historical dataset for Solar CSP capacity in **Figure 26** highlights a non-constant increasing trend with no growth at all between 2015 and 2021. Therefore, stagnation is the only possible trend to be considered for the evolution of CSP capacity, leading to a very slow growth up to almost 2.5 GW by 2100.

Marine energy technologies, as visible in **Figure 26**, present again very low installation levels and an almost null growth in the last decade. The observed doubling time is close to 60 years, thus out of the range 2-4 years required to identify a revolutionary phase, and sufficient to justify a stagnation, modeled using the parameters in **Table 32**. **Figure 27d** shows that projections made according to case 4 lead to slightly more than 3 GW installed by 2100.

Concerning constraints for the development of nuclear fusion, targets have been set for the development of ARC capacity by Dr. Mumgaard, CEO of Commonwealth Fusion Systems, the company aiming to build a compact fusion power plant based on the ARC tokamak power plant concept. It has been claimed that 2 TW of fusion power are expected to be developed by 2050, supposedly starting the operation of the first ARC in 2035 [223]. That would mean having 8000 reactors delivering 250 MW net electrical power each (as from **Table 27**). Roughly speaking, that target means to consider, in average, slightly more than 500 reactors per year entering into operation, thus more than one per day. If considering a simple exponential development as in **Equation** 28 (where P is the installed power and t represents time), the target of 2 TW capacity by 2050 may be reached with a doubling time (time needed for installed capacity to double in value) slightly higher than 1 year, as technology adoption usually follows an exponential law in the first development stages [199]. Note that currently the only source to have achieved doubling times lower than 2 years in the initial development phase at global level is solar PV, with slightly more than 1.4 years-doubling time (2.5 years at European level).

$$P_t = P_{t-1} \cdot 2^{\frac{1}{\text{doubling time}}} \qquad 28$$

Figure 30 shows what such a high development speed would mean when compared against the historical development of other power technologies in the last two decades at global level, considering data provided by the U.S. Energy Information Administration [218], the International Renewable Energy Agency for wind [219] and solar energy technologies [46] and thethe REN21 Project [224]. From a first look, the fifteen-year CFS target appears quite ambitious if compared to, e.g., the twenty-year development of solar PV and wind offshore which, at a certain point, experienced a bend in their growth that slowed down their development, as shown in [52]. With such a trend, nuclear fusion capacity would surpass the current global installations of both nuclear fission and hydropower plants, getting close to the current levels of fossil fuels installed capacity (around 4 TW in 2019).

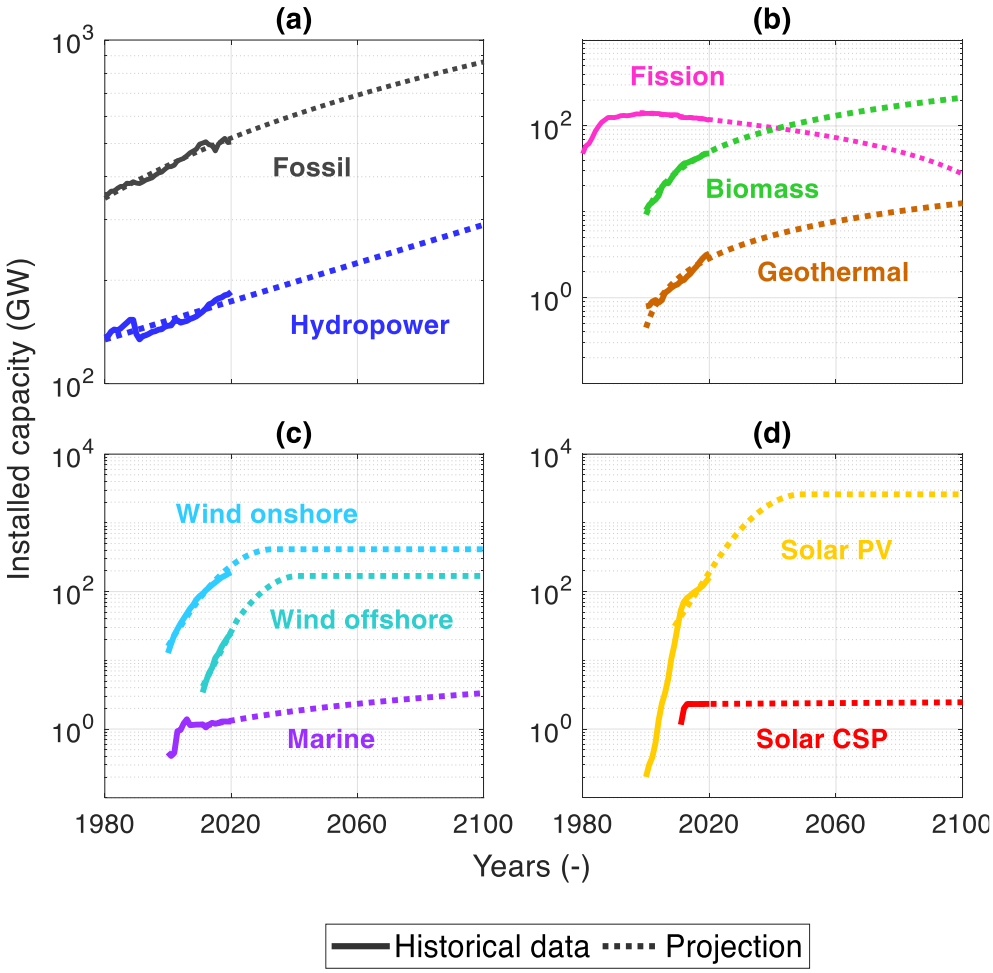

Figure 29. Historical data and installed capacity projections for a) fossil and hydropower technologies; b) nuclear fission, biomass and geothermal technologies; c) wind and marine technologies; d) solar technologies.

In particular, the trend targeted by CFS is definitely not in line with the development experienced by solar PV and wind technologies throughout the first 15 years for which data about installed capacity are available. Indeed, with a growth to 2 TW by 2050, nuclear fusion capacity would increase by 100 million times, compared to 3.4 million times for solar PV and wind offshore, and slightly more than 20 thousand times for wind onshore. Note that the size and technological complexity of NFPPs with respect to either solar PV panels or wind turbines makes the target look quite unlikely to be suitable, especially in a very limited time frame.

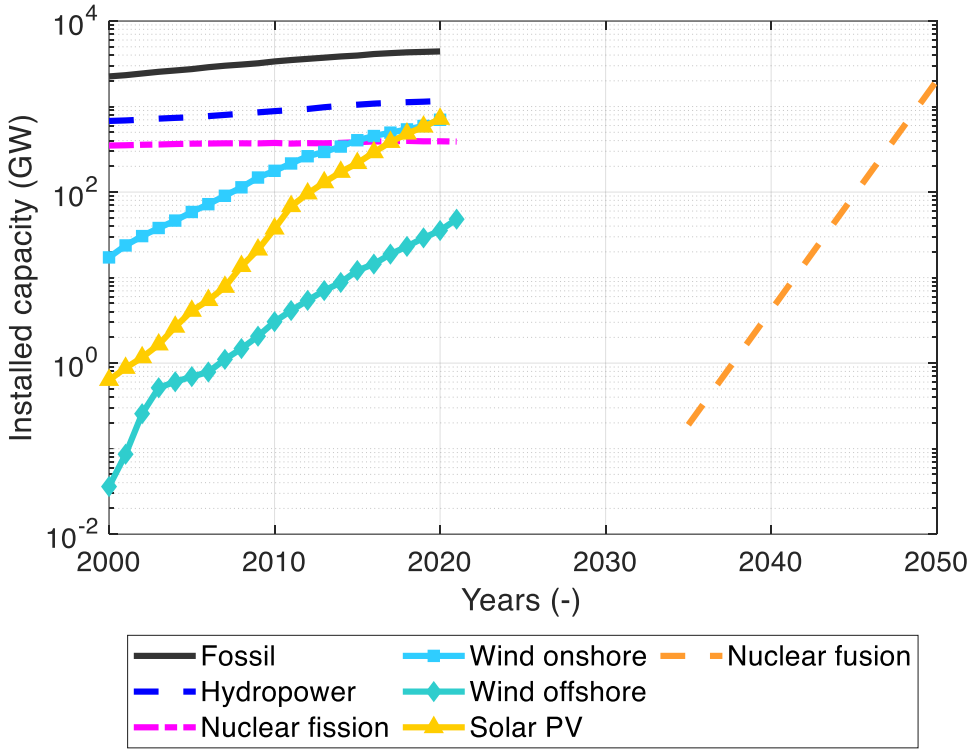

Figure 30. Global historical capacity development of fossil, hydropower, nuclear fission, wind and solar PV technologies against nuclear fusion according to the CFS target of 2 TW by 2050, following a trajectory computed according to a simple exponential growth deployment.

On those premises, the constraints adopted for fusion deployment are based on different development trends. Thus, three curves are developed here basing on the fastest growth model described in [208] and recalled in **Section 3.6.1**. Such model is feasible for the case of nuclear fusion as it is able to work when a target is set for P_{sat}, and in the case of nuclear fusion that will be set here at 2 TW. The capacity curves are computed according to three different doubling times up to 2100: the lower and the upper limits are set to identify the exponential phase mentioned above (2 and 4 years) and while the value of 1.4 years corresponds to the fastest doubling time in the exponential phase, as identified in the set of global historical data belonging to solar PV [52]. In all cases, the lifetime for fusion technologies is set at 40 years. The three curves are presented in **Figure 31**. When considering the fastest growth globally experienced in the exponential phase with 1.4 years-doubling time, the installed capacity in 2100 would almost reach 2 TW, thus very close to the targeted saturation capacity, while just 160 GW would be installed in 2050. On the other hand, with a 2 years-doubling time, the maximum achievable capacity results

in 1.8 TW in 2100. In that case, the installed capacity achieved by 2050 is just slightly below 30 GW. When considering instead a doubling time of 4 years, the installed capacity development is far slower in the exponential phase (with a duration of 40 years) and the final installation level in 2100 is slightly above 1 TW, and only 2.6 GW are installed by 2050.

Concerning other works developing constraints for fusion development, ETM takes into account a constraint for the maximum global cumulative fusion capacity development based on tritium availability for the basic and the advanced EU-DEMO-based reactors, considering just 184 GW to be possibly developed globally by 184, out of which just 15 GW in Europe [225]. Regarding the Asian-DEMO-based technology, the study in [48] assumes that the reactor is available in the countries participating to the ITER endeavor starting from 2050 (and in some other regions of the world starting from 2070), and that installed capacity cannot grow by more than 2 GW/year in every region. Note however that the growth rate there is not substantiated by any specific study in support of it.

In the following scenario analysis, the maximum capacity constraint for cumulative fusion capacity is selected to follow the "fastest growth" (1.4 years-doubling time) curve in **Figure 31**, despite the analysis carried out in a global perspective. Indeed, the constraint is regionalized considering that just one-fifth of the total fusion capacity would be available for Europe in the model developed here.

The computed capacity curves presented in **Figure 29** and (one-fifth of) the fastest growth curve (doubling time 1.4 years) for nuclear fusion in **Figure 31** are implemented in TEMOA-Europe adopting the MaxCapacityGroup constraint in **Equation 17**. However, fossil fuel and biomass plants equipped with CCS will not be constrained according to the trajectories in **Figure 29a** and **Figure 29b**, respectively, to be left free to contribute to decarbonization, even though their final installation/production level will be carefully examined to avoid an unrealistic behavior with exceptional growth in a short period of time. It has also to be highlighted again how nuclear fission is the only technology group envisaging a negative outlook throughout the time frame of the considered scenario.

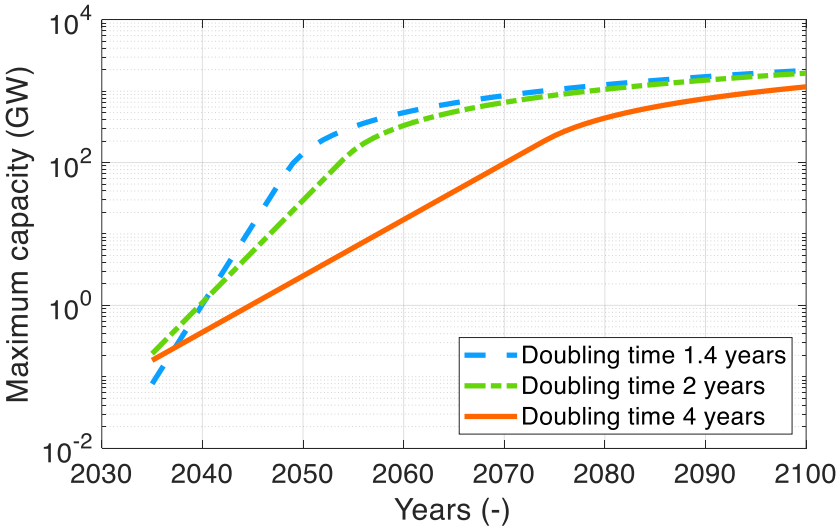

Figure 31. Installed capacity trends for nuclear fusion computed according to 1.4, 2 and 4 years-doubling times and constraint applied to EU-DEMO based on tritium availability.

3.7 Main results

TEMOA-Europe, as all the tools belonging to the ESOM family, is able to minimize the total cost of the system optimizing the construction of the RES network. Results are obtained in terms of installed capacity levels of the different technologies composing the optimized RES, along with their activity (i.e. output commodity flow) and the CO_2 emissions related to their use. A proper postprocessing of the activity levels, combining them with the commodity usage, defined through the efficiency and the share of commodities possibly used as input for the technologies, gives the possibility to obtain detailed results concerning energy supply and consumption.

3.7.1 Features of the presented scenarios

This section presents a set of results obtained from illustrative challenging scenarios considering stringent CO_2 emission trajectory coupled with good economic and moderate population growth, as even backed up by the targets of the European Green Deal [107]. Projections regarding GDP and population are taken from the latest version of the International Energy Outlook [193], which provides long-term projections on macroeconomic indicators until 2050. Figures until 2100 are simply extrapolated. The prescribed trajectory for the European GDP is reported in **Figure 32**, showing how more than doubling of the GDP

levels (+ 156%) reckoned for 2005 is envisaged by 2100. On the other hand, concerning population, **Figure 32** shows modest growth throughout the TEMOA-Europe time scale, with just a 13% increase with respect to 2005 levels and complete stagnation in the second half of this century. **Figure 32** also compares trends derived from the International Energy Outlook 2019 [226], showing how the effects of the COVID-19 on very-long term projections generally have no effect, while GDP growth has been reviewed downwards for the next decades and that has effects until the end of the century. Additional relevant constraints envisage the end of the dependence on Russian fossil fuels starting from 2025, as from the targets of the REPowerEU Plan [6] and the possibility to increasingly resort to afforestation to abate up to 1 Gt_{CO_2} per model period.

Results for three scenarios will be presented, solely differentiated according to the availability of nuclear fusion technologies: in the scenario "Fusion_2035", fusion (in particular, the ARC-based technology) is available starting from 2035, retracing the characterization in **Section 2.5**. The scenario "Fusion_2035" will be considered as a reference scenario for which detailed results will be presented in terms of CO_2 emission trajectories and composition of the electricity supply sector, along with an overview of the results concerning energy consumption and a technology assessment for the transport sector.

Two alternative scenarios are also considered to take into account the uncertainty about the possibility to actually develop nuclear fusion technologies: in "Fusion_2060", all the fusion technologies characterized in **Section 2.5** are available starting from 2060 and the constraint for the fastest capacity development depicted in **Figure 31** is applied, but shifted by 25 years (note that just one-fifth of the capacity depicted by the curve retracing the 1.4-years doubling time in the exponential phase is considered available for Europe, as mentioned above). The same happens for ARC features, so that lithium consumption and costs are reduced starting from 2080, instead of 2050 as it happens in the reference scenario. Eventually, a "No_fusion" scenario is analyzed, considering that fusion technologies are not available over the whole time horizon of TEMOA-Europe. Results for those two scenarios will be just presented in terms of the computed evolution of the electricity generation mix, to show the solutions adopted by TEMOA-Europe to contrast the absence of an electricity production alternative that may never be unlocked at commercial level.

In all the scenarios presented here, the maximum yearly CO_2 emission levels are constrained such as to allow net-zero emissions by 2050, as already performed

by IEA in the *World Energy Outlook 2021* [2] at the global level. The prescribed CO_2 trajectory is also in line with the European Commission Fit for 55 [227] target, aiming at reducing CO_2 emission levels by 55% by 2030 with respect to 1990 levels (~ 5 Gt [228]). **Table 33** reports the adopted emission limits and the relative reduction with respect to 1990 levels. Note that the emission limit is considered for the energy system as a whole, and not specified according to different sectors, so that the model can decide the sectors to be prioritized in the decarbonization process.

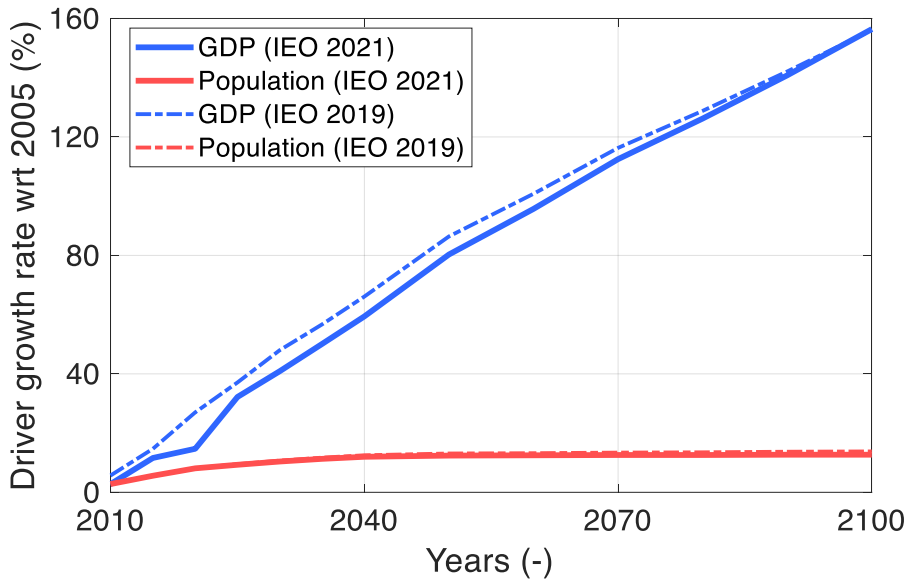

Figure 32. Projections of the GDP and population growth rate as prescribed in TEMOA-Europe.

Table 33. Emission reduction trajectory implemented in TEMOA-Europe.

Period	Emission limit (Gt)	Reduction with respect to 1990 (%)
2030	2.25	55
2035	1.50	70
2040	0.75	85
2050	0.00	100
2060	0.00	100
2070	0.00	100
2080	0.00	100
2090	0.00	100
2100	0.00	100

Note that the results of the scenarios presented here are only used to show the effects of the implementation of the technological modules and constraints described in this thesis and the capabilities of the model to reproduce future energy trends, while they should be tested both against historical data and also compared to other acknowledgeable energy outlooks. Therefore, they do not intend to have any policy-relevant significance at this stage.

3.7.2 CO_2 emissions trajectories

GHG emissions are computed in TEMOA-Europe according to a dynamic method that is able to take care of the possible evolution in the composition of some fuels to account for the contribution by either biofuels, synfuels (e.g. in traditional fuels like gasoline and diesel) or hydrogen (e.g. blended with natural gas with variable percentages), as explained in [229].

Figure 33 shows in detail the CO_2 emissions generated by each sector in TEMOA-Europe compared to the net CO_2 emissions for the "Fusion_2035" scenario. The net CO_2 reduction trajectory depicted by net emissions perfectly retraces the one in **Table 33** for the emission limit starting from 2030, highlighting how the model would possibly operate different economically optimal choices whenever left free of performing unconstrained optimization.

The adoption of afforestation measures is the reason for the large difference between gross sectoral CO_2 emissions and the net emission trajectory in **Figure 33** starting from 2030 on, when the net CO_2 trajectory starts significantly moving away from the stack of gross sectoral emissions. The constraint on the possibility to adopt increasing afforestation as mitigation strategy (mentioned at the end of the first paragraph of **Section 3.7.1**) is also the reason for gross CO_2 emissions to increase again from 2050 to 2100. The model is the able to find an optimal configuration for the RES while reaching the imposed decarbonization targets. Gross emission reduction alone, fostered by the transition of supply and demand sectors towards a cleaner energy mix, would just allow 85% reduction in CO_2 emissions by 2100 compared to 1990 levels, being below 1 Gt already starting from 2050 on.

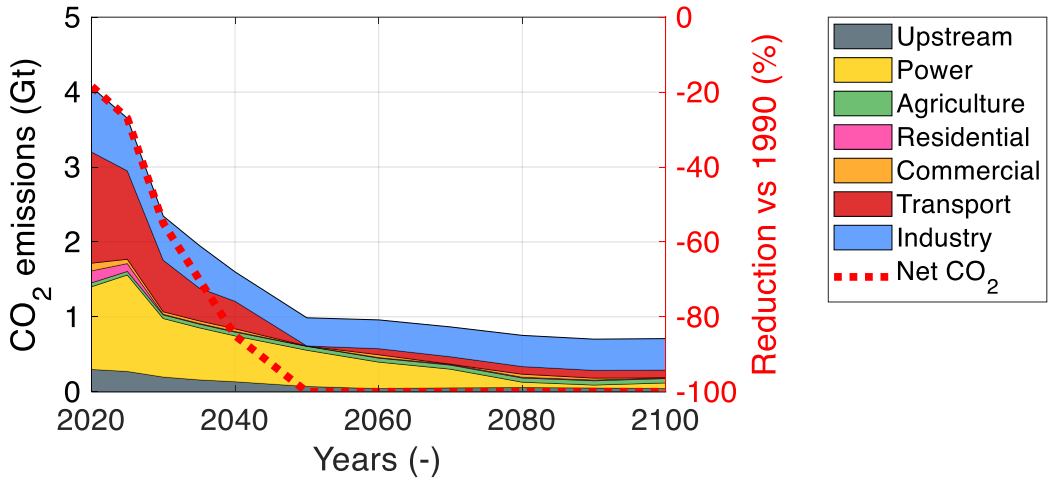

Figure 33. Gross sectoral CO_2 emission trajectories compared against the net-CO_2 emission curve depicted in the analyzed scenario.

In the "Fusion_2035" scenario, the commercial sector is the only one to be completely decarbonized by 2100. Nonetheless, the combined contribution of the residential and the commercial sectors is very low already at the beginning of the time scale represented in **Figure 33**, contributing together to the almost 7% of total emissions in 2020 and to less than 2% of gross CO_2 emissions in 2100.

The power sector experiences almost full decarbonization (over 90% reduction in 2100 with respect to 2020), anticipating the phase-out of traditional fossil fuel plants, currently representing the bulk of generation capacity in Europe, see **Figure 26**.

On the other hand, the agriculture sector is the only one experiencing an increase in carbon dioxide emissions (+ 12%), due to the unavailability of an alternative, low-carbon combination of fuels used to produce agricultural final demand which, instead, undergoes a significant increase.

The set of low-carbon technologies envisaged in the TEMOA-Europe database for the industrial sector allows a 50% reduction with respect to 2020 levels in 2100, making industry the hardest-to-abate end-use sector in TEMOA-Europe among those represented with a high level of technological disaggregation, even though mainly due to the impossibility of decarbonizing some processes relying on aggregated fuel consumption (other industries, non-specified industrial energy use and non-energy uses, see **Section 3.2**).

Also the transport sector presents an almost full decarbonization, with almost 95% reduction in 2100 with respect to 2020 levels and around 100 Mt_{CO_2} vented in 2100. In particular, that is also possible thanks to the inclusion of data concerning futuristic clean vehicles like ships and aircrafts using hydrogen as fuel.

Finally, the upstream sector (~ 85% reduction with respect to 2020 levels in 2100) is mostly decarbonized due to the indirect effect of a general reduction in the use of fossil fuels in the other sectors, resulting in dismissed refineries avoiding thus more than 100 Mt_{CO_2}.

3.7.3 Electricity supply

Figure 34 shows the results in terms of electricity generation mix for the scenario "Fusion_2035".

The effect of the application of the technology adoption curves depicted in **Section 3.6.3** is especially evident concerning the outlook on nuclear fusion. It contributes to the transition towards an almost fully decarbonized electricity generation sector with slightly more than 2000 TWh in 2100 – the 25% of the total electricity production computed by TEMOA-Europe in the "Fusion_2035" scenario. The only technology taken into account for nuclear fusion is ARC, which also corresponds to the cheapest reactor concept, as from **Table 27**. However, the global analysis performed in [110] concerning a less stringent scenario in terms of CO_2 emission reduction (still allowing 1 Gt_{CO_2} in 2100), but following the same fastest growth trajectory for nuclear fusion as in **Figure 31** (although based on the global level), showed how fusion would be more beneficial in regions of the world other than Europe. In particular, it shows that fusion is necessary where the current energy system lacks a prompt implementation of clean energy technologies due to a current mix almost completely based on fossil fuels (e.g. China), while not having any role in Europe. In both cases, ARC is selected as the only NFPP concept to be implemented, mainly due to its lower cost when compared to the EU-DEMO and the Asian-DEMO. All in all, fusion characterization would need further attention in the future development of this work, especially concerning constraints tailored to the European case, especially to consider that the fusion fuel value chain and the industry to support such a massive construction of NFPPs still does not exist in large part.

The total electricity production is more than doubled in 2100 with respect to 2020 (see **Figure 34a**) pointing out how electrification of end-uses is strictly related to an effective decarbonization process.

As visible in **Figure 34b**, the electricity generation mix at the end of the century in the "Fusion_2035" scenario envisages the largest contribution from solar energy (28%), with fossil fuels almost completely phased-out (3%), even when considering plants equipped with CCS, which are only marginally present in the energy mix depicted by TEMOA-Europe for this scenario and just starting from 2050 on (representing less than 2% of total electricity production in 2100). Indeed, an important result is that, with the characteristics implemented in TEMOA-Europe, fossil fuels plants with CCS are deemed as useless for the energy transition, despite allowing a 90% emission reduction with respect to their traditional counterparts in the TEMOA-Europe database [189]. Wind (25%) and hydropower (12%) also represent considerable electricity sources in 2100. Other renewables like biomass, geothermal and marine energy technologies slightly contribute to the energy mix in 2100 (4% of total generation when considered together), despite being clean energy sources. Actually, the role of biomass electricity is non-negligible until fusion is available, reaching almost 9% of total generation by 2050. The imposed constraint for fission phase-out also almost completely excludes that from the electricity generation mix at the end of the century (2% in 2100, starting from 24% in 2020).

All in all, the phase-out of fossil fuels and the increase of electricity demand are contrasted in the analyzed scenario adopting growing shares of solar, wind and fusion energy, while the role of biomass for electricity production is considerable only at mid-century, to contrast the decline of fossil fuel generation when fusion still covers a marginal role. Solar, hydropower and other minor renewables are the only technologies envisaging considerable growth in total generation even when fusion is made available to produce commercial electricity.

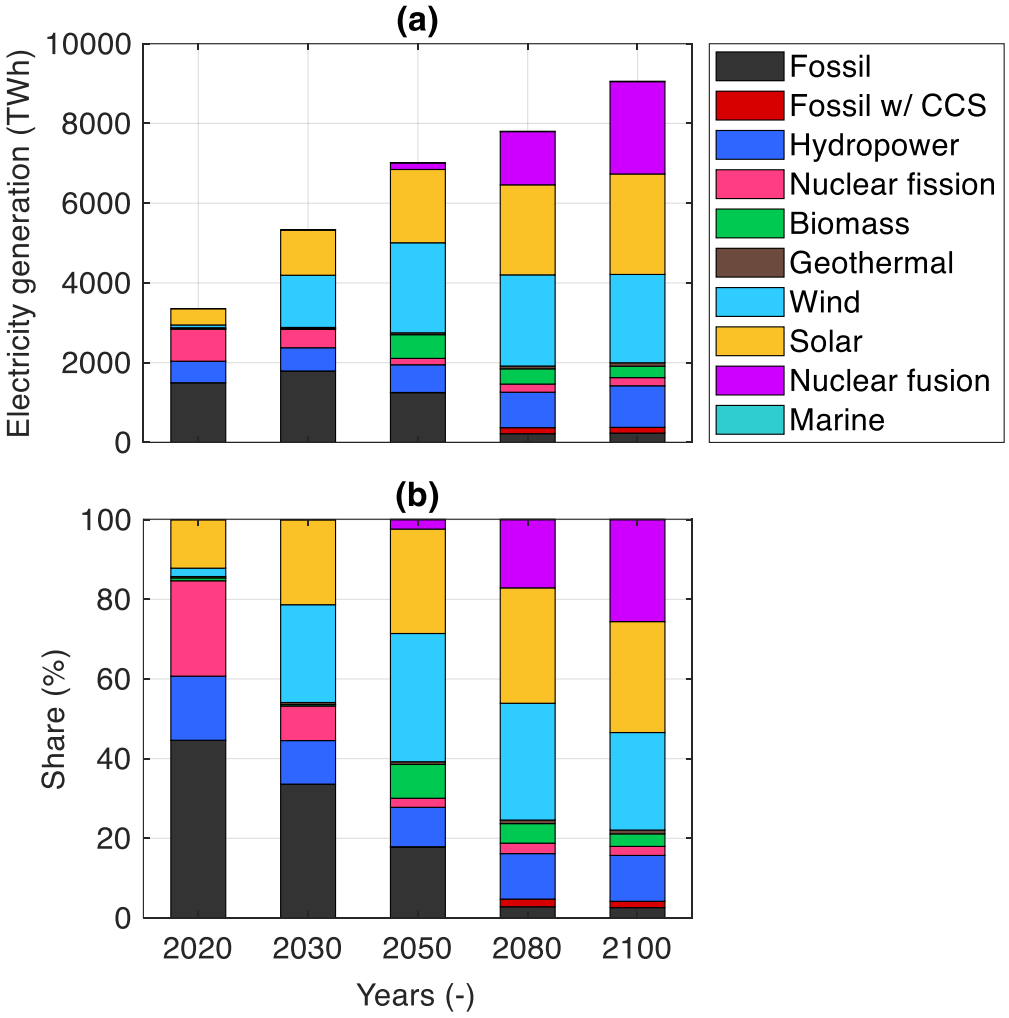

Figure 34. Evolution of the electricity generation mix at selected time steps in TEMOA-Europe for the "Fusion_2035" scenario.

The evolution of the electricity generation mix in **Figure 35** for the scenario "Fusion_2060" highlights just one single difference with respect to "Fusion_2035" in **Figure 34**: the missing shares of fusion electricity, due to the application of the 1.4 years-doubling constraint in **Figure 31** with a 25 years-delay, lead to a larger role of biomass electricity. Indeed, its contribution is always around 9% starting from 2050 on, as visible from **Figure 35b**.

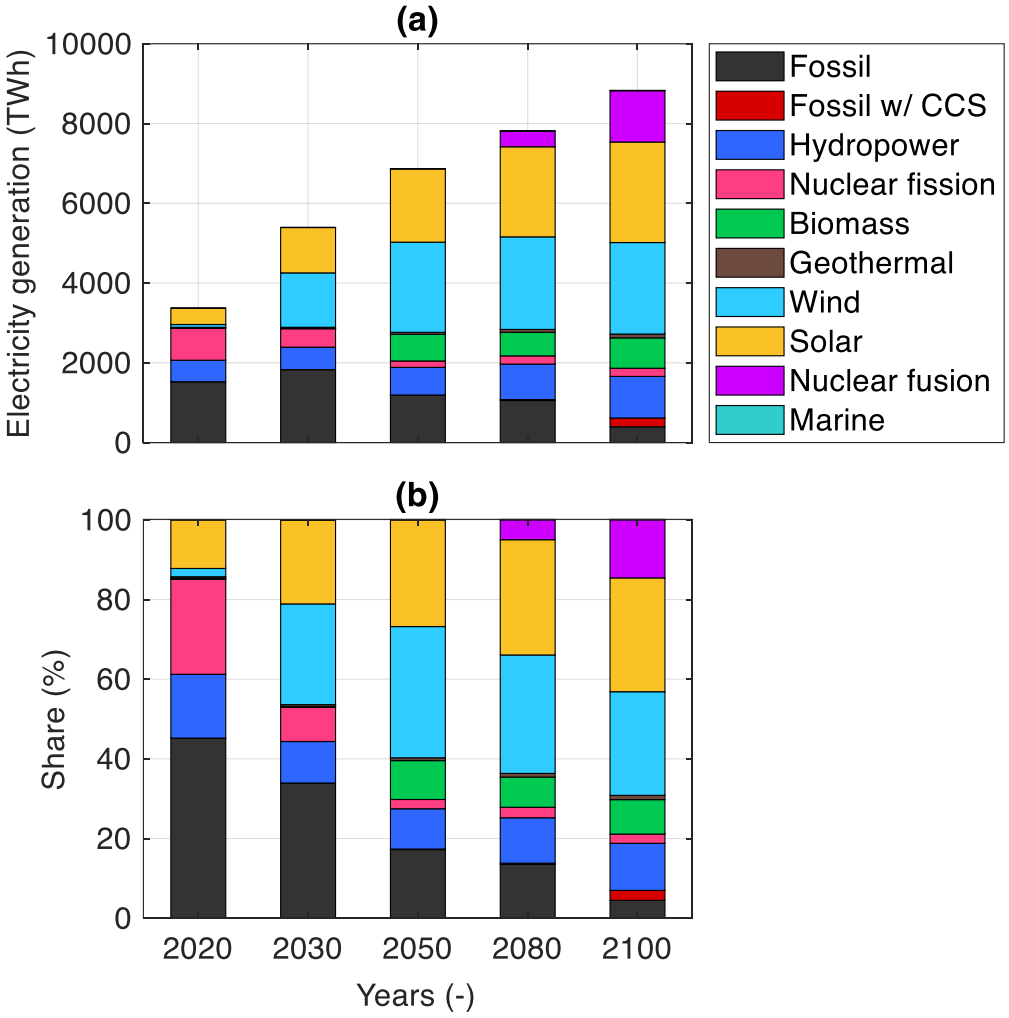

Figure 35. Evolution of the electricity generation mix at selected time steps in TEMOA-Europe for the "Fusion_2060" scenario.

Concerning the results of the "No_fusion" scenario reported in **Figure 36**, the complete absence of fusion is instead balanced by slightly growing shares of solar, wind and biomass electricity with respect to **Figure 35**, while the phase-out of fossil fuels is not possible. However, they contribute to an almost stable production level for the whole time scale, as visible from **Figure 36a**. On the other hand, **Figure 36b** shows how 80% of total electricity would come from renewable energy, despite a less effective decarbonization of the power sector.

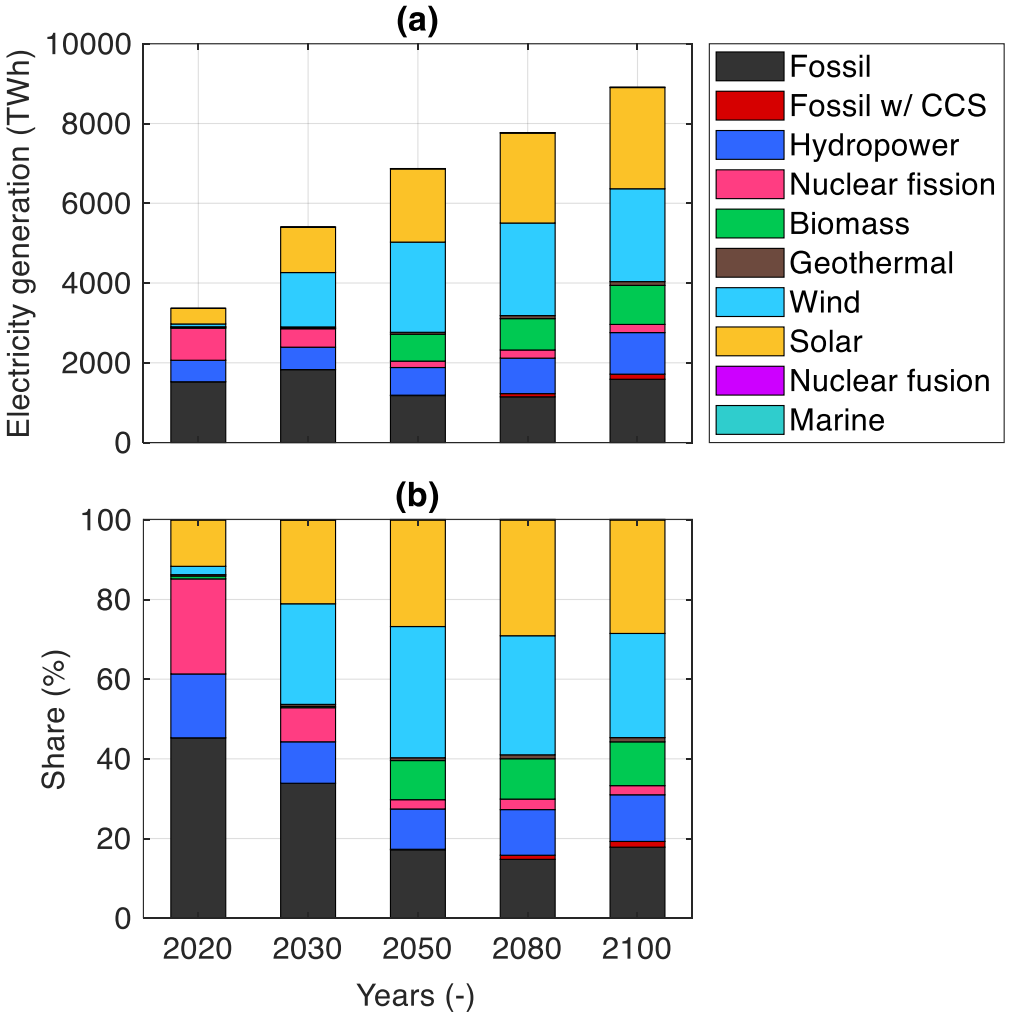

Figure 36. Evolution of the electricity generation mix at selected time steps in TEMOA-Europe for the "No_fusion" scenario.

3.7.4 Energy consumption and technology assessment

Concerning an end-use sector, the transport consumption mix allowing almost full decarbonization by 2100 computed by TEMOA-Europe for the "Fusion_2035" is shown in **Figure 37**. While total energy consumption is halved in 2100 with respect to 2020 due to the large contribution of electricity, allowing higher energy efficiency than traditional internal combustion engines and that can be used for all road transport modes and trains, as explained in **Sections 2.1** and **2.2**, TEMOA-Europe envisages an almost complete phase-out of gasoline vehicles already since 2040, despite the current actual transport framework still presents a large number

of gasoline vehicles, especially cars. On the other hand, natural gas always represents a negligible contribution.

Also gas oil (mostly used in heavy-duty road transport) consumption, undergoes almost 90% reduction and is mostly used in combination with electricity in plug-in hybrid heavy-duty vehicles by the end of the century.

Figure 37 also shows the full transition from kerosene to hydrogen in aviation, especially after 2050, when liquid hydrogen-fueled international aviation vehicles are made available in TEMOA-Europe. Also ammonia, available as low-carbon fuel for ships, represents a major choice to contribute to decarbonization, with over 2000 PJ consumed by 2100.

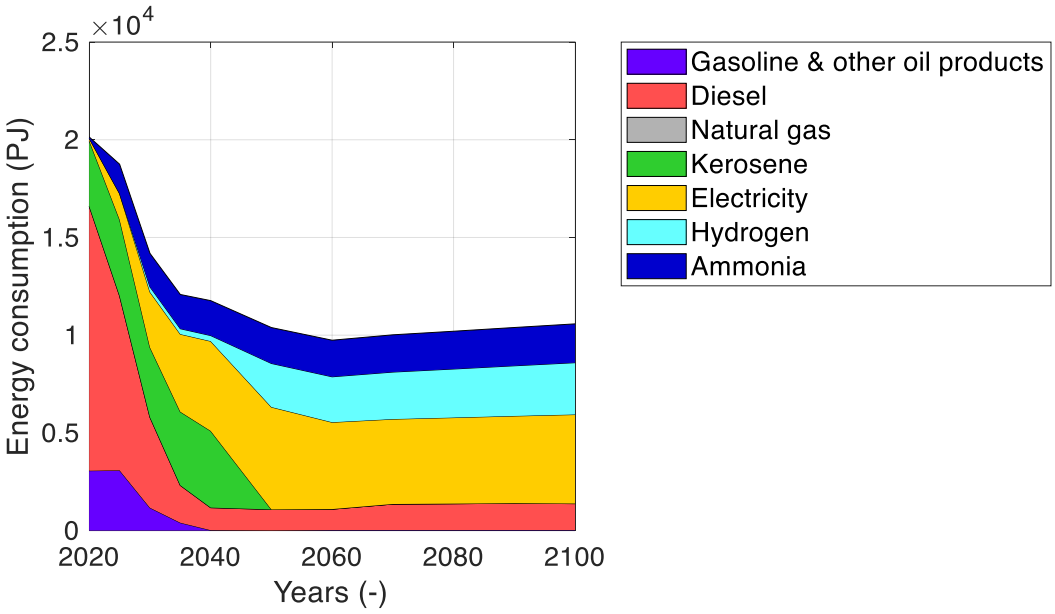

Figure 37. Evolution of the energy consumption mix for the transport sector in the "Fusion_2035" scenario.

An energy system optimization model like TEMOA-Europe is also able to provide details about the technology mix in different sectors. Indeed, **Figure 38** presents the choices made in the car sector with electric cars contributing to the totality of the demand share already starting from 2040, thus representing a necessary option to reach the full decarbonization target by 2050 despite the higher costs with respect to traditional vehicles. Nonetheless, it has to be noted that TEMOA-Europe cannot recognize, at this stage, possible issues like lithium availability for batteries, or other limitations to the diffusion of electric vehicles

due to, e.g., range anxiety. Gasoline, LPG and natural gas cars are instead disregarded already starting from the 2020 period, while full-hybrid cars contribute to substitute traditional internal combustion engines while the transition to a full-electric car sector happens.

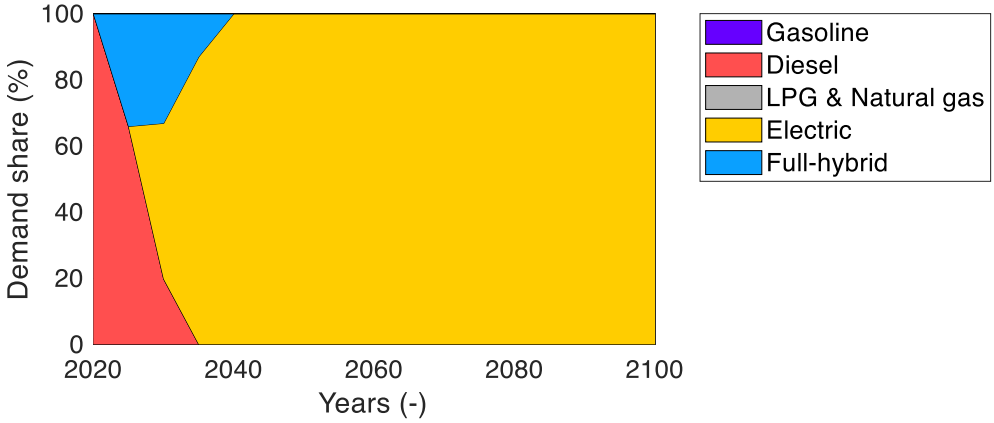

Figure 38. Technology mix computed for cars in the “Fusion_2035” scenario.

Chapter 4

Conclusion and perspectives

The pressing issue of climate change and the fast-changing economical and geopolitical dynamics require decision-makers to anticipate and shape possible future outcomes under a variety of different scenarios that consider resource availability and pricing, technology innovation, demand growth, and new energy and environmental strategies.

In the framework of the development of climate change mitigation and energy security issues to ease fast and effective decarbonization of the economy, energy system optimization models are key tools to drive investment choices and policy measures. Indeed, they include detailed, bottom-up technology specifications and adopt linear programming techniques to minimize the system-wide cost of energy provision and use by optimizing the installation of energy technology capacity and its utilization.

Since the deployment of new low-carbon technologies is strictly related to economic efforts to support research, development and commercialization, ESOMs play a crucial role in technology assessment to define their possible role in the climate change mitigation process. In this framework, the deployment of nuclear fusion technologies is experiencing an unprecedented effort concerning large financial expenditure in both public and private research, although any nuclear fusion reactor would be realistically available in the coming years. While private investors would be glad to know that they have bet on the winning horse, public financing is subject to the scrutiny of both governments and

taxpayers, and energy system models could play an important role in either justifying or discouraging huge monetary expenditures on projects that would not be able to respond to the expectations.

Nonetheless, the typical tendency of working with energy system models is to rely on proprietary frameworks based on hardly accessible databases that do not guarantee full transparency of the results. On the other hand, unavoidable future uncertainties grow with time, and the use of models to produce quantitative predictions is a perilous approach that often produces misleading conclusions. Since it is also clearly impossible to validate the results of models that assess future scenarios against the actual developments of the energy system before they are realized, the possibility to strongly bias the outcomes of the analyses appears evident.

In the framework of the EUROfusion Consortium to support the development of nuclear fusion, the EUROfusion TIMES Model (a global ESOM in 17 regions adopting a time scale from 2005 to 2100) is used to address design choices for an effective deployment of a reactor concept based on the outcomes of the ITER project that would be cost-effective once commercially available. However, the closed nature of this model both at the database and software level (TIMES is based on a fully accessible source code but relies on paid software) hinders the possibility of third-party verification and the guarantee of producing unbiased analyses.

Some open tools for energy system optimization like OSeMOSYS and TEMOA have been tested in recent years and have proven themselves comparable to the reference TIMES model generator despite the lower degree of detail and the possibility to solve just a simplified version of the optimization problem.

Given that, open-database and open-code partial equilibrium ESOMs allow to improve the reliability and transparency of such tools and their results, increasing their policy relevance.

The work aims to develop TEMOA-Europe, the first open-database and open-software model instance for energy system analysis concerning the European continent. The time scale is purposedly very long until 2100 to guarantee that the effects of the possible integration of nuclear fusion in the energy mix would be visible in the model outcomes. This activity takes advantage of the involvement in the EUROfusion WPSES with a three-year experience in the development and maintenance of technological modules for ETM. As TEMOA-Europe is mainly

based on the work carried out within the WPSES, this work presents a thorough explanation of the process to develop a techno-economic characterization for the industrial energy-intensive subsectors, for road transport and the hydrogen module as also currently implemented in ETM. The characterization of the industrial and road transport sectors presents a comprehensive portfolio of both well-established and innovative technologies, providing a very high level of disaggregation and considering some technological options which are not included in any other energy system model instance, like, for instance, steel production through electrolysis processes, fuel cell trucks or liquid hydrogen-fueled aircrafts.

Moreover, a new characterization for non-road transport and nuclear fusion technologies is expressly developed for TEMOA-Europe to overcome two ETM drawbacks: 1) the formulation of non-road transport demand in terms of consumed energy instead of traveled distance, which hinders the optimization process from considering differences in the performance of alternative vehicles and 2) the absence of competition in the nuclear fusion module as just a single technology in a basic and an advanced configurations – both based on the expected outcomes of the ITER project converging in a European DEMO reactor – is available in the Reference Energy System.

As realistic technical constraints are also crucial to enhance the reliability of energy models, a method to obtain capacity curves based on historical data series and the S-curve approach to forecast technological development is presented in this work for the application to a European case study. In particular, the focus is on the electricity generation sector. The method presents four cases for the evolution of the installed capacity of commercially available technologies, namely fossil, hydropower, nuclear fission, geothermal, biomass, wind (both onshore and offshore), solar (both PV and CSP) and marine energy plants.

To also define educated constraints for the adoption of nuclear fusion, another method, described in [208], is used here based on the claims presented by Commonwealth Fusion Systems [223]. As the target of 2 TW globally cumulative installed fusion power by 2050 appears quite far ambitious and unrealistic if compared to the actual development of currently available electricity generation technologies, the “fastest growth” trajectory towards 2 TW by 2100 is developed here and compared to constraints for the EU-DEMO retrieved for the European region in ETM and based on tritium availability [225]. However, just one-fifth of the 2 TW is conceived to be available for Europe in this work.

Some results from the TEMOA-Europe version developed for this thesis are also presented in terms of CO_2 emission trajectories for the different energy supply and demand sectors, electricity generation mix and, finally, energy consumption and technology mix in the transport sector. The most relevant result is that TEMOA-Europe is able to compute trajectories toward an almost full decarbonization of the energy system under a set of very stringent constraints.

In perspective, there is plenty of room for TEMOA-Europe, both concerning improvements in the methodology and practical applications of the model. Indeed, the TEMOA formulation shall still benefit from a continuous update to improve the capabilities to represent the technical features of energy technologies giving, for instance, the possibility to directly act on specific technology shares within groups, instead of setting absolute values for maximum capacities/activities. Moreover, the dual formulation of the TEMOA model will be explored to provide marginal costs of energy commodities as additional outputs in scenario analyses.

Concerning updates to the model, a thorough benchmark against historical trends will be carried out and, in case of significant deviations, the causes of the discrepancies will be investigated and, if necessary, proper constraints will be implemented to align the model with historical data. Regarding technological modules, the most recent updates performed on the industry and the hydrogen modules are the only ones requiring no major changes shortly. Concerning the transport sector, the road transport module would also benefit from further disaggregation of service demands, separating, for instance, urban and extra-urban mobility and, in the case of cars, providing techno-economic details for different car sizes to substitute the currently implemented representative car. Also, the current structure of the power sector calls for a deep improvement, first considering economic parameters to be updated according to the most recent trends expected for the future, especially for renewable energy technologies, advanced nuclear plants. Nonetheless, nuclear fusion still requires special attention to improve the modeling of the fusion fuel chain and to expand the set of techno-economic parameters associated with NFPPs. Moreover, the distribution of some service demands throughout different seasons and times of day should be explored. Also, storage technologies for renewable plants have to be implemented, possibly investigating a more refined time scale to better focus on short-term mechanisms of electricity production and consumption. Another focus will be on electro-fuels, concerning their production (even allowing direct air capture to subtract CO_2 from the atmosphere to produce fuels) and consumption in end-use sectors.

Concerning applications, a set of policy-relevant scenarios to represent and assess in detail the pathway to realize targets of the European Green Deal and the REpowerEU, along with the implementation of a set of different scenarios will be carried out to disseminate the model and test it in challenging frameworks.

References

[1] International Monetary Fund, “World Economic Outlook 2022: Countering the Cost-of-Living Crisis,” 2022. Accessed: Oct. 25, 2022. [Online]. Available: https://www.imf.org/en/Publications/WEO/Issues/2022/10/11/world-economic-outlook-october-2022#:~:text=Press Briefing%3A World Economic Outlook%2C October 2022,-October 11%2C 2022&text=The IMF forecasts global growth,acute phase of the pandemic.

[2] International Energy Agency, “World Energy Outlook 2021,” Paris, France, 2021. [Online]. Available: www.iea.org/weo.

[3] European Central Bank, “Why is inflation currently so high?,” 2021. https://www.ecb.europa.eu/ecb/educational/explainers/tell-me-more/html/high_inflation.en.html (accessed Oct. 25, 2022).

[4] Federal Reserve History, “Oil Shock of 1973–74,” 2013. https://www.federalreservehistory.org/essays/oil-shock-of-1973-74 (accessed Oct. 25, 2022).

[5] S. C. Bhattacharyya and G. R. Timilsina, “A review of energy system models,” *Int. J. Energy Sect. Manag.*, vol. 4, no. 4, p. 25, 2010, doi: 10.1108/17506221011092742.

[6] European Commission, “REPowerEU: affordable, secure and sustainable energy for Europe,” 2022. https://ec.europa.eu/info/strategy/priorities-2019-2024/european-green-deal/repowereu-affordable-secure-and-sustainable-energy-europe_en (accessed Oct. 25, 2022).

[7] Intergovernmental Panel on Climate Change, *Climate Change 2022 - Mitigation of Climate Change - Summary for Policymakers (SPM)*, no. 1. 2022.

[8] M. Gargiulo and B. Ó. Gallachóir, “Long-term energy models: Principles, characteristics, focus, and limitations,” *Wiley Interdiscip. Rev. Energy Environ.*, vol. 2, no. 2, pp. 158–177, 2013, doi: 10.1002/wene.62.

[9] Organization for Economic Co-operation and Development and International Energy Agency, “World Energy Model Documentation,” Paris, France, 2012.

[10] M. Gaeta and B. Baldissara, “Il modello energetico TIMES-Italia - Struttura e dati,” Rome, Italy, 2011.

[11] Ministero dello Sviluppo Economico; Ministero dell’Ambiente e della Tutela del Territorio e del Mare, “Strategia Energetica Nazionale (SEN), 2017,” 2017.

[12] S. Simoes *et al.*, *The JRC-EU-TIMES model. Assessing the long-term role of the SET Plan Energy technologies*, no. EUR 26292 EN. 2013.

[13] International Energy Agency and Energy Technology Systems Analysis Program, “TIMES,” 2005. https://iea-etsap.org/index.php/etsap-tools/model-generators/times (accessed Oct. 25, 2022).

[14] L. Schrattenholzer, “The Energy Supply Model MESSAGE; International Institute for Applied Systems Analysis,” 1981. http://pure.iiasa.ac.at/id/eprint/1542/ (accessed Oct. 25, 2022).

[15] D. Huppmann *et al.*, “The MESSAGEix Integrated Assessment Model and the ix modeling platform (ixmp): An open framework for integrated and cross-cutting analysis of energy, climate, the environment, and sustainable development,” *Environ. Model. Softw.*, vol. 112, pp. 143–156, 2019, doi: https://doi.org/10.1016/j.envsoft.2018.11.012.

[16] R. Loulou, G. Goldstein, A. Kanudia, A. Lehtilä, and U. Remme, *Documentation for the TIMES model: Part I*. 2016.

[17] K. Hunter, S. Sreepathi, and J. F. DeCarolis, “Modeling for insight using Tools for Energy Model Optimization and Analysis (Temoa),” *Energy Econ.*, vol. 40, pp. 339–349, 2013, doi: 10.1016/j.eneco.2013.07.014.

[18] International Renewable Energy Agency, “Accelerating the Energy Transition through Innovation,” Dubai, UAE, 2017. [Online]. Available: https://www.irena.org/-/media/Files/IRENA/Agency/Publication/2017/Jun/IRENA_Energy_Transition_Innovation_2017.pdf.

[19] International Renewable Energy Agency, *Global Renewables Outlook: Energy Transformation 2050*. Dubai, UAE, 2020.

[20] International Energy Agency, “Tracking Power 2021,” 2021. [Online]. Available: https://www.iea.org/reports/tracking-power-2021.

[21] K. W. Bandilla, “Carbon Capture and Storage,” in *Future Energy (Third Edition)*, Third Edit., T. M. Letcher, Ed. Elsevier, 2020, pp. 669–692.

[22] B. Viswanathan, “Chapter 6 - Nuclear Fusion,” in *Energy Sources*, B. Viswanathan, Ed. Amsterdam: Elsevier, 2017, pp. 127–137.

[23] International Energy Agency, “CCUS in Power,” 2021. https://www.iea.org/reports/ccus-in-power.

[24] World Nuclear Association, “Nuclear Fusion Power,” 2021. https://world-nuclear.org/information-library/economic-aspects/economics-of-nuclear-power.aspx (accessed Feb. 25, 2022).

[25] R. Mumgaard, “Fostering a New Era of Fusion Energy Research and Technology Development,” 2021.

[26] International Energy Agency, “World Energy Outlook 2022,” Paris, France, 2022. [Online]. Available: https://iea.blob.core.windows.net/assets/47be1252-05d6-4dda-bd64-4926806dd7f3/WorldEnergyOutlook2022.pdf.

[27] International Energy Agency, *Energy Technology Perspectives (ETP) - Catalysing Energy Technology Transformations*. Paris, France, 2017.

[28] J. H. B. Opschoor, “Fighting Climate Change - Human Solidarity in a Divided World,” *Dev. Change*, vol. 39, no. 6, pp. 1193–1202, 2008, doi: 10.1111/j.1467-7660.2008.00515.x.

[29] UK Atomic Energy Authority, “Spherical Tokamak for Energy Production,” 2022. https://step.ukaea.uk/ (accessed Oct. 09, 2022).

[30] D. Clery, “The bizarre reactor that might save nuclear fusion,” 2015. https://www.science.org/content/article/bizarre-reactor-might-save-nuclear-fusion.

[31] ITER, “What is ITER?,” 2022. https://www.iter.org/proj/inafewlines (accessed Jul. 28, 2022).

[32] T. Donné, “European Research Roadmap to the Realisation of Fusion Energy,” *EUROfusion*, 2018, [Online]. Available: https://www.euro-fusion.org/fileadmin/user_upload/EUROfusion/Documents/TopLevelRoadmap.pdf.

[33] J. Zheng *et al.*, “Recent progress in Chinese fusion research based on superconducting tokamak configuration,” *Innov.*, vol. 3, no. 4, p. 100269, 2022, doi: https://doi.org/10.1016/j.xinn.2022.100269.

[34] K. Tobita *et al.*, “Japan’s Efforts to Develop the Concept of JA DEMO During the Past Decade,” *Fusion Sci. Technol.*, vol. 75, no. 5, pp. 372–383,

2019, doi: 10.1080/15361055.2019.1600931.

[35] B. S. Kim, S.-H. Hong, and K. Kim, “Preliminary assessment of the safety factors in K-DEMO for fusion compatible regulatory framework,” *Sci. Rep.*, vol. 12, p. 8276, 2022.

[36] B. N. Sorbom *et al.*, “ARC: A compact, high-field, fusion nuclear science facility and demonstration power plant with demountable magnets,” *Fusion Eng. Des.*, vol. 100, pp. 378–405, 2015, doi: https://doi.org/10.1016/j.fusengdes.2015.07.008.

[37] Z. S. Hartwig *et al.*, “VIPER: an industrially scalable high-current high-temperature superconductor cable,” *Supercond. Sci. Technol.*, vol. 33, no. 11, p. 11LT01, 2020, doi: 10.1088/1361-6668/abb8c0.

[38] V. Corato *et al.*, “The DEMO magnet system – Status and future challenges,” *Fusion Eng. Des.*, vol. 174, p. 112971, 2022, doi: https://doi.org/10.1016/j.fusengdes.2021.112971.

[39] S. Meschini, “Sustainability of compact, high magnetic field fusion reactors: environment, society and economy,” *Fresenius Environ. Bull.*, vol. 30, no. 06, pp. 5974–5984, 2021.

[40] D. Lerede, C. Bustreo, F. Gracceva, M. Saccone, and L. Savoldi, “Techno-economic and environmental characterization of industrial technologies for transparent bottom-up energy modeling,” *Renew. Sustain. Energy Rev.*, vol. 140, p. 110742, Apr. 2021, doi: 10.1016/j.rser.2021.110742.

[41] B. Nie, M. Ni, J. Liu, Z. Zhu, Z. Zhu, and F. Li, “Insights into potential consequences of fusion hypothetical accident, lessons learnt from the former fission accidents,” *Environ. Pollut.*, vol. 245, pp. 921–931, 2019, doi: https://doi.org/10.1016/j.envpol.2018.11.075.

[42] S. Sandri *et al.*, “A Review of Radioactive Wastes Production and Potential Environmental Releases at Experimental Nuclear Fusion Facilities,” *Environments*, vol. 7, no. 1, 2020, doi: 10.3390/environments7010006.

[43] ITER, “ITER - Frequently Asked Questions,” 2022. https://www.iter.org/FAQ#collapsible_5 (accessed Sep. 16, 2022).

[44] D. Lerede, M. Saccone, C. Bustreo, F. Gracceva, and L. Savoldi, “Could clean industrial progresses and the rise of electricity demand foster the penetration of nuclear fusion in the European energy mix?,” *Fusion Eng. Des.*, vol. 172, no. July, p. 112880, 2021, doi: 10.1016/j.fusengdes.2021.112880.

[45] E. Gnansounou and D. Bednyagin, “Multi-Regional Long-Term Electricity Supply Scenarios with Fusion,” *Fusion Sci. Technol.*, vol. 52, no. 3, pp. 388–393, 2007, doi: 10.13182/FST07-A1518.

[46] K. Vaillancourt, M. Labriet, R. Loulou, and J.-P. Waaub, “The role of nuclear energy in long-term climate scenarios: An analysis with the World-TIMES model,” *Energy Policy*, vol. 36, no. 7, pp. 2296 – 2307, 2008, doi: 10.1016/j.enpol.2008.01.015.

[47] K. Tokimatsu, K. Okano, T. Yoshida, K. Yamaji, and M. Katsurai, “Study of design parameters for minimizing the cost of electricity of tokamak fusion power reactors,” *Nucl. Fusion*, vol. 38, no. 6, pp. 885–902, 1998, doi: 10.1088/0029-5515/38/6/307.

[48] K. Gi, F. Sano, K. Akimoto, R. Hiwatari, and K. Tobita, “Potential contribution of fusion power generation to low-carbon development under the Paris Agreement and associated uncertainties,” *Energy Strateg. Rev.*, vol. 27, no. October 2019, p. 100432, 2020, doi: 10.1016/j.esr.2019.100432.

[49] Y. Fujii and K. Yamaji, “Assessment of technological options in the global energy system for limiting the atmospheric CO2 concentration,” *Environ. Econ. Policy Stud.*, vol. 1, no. 2, pp. 113–139, 1998, doi: 10.1007/bf03353897.

[50] K. Okano *et al.*, “Compact reversed shear tokamak reactor with a superheated steam cycle,” *Nucl. Fusion*, vol. 40, no. SPEC. ISS. 3, pp. 635 – 646, 2000, doi: 10.1088/0029-5515/40/3Y/326.

[51] K. Tobita *et al.*, “SlimCS - Compact low aspect ratio DEMO reactor with reduced-size central solenoid,” *Nucl. Fusion*, vol. 47, no. 8, pp. 892 – 899, 2007, doi: 10.1088/0029-5515/47/8/022.

[52] D. Lerede and L. Savoldi, “Might future electricity generation suffice to meet the global demand?,” *Submitt. to Energy Strateg. Rev.*, 2022.

[53] C. Allwood, J M; Bosetti, V; Dubash, N K; Gómez-Echeverri, L; von Stechow, “Glossary. In Climate Change 2014: Mitigation of Climate Change; Contribution of Working Group III to the Fifth Assessment Report of the Intergovernmental Panel on Climate Change,” Cambridge, USA, 2014.

[54] International Energy Agency, Energy Technology Systems Analysis Program, and Decisionware Group August, “TIMES - Starter Model Guidelines for Use,” no. August, 2016.

[55] R. Loulou, A. Lehtilä, A. Kanudia, U. Remme, and G. Goldstein, "Documentation for the TIMES Model Part II," 2016.

[56] North Carolina State University, "TEMOA Database Construction," 2022. https://temoacloud.com/temoaproject/Documentation.html#database-construction (accessed Oct. 24, 2022).

[57] M. Gargiulo, K. Vailancourt, and R. De Miglio, *Documentation for the TIMES Model Part IV*. 2016.

[58] IPCC, *Climate Change 2021: The Physical Science Basis. Contribution of Working Group I to the Sixth Assessment Report of the Intergovernmental Panel on Climate Change*. Cambridge University Press. In Press, 2021.

[59] International Renewable Energy Agency, *Planning for the Renewable Future: Long-term modelling and tools to expand variable renewable power in emerging economices*. Dubai, UAE, 2017.

[60] International Energy Agency and Energy Technology Systems Analysis Program, "Applications," 2005. https://iea-etsap.org/index.php/applications (accessed Nov. 02, 2022).

[61] International Energy Agency and Energy Technology Systems Analysis Program, "MARKAL," 2005. https://iea-etsap.org/index.php/etsap-tools/model-generators/markal (accessed Nov. 02, 2022).

[62] International Energy Agency, *Energy Technology Perspectives 2006*. Paris, France, 2007.

[63] W. Nijs and P. Ruiz, "01_JRC-EU-TIMES Full model," 2019. http://data.europa.eu/89h/8141a398-41a8-42fa-81a4-5b825a51761b (accessed Oct. 20, 2022).

[64] International Energy Agency, "The Future of Petrochemicals - Towards more sustainable plastics and fertilizers: Methodological Annex," Paris, France, 2018.

[65] R. Vicente-Saez, R. Gustafsson, and L. Van den Brande, "The dawn of an open exploration era: Emergent principles and practices of open science and innovation of university research teams in a digital world," *Technol. Forecast. Soc. Change*, vol. 156, p. 120037, Jul. 2020, doi: 10.1016/J.TECHFORE.2020.120037.

[66] European Commission, "The EU's open science policy," 2020. https://ec.europa.eu/info/research-and-innovation/strategy/strategy-2020-2024/our-digital-future/open-science_en#the-eus-open-science-policy

(accessed Nov. 02, 2022).

[67] S. Pfenninger, J. DeCarolis, L. Hirth, S. Quoilin, and I. Staffell, “The importance of open data and software: Is energy research lagging behind?,” *Energy Policy*, vol. 101, pp. 211–215, Feb. 2017, doi: 10.1016/J.ENPOL.2016.11.046.

[68] J. Skea, R. van Diemen, J. Portugal-Pereira, and A. Al Khourdajie, “Outlooks, explorations and normative scenarios: Approaches to global energy futures compared,” *Technol. Forecast. Soc. Change*, vol. 168, no. July 2020, pp. 16–18, 2021, doi: 10.1016/j.techfore.2021.120736.

[69] Risø National Laboratory Denmark *et al.*, *Balmorel: A Model for Analyses of the Electricity and CHP Markets in the Baltic Sea Region*. 2001.

[70] J. Hörsch, F. Hofmann, D. Schlachtberger, and T. Brown, “PyPSA-Eur: An open optimisation model of the European transmission system,” *Energy Strateg. Rev.*, vol. 22, pp. 207–215, 2018, doi: https://doi.org/10.1016/j.esr.2018.08.012.

[71] J. Johnston, R. Henriquez-Auba, B. Maluenda, and M. Fripp, “Switch 2.0: A modern platform for planning high-renewable power systems,” *SoftwareX*, vol. 10, p. 100251, 2019, doi: https://doi.org/10.1016/j.softx.2019.100251.

[72] KTH-dESA, *OSeMOSYS Documentation*. Stockholm, Sweden, 2021.

[73] J. F. Decarolis, K. Hunter, and S. Sreepathi, “The TEMOA Project : Tools for Energy Model Optimization and Analysis,” *Energy Econ.*, vol. 40, pp. 339–349, 2010, doi: 10.1016/j.eneco.2013.07.014.

[74] J. F. DeCarolis, S. Babaee, B. Li, and S. Kanungo, “Modelling to generate alternatives with an energy system optimization model,” *Environ. Model. Softw.*, vol. 79, pp. 300–310, 2016, doi: 10.1016/j.envsoft.2015.11.019.

[75] T. Santos, “Regional energy security goes South: Examining energy integration in South America,” *Energy Res. Soc. Sci.*, vol. 76, p. 102050, Jun. 2021, doi: 10.1016/J.ERSS.2021.102050.

[76] M. V. Rocco, E. Fumagalli, C. Vigone, A. Miserocchi, and E. Colombo, “Enhancing energy models with geo-spatial data for the analysis of future electrification pathways: The case of Tanzania,” *Energy Strateg. Rev.*, vol. 34, p. 100614, Mar. 2021, doi: 10.1016/J.ESR.2020.100614.

[77] A. Dhakouani, E. Znouda, and C. Bouden, “Impacts of energy efficiency policies on the integration of renewable energy,” *Energy Policy*, vol. 133,

p. 110922, Oct. 2019, doi: 10.1016/J.ENPOL.2019.110922.

[78] Y. Chung, C. Paik, and Y. J. Kim, “Open source-based modeling of power plants retrofit and its application to the Korean electricity sector,” *Int. J. Greenh. Gas Control*, vol. 81, pp. 21–28, Feb. 2019, doi: 10.1016/J.IJGGC.2018.12.005.

[79] J. Anjo, D. Neves, C. Silva, A. Shivakumar, and M. Howells, “Modeling the long-term impact of demand response in energy planning: The Portuguese electric system case study,” *Energy*, vol. 165, pp. 456–468, Dec. 2018, doi: 10.1016/J.ENERGY.2018.09.091.

[80] M. Welsch *et al.*, “Incorporating flexibility requirements into long-term energy system models – A case study on high levels of renewable electricity penetration in Ireland,” *Appl. Energy*, vol. 135, pp. 600–615, 2014, doi: https://doi.org/10.1016/j.apenergy.2014.08.072.

[81] J. F. DeCarolis, K. Hunter, and S. Sreepathi, “Multi-stage stochastic optimization of a simple energy system,” 2012.

[82] P. Seljom, L. Kvalbein, L. Hellemo, M. Kaut, and M. M. Ortiz, “Stochastic modelling of variable renewables in long-term energy models: Dataset, scenario generation & quality of results,” *Energy*, vol. 236, p. 121415, 2021, doi: https://doi.org/10.1016/j.energy.2021.121415.

[83] H. Eshraghi, A. R. de Queiroz, and J. F. DeCarolis, “US Energy-Related Greenhouse Gas Emissions in the Absence of Federal Climate Policy.,” *Environ. Sci. Technol.*, vol. 52, no. 17, pp. 9595–9604, Sep. 2018, doi: 10.1021/acs.est.8b01586.

[84] M. McGrath, “Climate change: US formally withdraws from Paris agreement,” *BBC News*, 2020.

[85] A. J. Blinken, “US makes official return to Paris climate pact.” 2021, [Online]. Available: https://www.state.gov/the-united-states-officially-rejoins-the-paris-agreement/.

[86] C. Lenox, R. Dodder, C. Gage, O. Kaplan, D. Loughlin, and W. Yelverton, “EPA U .S . Nine-region MARKAL Database Database Documentation,” 2013.

[87] O. E. Outlook, “Open Energy Outlook for the United States,” 2016. https://openenergyoutlook.org/ (accessed Aug. 13, 2021).

[88] B. Li, J. Thomas, A. R. de Queiroz, and J. F. DeCarolis, “Open Source Energy System Modeling Using Break-Even Costs to Inform State-Level

Policy: A North Carolina Case Study," *Environ. Sci. Technol.*, vol. 54, no. 2, pp. 665–676, Jan. 2020, doi: 10.1021/acs.est.9b04184.

[89] N. Patankar, A. R. de Queiroz, J. F. DeCarolis, M. D. Bazilian, and D. Chattopadhyay, "Building conflict uncertainty into electricity planning: A South Sudan case study," *Energy Sustain. Dev.*, vol. 49, pp. 53–64, Apr. 2019, doi: 10.1016/J.ESD.2019.01.003.

[90] N. Patankar, H. Eshraghi, A. R. de Queiroz, and J. F. DeCarolis, "Using robust optimization to inform US deep decarbonization planning," *Energy Strateg. Rev.*, vol. 42, p. 100892, 2022, doi: https://doi.org/10.1016/j.esr.2022.100892.

[91] C. L. Henry *et al.*, "Promoting reproducibility and increased collaboration in electric sector capacity expansion models with community benchmarking and intercomparison efforts," *Appl. Energy*, vol. 304, p. 117745, 2021, doi: https://doi.org/10.1016/j.apenergy.2021.117745.

[92] M. Nicoli, F. Gracceva, D. Lerede, and L. Savoldi, "Can we rely on open-source Energy System Optimization Models? The TEMOA-Italy case study," *Energies*, vol. 15, no. 18, p. 6505, 2022, doi: https://doi.org/10.3390/en15186505.

[93] L. Ford, A. de Queiroz, J. DeCarolis, and A. Sankarasubramanian, "Co-Optimization of Reservoir and Power Systems (COREGS) for seasonal planning and operation," *Energy Reports*, vol. 8, pp. 8061–8078, Nov. 2022, doi: 10.1016/J.EGYR.2022.06.017.

[94] A. R. de Queiroz *et al.*, "Repurposing an energy system optimization model for seasonal power generation planning," *Energy*, vol. 181, pp. 1321–1330, 2019, doi: https://doi.org/10.1016/j.energy.2019.05.126.

[95] J. A. Bennett *et al.*, "Extending energy system modelling to include extreme weather risks and application to hurricane events in Puerto Rico," *Nat. Energy*, vol. 6, no. 3, pp. 240–249, 2021, doi: 10.1038/s41560-020-00758-6.

[96] Y. Almulla *et al.*, *Model Management Infrastructure (MoManI) Training Manual*. 2017.

[97] J. Decarolis, "Temoa on the Cloud," 2021. https://www.youtube.com/watch?v=fxYO_kIs364&ab_channel=JoeDeCarolis (accessed Nov. 02, 2022).

[98] The Editors of Encyclopaedia Britannica, "SQL computer language," 2009.

https://www.britannica.com/technology/SQL (accessed Nov. 02, 2022).

[99] E. Wright, A. Kanudia, R. Loulou, and G. Goldstein, *Documentation for the TIMES Model Part V*. 2016.

[100] IBM Corp., "CPLEX Optimizer," 2022. https://www.ibm.com/it-it/analytics/cplex-optimizer (accessed Nov. 02, 2022).

[101] Energy Technology Systems Analysis Program, "Letter of Agreement."

[102] Free Software Foundation, "GNU Linear Programming Kit, Version 4.52," 2014. [Online]. Available: http://www.gnu.org/software/glpk/glpk.html.

[103] Python Software Foundation, "Python," 2022. https://www.python.org/ (accessed Nov. 02, 2022).

[104] GAMS Development Corporation and GAMS Software GmbH, "Gams Documentation Center," 2022. https://www.gams.com/latest/docs/ (accessed Nov. 02, 2022).

[105] IBM Corp., "User's Manual for CPLEX," *International Business Machines Corporation*, 2009. http://scholar.google.com/scholar?hl=en&btnG=Search&q=intitle:User's+Manual+for+CPLEX#1 (accessed Aug. 12, 2021).

[106] Gurobi Optimization, "Gurobi Optimizer Reference Manual." https://www.gurobi.com/documentation/9.1/refman/index.html (accessed Aug. 12, 2021).

[107] European Commission, "A European Green Deal," 2019. https://ec.europa.eu/info/strategy/priorities-2019-2024/european-green-deal_en (accessed Feb. 23, 2022).

[108] M. Windridge, "Huge Growth In Fusion Energy Industry, Shows New Report," *Forbes*, 2022.

[109] D. Lerede, C. Bustreo, F. Gracceva, Y. Lechón, and L. Savoldi, "Analysis of the effects of electrification of the road transport sector on the possible penetration of nuclear fusion in the long-term european energy mix," *Energies*, vol. 13, no. 14, 2020, doi: 10.3390/en13143634.

[110] D. Lerede, M. Nicoli, L. Savoldi, and A. Trotta, "Analysis of the possible contribution of different nuclear fusion technologies to the global energy transition," *sumbitted to Energy Strateg. Rev.*, 2023.

[111] S. Pfenninger *et al.*, "Opening the black box of energy modelling:

Strategies and lessons learned," *Energy Strateg. Rev.*, vol. 19, pp. 63–71, 2018, doi: 10.1016/j.esr.2017.12.002.

[112] Deutsche Automobil Treuhand GmbH, "Leitfaden über den Kraftstoffverbrauch,die CO2-Emissionen und den Stromverbrauch aller neuen Personenkraftwagenmodelle, die in Deutschland zum Verkauf angeboten werden," 2018. [Online]. Available: https://www.dat.de/co2/.

[113] Engineering Toolbox, "Fuels properties database," 2019. https://www.engineeringtoolbox.com (accessed Oct. 13, 2022).

[114] European Environment Agency, "Occupancy rates of passenger vehicles," 2021. https://www.eea.europa.eu/data-and-maps/indicators/occupancy-rates-of-passenger-vehicles/occupancy-rates-of-passenger-vehicles (accessed Feb. 10, 2023).

[115] The Real Urban Emissions Initiative, "Explanation of the TRUE real-world passenger vehicle emissions rating system," 2018. https://theicct.org/sites/default/files/publications/TRUE_explanation_technical_20180604.pdf (accessed Nov. 26, 2019).

[116] L. Mårtensson, "Emissions from Volvo ' s trucks Emissions from Volvo's trucks to facilitate emission calculation from transport," 2018.

[117] European Automobile Manufacturers' Association, "Tax Guide 2019," 2019. [Online]. Available: https://www.acea.be/uploads/news_documents/ACEA_Tax_Guide_2019.pdf.

[118] M. Redelbach, P. B., D. Santini, and H. E. Friedrich, "Cost analysis of Plug in Hybrid Electric Vehicles including Maintenance & Repair costs and Resale Value," 2016.

[119] P. Muehlich and T. Hamacher, "Global transportation scenarios in the multi-regional EFDA-TIMES energy model," *Fusion Eng. Des.*, vol. 84, no. 7, pp. 1361–1366, 2009, doi: https://doi.org/10.1016/j.fusengdes.2008.12.016.

[120] M. Mantzos, Leonidas; Wiesenthal, Tobias; Neuwahl, Frederik; Rózsai, "POTEnCIA Central-2018 scenario," *European Commission, Joint Research Centre*, 2019. .

[121] Organization for Economic Co-operation and Development and International Energy Agency, *Energy Balances of OECD Countries (2009 Edition)*. 2009.

[122] Airbus, “Hydrogen,” 2022. https://www.airbus.com/en/innovation/zero-emission-journey/hydrogen (accessed Feb. 10, 2022).

[123] Energy Technology Systems Analysis Program, “Technology Brief T12 - Aviation Transport,” 2011.

[124] Energy Technology Systems Analysis Program, “Technology Brief T11 - Rail Transport,” 2011.

[125] Energy Technology Systems Analysis Program, “Technology Brief T13 - Shipping Transport,” 2011.

[126] Energy Technology Systems Analysis Program, “E-TechDS – Energy Technology Data Source,” 2013. https://iea-etsap.org/index.php/energy-technology-data (accessed Oct. 19, 2022).

[127] Energy Technology Systems Analysis Program, “Energy Supply Technology Data,” 2013. https://iea-etsap.org/index.php/energy-technology-data/energy-supply-technologies-data (accessed Oct. 19, 2022).

[128] Energy Technology Systems Analysis Program, “Energy Demand Technology Data,” 2013. https://iea-etsap.org/index.php/energy-technology-data/energy-demand-technologies-data (accessed Oct. 19, 2022).

[129] T. Ekholm and A. Lehtilä, “EFDA-TIMES Model Industry Update,” Espoo, Finland, 2008.

[130] K.-K. Cao, F. Cebulla, J. J. Gómez Vilchez, B. Mousavi, and S. Prehofer, “Raising awareness in model-based energy scenario studies—a transparency checklist,” *Energy. Sustain. Soc.*, vol. 6, no. 1, p. 28, 2016, doi: 10.1186/s13705-016-0090-z.

[131] A. Jaques, F. Neitzert, and P. Boileau Hull, *Trends in Canada`s greenhouse gas emissions (1990-1995)*. Canada: Environment Canada, Ottawa, ON (Canada), 1997.

[132] S. Hornby Anderson and D. R. Urban, “Cost and Quality Effectiveness of Carbon Dioxide in Steel Mills,” 1989.

[133] R. Remus, M. A. Aguado-Monsonet, S. Roudier, and L. Delgado Sancho, “Best Available Techniques (BAT) Reference Document for Iron and Steel Production,” Luxembourg, Luxembourg, 2013.

[134] E. Worrell, L. Price, M. Neelis, C. Galitsky, and N. Zhou, “World Best Practice Energy Intensity Values for Selected Industrial Sectors,” 2007.

[135] International Energy Agency and UNIDO, “Technology Roadmap - Carbon Capture and Storage in Industrial Applications,” Paris, France, 2011. doi: 10.4324/9781315264783-86.

[136] Tata Steel, “HISARNA - Building a sustainable steel industry,” Mumbai, India, 2019. [Online]. Available: https://www.tatasteeleurope.com/sites/default/files/tata-steel-europe-factsheet-hisarna.pdf.

[137] H. Croezen and M. Korteland, “Technological developments in Europe - A long-term view of CO2 efficient manufacturing in the European region,” Delft, The Netherlands, 2010.

[138] V. Vogl, M. Åhman, and L. J. Nilsson, “Assessment of hydrogen direct reduction for fossil-free steelmaking,” *J. Clean. Prod.*, vol. 203, pp. 736–745, 2018, doi: https://doi.org/10.1016/j.jclepro.2018.08.279.

[139] H. Lavelaine *et al.*, *Iron production by electrochemical reduction of its oxide for high CO2 mitigation*. Brussels, Belgium, 2016.

[140] M. Gasik, *Handbook of Ferroalloys*. Espoo, Finland, 2013.

[141] S. Singerling *et al.*, “Geological Survey Minerals Yearbook - Ferroalloys,” Reston, USA, 2015.

[142] M. Wörtler *et al.*, “Steel’s contribution to a low-carbon Europe 2050 - Technical and economic analysis of the sector’s CO2 abatement potential,” Boston, USA, 2013.

[143] J. Mayer, G. Bachner, and K. W. Steininger, “Macroeconomic implications of switching to process-emission-free iron and steel production in Europe,” *J. Clean. Prod.*, vol. 210, pp. 1517–1533, 2019, doi: https://doi.org/10.1016/j.jclepro.2018.11.118.

[144] T. Kuramochi, A. Ramírez, W. Turkenburg, and A. Faaij, “Comparative assessment of CO2 capture technologies for carbon-intensive industrial processes,” *Prog. Energy Combust. Sci.*, vol. 38, no. 1, pp. 87–112, 2012, doi: https://doi.org/10.1016/j.pecs.2011.05.001.

[145] B. Anameric and S. K. Kawatra, “Direct Iron Smelting Reduction Processes,” *Miner. Process. Extr. Metall. Rev.*, vol. 30, no. 1, pp. 1–51, 2008, doi: 10.1080/08827500802043490.

[146] Organization for Economic Co-operation and Development, “Exchange rates,” 2020. https://data.oecd.org/conversion/exchange-rates.htm (accessed Oct. 19, 2022).

[147] H. L. Brunjes and M. J. Manning, “Determination of Sulfur in Coal and Coke,” *Ind. Eng. Chem. Anal. Ed.*, vol. 12, no. 12, pp. 718–720, Dec. 1940, doi: 10.1021/ac50152a004.

[148] World Aluminum, “Metallurgical alumina refining fuel consumption,” 2020. www.world-aluminum.org/statistics (accessed Oct. 19, 2022).

[149] J. A. Moya *et al.*, “Energy Efficiency and GHG Emissions: Prospective Scenarios for the Aluminum Industry,” Luxembourg, Luxembourg, 2015.

[150] European Aluminum Association, “Environmental Profile Report for the Aluminum Industry,” Brussels, Belgium, 2018.

[151] Energy Technology Systems Analysis Program, “Technology Brief I10 - Aluminum Production,” 2012.

[152] International Energy Agency, “Industry,” *Tracking Report - September 2022*, 2022. https://www.iea.org/reports/industry (accessed Oct. 20, 2022).

[153] Sayad-Yaghoubi and G. Smith, “Low Temperature Aluminum Carbothermic Smelting Process,” 2013.

[154] J. A. S. Green, *Aluminum Recycling and Processing for Energy Conservation and Sustainability*. 2007.

[155] S. Alvarado, P. Maldonado, A. Barrios, and I. Jaques, “Long term energy-related environmental issues of copper production,” *Energy*, vol. 27, no. 2, pp. 183–196, 2002, doi: https://doi.org/10.1016/S0360-5442(01)00067-6.

[156] International Energy Agency, “Tracking Industrial Energy Efficiency and CO2 Emissions,” Paris, France, 2007.

[157] C. A. Dunne, Robert C.; Kawatra, S Komar; Young, *SME Mineral Processing and Extractive Metallurgy Handbook*. Englewood, USA, 2019.

[158] F. Schorcht, I. Kourti, S. Bianca Maria, S. Roudier, and L. Delgado Sancho, “Best Available Techniques (BAT) Reference Document for the Production of Cement, Lime and Magnesium Oxide,” Luxembourg, Luxembourg, 2013.

[159] N. A. Madlool, R. Saidur, M. S. Hossain, and N. A. Rahim, “A critical review on energy use and savings in the cement industries,” *Renew. Sustain. Energy Rev.*, vol. 15, no. 4, pp. 2042–2060, 2011, doi: https://doi.org/10.1016/j.rser.2011.01.005.

[160] Energy Technology Systems Analysis Program, “Technology Brief I03 -

Cement Production," 2010.

[161] IEAGHG, "Deployment of CCS in the cement industry," Stoke Orchard, Cheltenham, United Kingdom, 2013. [Online]. Available: https://ieaghg.org/docs/General_Docs/Reports/2013-19.pdf.

[162] A. Nazari and J. G. Sangjayan, "Handbook of Low Carbon Concrete," Oxford, United Kingdom, 2017.

[163] International Energy Agency, "Technology Roadmap, Low-Carbon Transition in the Cement Industry," Paris, France, 2018.

[164] B. M. Scalet, M. Garcia Muñoz, A. Q. Sissa, S. Roudier, and L. Delgado Sancho, "Best Available Techniques (BAT) Reference Document for the Manufacture of Glass," Luxembourg, Luxembourg, 2014.

[165] Statista, "Average price of crude gypsum on a free-on board (FOB) mine basis," 2020. https://www.statista.com/statistics/219363/wallboard-products-crude-price-in-the-us/ (accessed Oct. 20, 2022).

[166] B. Tempest, C. Snell, T. Gentry, M. Trejo, and K. Isherwood, "Manufacture of full-scale geopolymer cement concrete components: A case study to highlight opportunities and challenges," *PCI J.*, vol. 60, no. 6, pp. 39–50, 2015, doi: 10.15554/pcij.11012015.39.50.

[167] G. Kotsay and R. Jaskulski, "Belite cement as an ecological alternative to Portland cement-a review," *Mater. Struct. Technol.* , vol. 2, no. 1, pp. 70–76, 2019, doi: 10.31448/mstj.02.01.2019.70-76.

[168] International Energy Agency, "The Future of Petrochemicals - Towards more sustainable plastics and fertilizers," Paris, France, 2018.

[169] T. Brinkmann, G. G. Santonja, F. Schorcht, R. Serge, and L. Delgado Sancho, "Best Available Techniques (BAT) Reference Document for the Production of Chlor-Alkali," Luxembourg, Luxembourg, 2014.

[170] P. Bajpai, "Pulp and Paper Production Processes and Energy Overview," in *Pulp and Paper Industry*, Elsevier, Ed. 2016, pp. 15–49.

[171] US Department of Energy, "Energy and environmental profile of the U.S. pulp and paper industry," Columbia, USA, 2005.

[172] M. Suhr *et al.*, "Best Available Techniques (BAT) Reference Document for the Production of Paper, Pulp and Board," Luxembourg, Luxembourg, 2015.

[173] European Commission, “A hydrogen strategy for a climate-neutral Europe,” *Hydrogen Strategy*, 2022. https://ec.europa.eu/energy/sites/ener/files/hydrogen_strategy.pdf (accessed Mar. 10, 2022).

[174] H. Blanco, W. Nijs, J. Ruf, and A. Faaij, “Potential for hydrogen and Power-to-Liquid in a low-carbon EU energy system using cost optimization,” *Appl. Energy*, vol. 232, no. October, pp. 617–639, 2018, doi: 10.1016/j.apenergy.2018.09.216.

[175] A. Balbo, “Will hydrogen be a game-changer in the Italian decarbonization pathways? Exploiting an Energy System Optimization Model for scenario analysis,” Politecnico di Torino, 2022.

[176] International Energy Agency, “Global Hydrogen Review 2021,” 2021.

[177] M. W. Melaina, O. Antonia, and M. Penev, “Blending Hydrogen into Natural Gas Pipeline Networks : A Review of Key Issues Blending Hydrogen into Natural Gas Pipeline Networks : A Review of Key Issues,” no. March, 2013.

[178] H. Cabal *et al.*, “Fusion power in a future low carbon global electricity system,” *Energy Strateg. Rev.*, vol. 15, pp. 1–8, 2017, doi: https://doi.org/10.1016/j.esr.2016.11.002.

[179] Y. Lechon *et al.*, “A global energy model with fusion,” *Fusion Eng. Des.*, vol. 75–79, no. SUPPL., pp. 1141–1144, 2005, doi: 10.1016/j.fusengdes.2005.06.078.

[180] M. Kovari, R. Kemp, H. Lux, P. Knight, J. Morris, and D. J. Ward, “‘PROCESS’: A systems code for fusion power plants—Part 1: Physics,” *Fusion Eng. Des.*, vol. 89, no. 12, pp. 3054–3069, 2014, doi: https://doi.org/10.1016/j.fusengdes.2014.09.018.

[181] D. N. Dongiovanni and M. T. Porfiri, “Methodology for Investigating Safety Impact on Design and Costs,” Garching bei München, 2016.

[182] W. E. Han and D. J. Ward, “A preliminary scoping study of the role of fusion in the future energy market using the EFDA/TIMES Model,” 2007.

[183] J. Raeder *et al.*, “Review of the safety concept for fusion reactor concepts and transferability of the nuclear fission regulation to potential fusion power plants,” 2016. [Online]. Available: https://www.grs.de/sites/default/files/publications/grs-389_1.pdf.

[184] S. Segantin, A. Bersano, N. Falcone, and R. Testoni, “Exploration of power

conversion thermodynamic cycles for ARC fusion reactor," *Fusion Eng. Des.*, vol. 155, p. 111645, 2020, doi: https://doi.org/10.1016/j.fusengdes.2020.111645.

[185] E. Albagli, F. Grigoli, and E. Luttini, "Inflation Expectations and the Supply Chain," 2022.

[186] G. Federici, W. Biel, M. R. Gilbert, R. Kemp, and N. Taylor, "European DEMO design strategy and consequences for materials," *Nucl. Fusion*, vol. 57, no. 9, p. 092002, 2017.

[187] ORDECSYS, KanORS, HALOA, and KU Leuven Energy Institute, "EFDA World TIMES Model," 2004.

[188] MAHTEP Group, "MAHTEP/TEMOA," *GitHub*, 2023. https://github.com/MAHTEP/TEMOA (accessed Feb. 15, 2023).

[189] D. Lerede, "MAHTEP/TEMOA-Europe release 1.0." MAHTEP Group, 2023, [Online]. Available: https://github.com/MAHTEP/TEMOA-Europe/releases/tag/1.0.

[190] U. Remme, M. Blesl, and T. Kober, "The Dual Solution of a TIMES Model : its interpretation and price formation equations," 2009.

[191] M. Nicoli, G. Colucci, D. Lerede, and L. Savoldi, "GitHub - MAHTEP/TEMOA-Italy," *MAHTEP Group*, 2022. https://github.com/MAHTEP/TEMOA-Italy (accessed May 11, 2022).

[192] North Carolina State University, "Github - An open source energy system model: TemoaProject," 2022. https://github.com/TemoaProject/ (accessed Nov. 14, 2022).

[193] U.S. Energy Information Administration, "International Energy Outlook 2021," 2022. https://www.eia.gov/outlooks/aeo/data/browser/#/?id=3-IEO2021&cases=Reference&sourcekey=0 (accessed Feb. 09, 2023).

[194] N. Patankar, H. G. Fell, A. Rodrigo de Queiroz, J. Curtis, and J. F. DeCarolis, "Improving the representation of energy efficiency in an energy system optimization model," *Appl. Energy*, vol. 306, p. 118083, 2022, doi: https://doi.org/10.1016/j.apenergy.2021.118083.

[195] International Energy Agency, "Key World Energy Statistics 2021," Paris, France, 2021. [Online]. Available: https://www.iea.org/reports/key-world-energy-statistics-2021.

[196] International Energy Agency, "Electricity statistics," 2020.

https://www.iea.org/fuels-and-technologies/electricity (accessed Feb. 24, 2022).

[197] International Monetary Fund, *World Economic Outlook: crisis and recovery*, vol. 6. 2009.

[198] U.S Energy Information Administration, "Short-Term Energy Outlook Forecast highlights," 2022.

[199] R. Gunther McGrath, "The Pace of Technology Adoption is Speeding Up," *Harvard Business Review*, 2019.

[200] P. A. Geroski, "Models of technology diffusion," *Res. Policy*, vol. 29, no. 4, pp. 603–625, 2000, doi: https://doi.org/10.1016/S0048-7333(99)00092-X.

[201] A. Cherp, V. Vinichenko, J. Tosun, J. A. Gordon, and J. Jewell, "National growth dynamics of wind and solar power compared to the growth required for global climate targets," *Nat. Energy*, vol. 6, no. July, pp. 742–754, 2021, doi: 10.1038/s41560-021-00863-0.

[202] Z. Griliches, "Hybrid Corn: An Exploration in the Economics of Technological Change," *Econometrica*, vol. 25, no. 4, pp. 501–522, Nov. 1957, doi: 10.2307/1905380.

[203] B. Gompertz, "XXIV. On the nature of the function expressive of the law of human mortality, and on a new mode of determining the value of life contingencies. In a letter to Francis Baily, Esq. F. R. S. &c," *Philos. Trans.*, vol. 115, pp. 513–583, 1825.

[204] K. A. Collett, S. M. Bhagavathy, and M. D. McCulloch, "Forecast of electric vehicle uptake across counties in England: Dataset from S-curve analysis," *Data Br.*, vol. 39, p. 107662, 2021, doi: https://doi.org/10.1016/j.dib.2021.107662.

[205] M. Taylor and A. Taylor, "The technology life cycle: Conceptualization and managerial implications," *Int. J. Prod. Econ.*, vol. 140, no. 1, pp. 541–553, 2012, doi: https://doi.org/10.1016/j.ijpe.2012.07.006.

[206] M. Nieto, F. Lopéz, and F. Cruz, "Performance analysis of technology using the S curve model: the case of digital signal processing (DSP) technologies," *Technovation*, vol. 18, no. 6, pp. 439–457, 1998, doi: https://doi.org/10.1016/S0166-4972(98)00021-2.

[207] E. R. Otto, *Innovation: the attacker's advantage*. 1986.

[208] N. J. Lopes Cardozo, A. G. G. Lange, and G. J. Kramer, “Fusion: Expensive and Taking Forever?,” *J. Fusion Energy*, vol. 35, no. 1, pp. 94–101, 2016, doi: 10.1007/s10894-015-0012-7.

[209] S. A. Gabriel, A. S. Kydes, and P. Whitman, “The national energy modeling system: A large-scale energy-economic equilibrium model,” *Oper. Res.*, vol. 49, no. 1, pp. 14–25, 2001, doi: 10.1287/opre.49.1.14.11195.

[210] G. J. Kramer and M. Haigh, “No quick switch to low-carbon energy,” *Nature*, vol. 462, no. 7273, pp. 568–569, 2009, doi: 10.1038/462568a.

[211] United Nations Scientific Committee on the Effects of Atomic Radiation, “Assessments of the radiation effects from the Chernobyl nuclear reactor accident,” 2008. https://www.unscear.org/unscear/en/areas-of-work/chernobyl.html (accessed Oct. 24, 2022).

[212] World Nuclear Association, “Fukushima Daiichi Accident,” 2022. https://world-nuclear.org/information-library/safety-and-security/safety-of-plants/fukushima-daiichi-accident.aspx (accessed Oct. 24, 2022).

[213] A. Breidthardt, “German government wants nuclear exit by 2022 at latest,” *Reuters*, 2011.

[214] J. Joly, “Germany begins nuclear phase-out, shuts down three of six nuclear power plants,” *Euronews*, 2021. https://www.euronews.com/2021/12/31/germany-begins-nuclear-phase-out-shuts-down-three-of-six-nuclear-power-plants.

[215] Microsoft, “LOGEST function.” https://support.microsoft.com/en-us/office/logest-function-f27462d8-3657-4030-866b-a272c1d18b4b (accessed Jul. 18, 2022).

[216] Microsoft, “LINEST function.” https://support.microsoft.com/en-us/office/linest-function-84d7d0d9-6e50-4101-977a-fa7abf772b6d#:~:text=The LINEST function calculates the,array that describes the line. (accessed Jul. 18, 2022).

[217] N. R. Draper and H. Smith, *Applied Regression Analysis*. 1998.

[218] U.S Energy Information Administration, “International data - Electricity,” 2021. https://www.eia.gov/international/data/world (accessed Mar. 04, 2022).

[219] International Renewable Energy Agency, “Wind energy,” *Wind*, 2021. https://www.irena.org/wind#:~:text=Global installed wind-generation

capacity,according to IRENA's latest data. (accessed Mar. 29, 2022).

[220] International Renewable Energy Agency, "Solar energy," *Solar*, 2021. https://www.irena.org/solar (accessed Mar. 29, 2022).

[221] World Nuclear Association, "Nuclear Power in France," 2022. https://world-nuclear.org/information-library/country-profiles/countries-a-f/france.aspx (accessed Oct. 25, 2022).

[222] L. Ziegler, E. Gonzalez, T. Rubert, U. Smolka, and J. J. Melero, "Lifetime extension of onshore wind turbines: A review covering Germany, Spain, Denmark, and the UK," *Renew. Sustain. Energy Rev.*, vol. 82, pp. 1261–1271, Feb. 2018, doi: 10.1016/J.RSER.2017.09.100.

[223] R. Mumgaard, "CFS and the new public-private fusion energy landscape," 2022, [Online]. Available: https://www.ipp.mpg.de/events/30326/4042067.

[224] REN21, "REN21: Renewables 2017 Global Status Report," 2021. [Online]. Available: http://www.ren21.net/status-of-renewables/global-status-report/.

[225] D. N. Dongiovanni, A. V. Müller, and S. Banacloche Sánchez, "Resources and materials availabilty for fusion reactors - 2021," Garching bei München, 2021.

[226] U.S. Energy Information Administration, "International Energy Outlook 2019," 2019. doi: 10.5860/choice.44-3624.

[227] European Commission, "Fit for 55," 2022. https://www.consilium.europa.eu/en/policies/green-deal/fit-for-55-the-eu-plan-for-a-green-transition/ (accessed Dec. 07, 2022).

[228] Climate Action Tracker, "Country Summary - EU," 2022. https://climateactiontracker.org/countries/eu/ (accessed Dec. 07, 2022).

[229] G. Colucci, M. Nicoli, D. Lerede, and L. Savoldi, "Dynamic Accounting for End-Use CO2 Emissions FromLow-Carbon Fuels in Energy System Optimization Models," in *Energy Proceedings*, 2022, p. 10294, doi: https://doi.org/10.46855/energy-proceedings-10294.

[230] Cepi, "Energy Efficiency and CO2 Reduction in the Pulp and Paper Industry," 2012. https://setis.ec.europa.eu/system/files/Technology_Information_Sheet_Energy_Efficiency_and_CO2_Reducton_in_the_Pulp_and_Paper_Industry.pdf (accessed Oct. 19, 2022).

[231] J. P. Birat, "ULCOS program: status & progress." Brussels, Belgium, 2010,

[Online]. Available: https://www.eesc.europa.eu/sites/default/files/resources/docs/estep_ulcos_nov_2010.pdf.

[232] Cemembrau, "Clinker substitution," 2018. https://lowcarboneconomy.cembureau.eu/5-parallel-routes/resource-efficiency/clinker-substitution/ (accessed Oct. 19, 2022).

[233] F. Pacheco-Torgal, J. Labrincha, C. Leonelli, A. Palomo, and P. Chindaprasit, "Handbook of alkali-activated Cements, Mortars and Concretes," 2015.

[234] International Energy Agency, "Projected Costs of Generating Electricity," Paris, France, 2010. doi: 10.1787/9789264008274-en.

Appendix

A summary of the energy-intensive technologies included in TEMOA-Europe and described in **Section 2.3** is provided here. The industrial database presented in this work is compared to the IEA ETP Model and the JRC-EU-TIMES in terms of availability of the different technologies.

In the TEMOA-Europe database, steel production is articulated over a set of 13 technologies including the whole manufacturing process starting from raw materials, to give steel as final product. The same happens in the IEA ETP Model, where, however, electrowinning (electrolysis-based) technologies are missing. In the JRC-EU-TIMES, instead, steel production is split in a set of processes starting from sintering and pelletizing of the iron ore, which can be then reduced either in a blast furnace or through direct reduction, and then further processed to give steel. Instead of modeling a secondary route for steel production from scrap, as it happens in this work and in IEA ETP, scrap iron is considered in the JRC-EU-TIMES as input for basic oxygen furnaces, electric arc furnaces and cast-iron cupola furnaces (the latter not considered in this work), along with quick lime. Concerning carbon capture and storage CCS-equipped technologies, they are considered for smelting reduction, BF-BOF and DRI-EAF processes, as done in this work, while electrowinning technologies are absent.

Ferroalloys production is modeled according to a single process in the present database, considering a weighted average energy consumption of global production processes, while they are not taken into account in the ETP Model and the JRC-EU-TIMES only considers ferrochromium as representative for the entire production field.

Eleven non-ferrous metals manufacturing technologies are characterized in this work and reported in **Table 35**. Six technologies are related to the production of aluminum. Aluminum production is articulated over two steps, namely alumina production and proper manufacturing of the aluminum. The first step is represented by the Bayer process, whose alumina output is given as input for aluminum technologies (except for the secondary route and kaolinite reduction). In the IEA ETP Model, aluminum production considers two primary (Hall-Héroult and Hall-Héroult with inert anodes) and one secondary processes,

neglecting alumina and the Bayer process. The same happens in the JRC-EU-TIMES, where the joint transformation of bauxite into alumina and the subsequent processing into aluminum occurs through the Hall-Héroult process (which is presented in a traditional variant and in four enhanced versions, one taking into account the use of inert anodes), while the secondary route is modelled considering scrap as input material (the limit on production from this route could be then explicitly derived by the model, instead of adopting user constraints).

Copper production is represented in this work by a single process, while it is not considered in the ETP Model and, in the JRC-EU-TIMES, an additional process with recycling is included, too (here not considered since the primary route already takes into account the presence of scrap).

A minor non-ferrous metal like zinc is considered only in this work.

A total of 11 non-metallic mineral manufacturing technologies are considered in the database for TEMOA-Europe and reported in **Table 36**.

Cement production is modelled in the JRC-EU-TIMES as it is done here, considering a clinker production step prior to cement blending, but innovative alternatives as alkali-activated concrete and belite cement, or the application of CCS for clinker production, are taken into account for TEMOA-Europe. Clinker is also considered in the ETP Model, but not explicitly modeling its production.

Lime production, ignored in the ETP model, is modelled in the JRC-EU-TIMES as a single process using a generic fuel representing a combination of coal, coke, thus not relying on any specific existing process, while a single reference technology is taken into account here.

Glass production in TEMOA-Europe just considers two processes relying either on fossil fuels or electricity. The JRC-EU-TIMES considers both standard and improved processes for hollow and flat glass production, including a process for glass recycling, since different commodities are considered to represent glass. Here, as in [129], a single generic type of glass is modeled, while glass production technologies are not at all present in the ETP Model.

Ceramics as energy-intensive materials are only taken into account here as in [129], and their production is modeled according to a single technology.

Twenty-three technologies are characterized here for the chemical sub-sector, eight for high value chemicals, which include olefins and aromatics, six for ammonia production, six for methanol production and three for chlorine production, exactly retracing the ETP Model (full details about techno-economic characterization of chemical technologies in the ETP are provided in [168]), as in **Table 37**. In the JRC-EU-TIMES, instead, chlorine production considers the same processes already described in this work, plus an advanced membrane technology (neglected here due to no reference found in the literature about such process), but bulk chemicals as HVCs and methanol are totally neglected.

Six "traditional" pulp-processing technologies are included in the TEMOA-Europe database, plus one representative papermaking plant, as reported in **Table 38**. In the JRC-EU-TIMES, instead, pulp production accounts for mechanical pulping, chemical pulping and recycled fiber pulping, while paper production includes low- and high-quality standard and advanced processes. For both, CCS is considered, differently from here. This last issue is quite relevant, because no directly emitting input sources are considered for pulp and paper production in this work, while natural gas use is considered in the JRC-EU-TIMES: CO_2 emissions from the pulp and paper industry are mainly related to the production of heat and steam for drying, which is not a subject of this work; furthermore, the European 2050 roadmap for pulp and paper does not include CCS as an option [230]. Pulping in the ETP Model considers again mechanical, chemical and recycled fiber techniques, while no details are provided on papermaking. Moreover, some innovative technologies at the R&D stage are mentioned in [27], but they are not modeled (an attempt was made for this work, but highlighting a lack of data to provide plausible estimations).

Table 34. Steelmaking technologies, with their deployment state and starting year for the introduction in the production system. The "×" indicates that a technology is present in the considered databases, the contrary for "-".

Product	Technology	IEA ETP 2017	JRC-EU-TIMES	TEMOA-Europe	Starting date (TEMOA-Europe)	Deployment state	Main references
Steel	BF-BOF	×	×	×	Base year	Traditional	[27], [129], [133], [134]
	DRI-EAF	×	×	×	Base year	Traditional	[27], [134]
	Steel from scrap-EAF	×	×	×	Base year	Traditional	[27], [134]
	Cast iron cupola furnace-BOF/EAF	-	×	-	-	-	-
	Smelting reduction-BOF	×	×	×	2006	Innovative – commercial	[133]
	BF-BOF with CCS	×	×	×	2020	Demonstration phase	[27], [129], [133], [134], [135]
	BF with top gas recovery-BOF	×	×	×	2020	Demonstration phase	[27], [129], [134], [135], [231]
	DRI-EAF with CCS	×	-	×	2020	Demonstration phase	[27], [134], [135]
	HIsarna-BOF	×	-	×	2025	Demonstration phase	[27], [129], [133], [134], [137]
	HIsarna-BOF with CCS	×	-	×	2025	Demonstration phase	[27], [129], [133], [134], [135]
	Hydrogen direct reduction-EAF	×	-	×	2030	Demonstration phase	[138]
	Ulcored with CCS	×	-	×	2030	Demonstration phase	[27], [134], [135]
	Ulcolysis	×	-	×	2030	R&D phase	[139]
	Ulcowin	×	-	×	2030	R&D phase	[139]
Ferroalloys	Ferroalloys production	-	-	×	Base year	Traditional	[140], [141]

Table 35. Technologies for alumina and aluminum production, with their deployment state and starting year for the introduction in the production system. The "×" indicates that a technology is present in the considered databases, the contrary for "-".

Product	Technology	IEA ETP 2017	JRC-EU-TIMES	TEMOA-Europe	Starting date (TEMOA-Europe)	Deployment state	Main references
Alumina	Bayer process	×	-	×	Base year	Traditional	[27], [148]
Aluminum	Hall-Héroult	×	×	×	Base year	Traditional	[149]
	Secondary aluminum	×	×	×	Base year	Traditional	[151],
	Hall-Héroult with inert anodes	×	×	×	2030	Innovative – commercial	[149]
	Carbothermic reduction	×	-	×	2050	Demonstration phase	[149], [153]
	Kaolinite reduction	×	-	×	2050	Demonstration phase	[154]
Copper	Primary copper production	-	×	×	Base year	Traditional	[156], [155]
	Secondary copper production	-	×	-	-	-	-
Zinc	Zinc production	-	-	×	Base year	Traditional	[156]

Table 36. Technologies for non-metallic minerals production, with their deployment state and starting year for the introduction in the production system. The "×" indicates that a technology is present in the considered databases, the contrary for "-".

Product	Technology	IEA ETP 2017	JRC-EU-TIMES	TEMOA-Europe	Starting date (TEMOA-Europe)	Deployment state	Main references
Clinker	Dry process	-	×	×	Base year	Traditional	[158], [159], [160]
	Wet process	-	×	×	Base year	Traditional	[158], [159], [160]
	Dry process with post-combustion CCS	-	×	×	2025	Demonstration phase	[135], [158], [159], [160]
	Dry process with oxy-fuel combustion CCS	-	-	×	2025	Demonstration phase	[158], [159], [160], [161]
Cement	Cement blending	×	×	×	Base year	Traditional	[232]
	Alkali-activated cement-based binders	-	-	×	2010	Innovative – commercial	[233], [162]
	Belite cement	-	-	×	2010	Innovative – commercial	[163]
Lime	Long rotary kiln	×	-	×	Base year	Traditional	[158]
	Generic process	-	×	-	-	-	-
Glass	Fossil fuel-fired furnace	-	-	×	Base year	Traditional	[164]
	All-electric furnace	-	-	×	Base year	Traditional	[164]
	Hollow glass furnaces	-	×	-	-	-	-
	Flat glass furnaces	-	×	-	-	-	-
Ceramics	Ceramics production	-	-	×	Base year	Traditional	[129], [156]

Table 37. Technologies for chemicals production, with their deployment state and starting year for the introduction in the production system. The "×" indicates that a technology is present in the considered databases, the contrary for "-".

Product	Technology	IEA ETP 2017	JRC-EU-TIMES	TEMOA-Europe	Starting date (TEMOA-Europe)	Deployment state	Main references
HVC	Naphtha steam cracking (SC)	×	-	×	Base year	Traditional	[168], [64]
	Ethane SC	×	-	×	Base year	Traditional	[168], [64]
	Gas oil SC	×	-	×	Base year	Traditional	[168], [64]
	LPG SC	×	-	×	Base year	Traditional	[168], [64]
	PDH	×	-	×	2010	Innovative – commercial	[168], [64]
	NCC	×	-	×	2011	Innovative – commercial	[168], [64]
	MTO	×	-	×	2015	Innovative – commercial	[168], [64]
	Bioethanol dehydration	×	-	×	2020	Demonstration phase	[168], [64]
Ammonia	NG SR	×	×	×	Base year	Traditional	[168], [64]
	Naphtha POX	×	-	×	Base year	Traditional	[168], [64]
	Coal GSF	×	-	×	Base year	Traditional	[168], [64]
	Synthesis via electrolysis	×	-	×	2015	Innovative – commercial	[168], [64]
	Biomass GSF	×	-	×	2025	Demonstration phase	[168], [64]
	NG SR with CCS	×	×	×	2025	Demonstration	[168], [64]

						phase	
Methanol	NG SR	×	-	×	Base year	Traditional	[168], [64]
	Coke oven gas steam reforming	×	-	×	Base year	Traditional	[168], [64]
	LPG POX	×	-	×	Base year	Traditional	[168], [64]
	Coal GSF	×	-	×	Base year	Traditional	[168], [64]
	Synthesis via electrolysis	×	-	×	2015	Innovative – commercial	[168], [64]
	Biomass GSF	×	-	×	2025	Demonstration phase	[168], [64]
Chlorine	Mercury cell	-	-	×	Base year	Traditional	[169]
	Diaphragm cell	-	-	×	Base year	Traditional	[169]
	Membrane cell	-	×	×	Base year	Traditional	[169]
	Advanced membrane cell	-	×	-	-	-	-
Other chemicals	Generic production processes	-	×	-	-	-	-

Table 38. Technologies for pulp and paper production, with their deployment state and starting year for the introduction in the production system. The × indicates that a technology is present in the considered databases, the contrary for "-".

Product	Technology	IEA ETP 2017	JRC-EU-TIMES	TEMOA-Europe	Starting date (TEMOA-Europe)	Deployment state	Main references
Pulp	Mechanical pulping	×	×	×	Base year	Traditional	[10], [11]
	Semi-chemical pulping	×	-	×	Base year	Traditional	[10]
	Kraft process	×	×	×	Base year	Traditional	[10]
	Sulfite process	-	-	×	Base year	Traditional	[10]
	Recycled fiber pulping	×	×	×	Base year	Traditional	[11], [12]
Paper	Paper production	×	×	-	Base year	Traditional	[10]
	High quality paper production	-	-	×	-	-	-
	Low quality paper production	-	-	×	-	-	-

Table 39 reports the detailed input/output energy-intensity breakdown by fuels and energy carriers for all the technologies taken into account in the iron and steel subsector. The most evident outcome is that the scrap-EAF route requires far lower energy with respect to all other technologies, even the most innovative ones. It has to be highlighted that CCS-equipped technologies, instead, rely on the same sources as traditional processes, and the additional electricity consumption has in general a slight impact on the overall energy intensity. On the other hand, the most innovative hydrogen- and electrolysis-based technologies (HDR-EAF, Ulcolysis, Ulcowin) require very low amount of direct CO_2 emitting sources (natural gas above all).

Table 40 reports the detailed energy-intensity for alumina and aluminum production technologies.

Detailed energy-intensity breakdown for clinker and cement production is reported in **Table 41**. **Table 41** makes it evident that energy consumption related to the wet process is not comparable with all of the other routes and, in addition, it is mainly fueled by the most polluting source, coal.

Table 42, Table 43 and **Table 44** report the data considered in TEMOA-Europe for HVC, ammonia and methanol production technologies, respectively.

Table 45 reports the detailed energy-intensity breakdown by energy carriers and materials required for pulp and paper production processes.

Table 39. Energy-intensity breakdown for steelmaking technologies.

Technology	Input energy intensity (GJ/t_{CS})											Output energy intensity (GJ/t_{CS})	
	BF reductant	BF gas	Coal	Coke oven gas	Natural gas	Electricity	Machine drive	Steam	Oxygen	Hydrogen	Total	Recovered off-gas	Steam
BF-BOF (2020)	13.3	3.06		0.9	0.7		0.6	0.2			18.7		
BF-BOF (2050)	11.7	2.70		0.8	0.6		0.5	0.2			16.5		
DRI-EAF (2020)					21.2	1.2					22.4		0.2
DRI-EAF (2050)					17.5	1.0					18.5		
Steel from scrap-EAF (2020)					3.4	2.8			0.5		6.7		
Steel from scrap-EAF (2050)					2.2	1.8			0.3		4.3		
Smelting reduction-BOF			15.9	0.4	0.4	0.4		0.1	1.2		18.4	0.4	
BF-BOF with CCS (2020)	13.3	3.06		0.9	0.7		1.0	0.2			19.1		3.1
BF-BOF with CCS (2050)	11.7	2.70		0.8	1.8		0.9	0.2			16.9		
BF-TGR-BOF with CCS	10.9	3.06		0.9	1.8		0.5	0.2			17.3		
DRI-EAF with CCS					17.5	1.0	0.4				18.8		0.2

HIsarna-BOF	13.1	0.8	0.6		0.6	0.2		14.3	0.7		
HIsarna-BOF with CCS	13.1	0.8	0.6		1.0	0.2		15.6	0.7		
Ulcored with CCS			17.5	1.0	0.7			19.2			
HDR-EAF			2.2	1.8	1.3		6.1	11.4		0.2	
Ulcolysis			1.2	14.5				15.7			
Ulcowin	0.9		2.27	12.6				15.7			

Table 40. Energy-intensity breakdown and energy-intensive material requirement for alumina and aluminum production technologies.

Technology	**Input energy-intensity (GJ/t_{NM})**					**Material input ($t_{Al_2O_3}/t_{Al}$)**
	Coal	**Heavy fuel oil**	**Natural gas**	**Electricity**	**Total**	**Alumina**
Bayer process (2020)	8.5	1.1	4.0	1.1	14.7	
Bayer process (2050)	6.0	0.8	2.9	0.8	10.4	
Hall-Héroult (2020)			2.8	48.7	51.5	1.9
Hall-Héroult (2050)			2.6	44.6	47.2	1.9
Secondary aluminum		0.1	3.7	0.5	4.3	
Hall-Héroult with inert anodes			2.2	38.3	40.5	1.9
Carbothermic reduction of alumina			2.0	34.1	36.0	1.9
Kaolinite reduction				50.4	50.4	

Table 41. Energy-intensity breakdown and energy-intensive material requirement for clinker production.

Technology	Input energy-intensity (GJ/t_{NM})							Material input (t/t_{NM})
	Heavy fuel oil	Coal	Natural gas	Biomass	Electricity	Machine drive	Total	Clinker
Dry process	1E-2	1.9	1E-2	0.2	0.5		2.7	
Wet process	1.0	4.2	0.5	0.4	0.4		6.5	
Dry process with post-combustion CCS	1E-2	1.9	1E-2	0.2	0.1	0.3	2.6	
Dry process with oxy-fuel CCS	1E-2	1.9	1E-2	0.2	0.5		2.7	
Cement blending								0.7
AAC	0.2	0.7	0.1	0.1	0.1		1.2	
Belite cement	0.6	2.4	0.3	0.2	0.4		3.9	

Table 42. Energy-intensity breakdown for HVC production, based on [64].

Technology	Input energy-intensity (GJ/t_{HVC})								Feedstock input (GJ/t_{HVC})						Output energy intensity (GJ/t_{HVC})
	Naphtha	Ethane	Gas oil	LPG	Biomass	Steam	Machine drive	Total	Naphtha	Ethane	Gas oil	LPG	Methanol	Biomass	Steam
Naphtha SC (2020)	13.1						0.3	13.4	80.8						1.4
Naphtha SC (2050)	11.8						0.3	12.1	72.7						2.1
Ethane SC (2020)		13.6					0.3	13.9		56.7					1.4
Ethane SC (2050)		12.2					0.3	12.5		51.0					3.0
Gas oil SC (2020)			12.0				0.3	12.3			89.9				1.4
Gas oil SC (2050)			10.8				0.3	11.1			80.9				1.4
LPG SC (2020)				13.5			0.3	13.8				79.2			1.4
LPG SC (2050)				12.2			0.3	12.5				71.3			2.8
PDH (2020)				10.7		2.7	0.1	13.5				55.9			0.1
PDH (2020)				8.9		2.2	0.1	11.2				50.3			0.1
NCC (2020)	10.9						0.3	11.2	62.9						1.2
NCC (2050)	9.8						0.3	10.1	56.6						1.2
MTO (2020)	5.9						0.2	6.1					53.7		1.1
BDH					1.6	45.5	1.9	49.0						45.9	

Table 43. Energy-intensity breakdown for ammonia production, based on [64].

Technology	Input energy-intensity (GJ/t_{NH_3})							Feedstock input (GJ/t_{NH_3})				Output energy intensity (GJ/t_{NH_3})	
	Naphtha	Biomass	Natural gas	Coal	Electricity	Machine drive	Total	Naphtha	Biomass	Natural gas	Coal	Hydrogen	Steam
NG SR (2020)			26.3		0.3		26.6			19.5			9.3
NG SR (2050)			15.5		0.3		15.8			19.5			11.4
Naphtha POX (2020)	27.9				2.0		29.9	18.4					8.4
Naphtha POX (2050)	20.6				2.0		22.6	18.4					9.7
Coal GSF (2020)				23.6	3.7		27.3				18.5		1.5
Coal GSF (2050)				19.6	3.7		23.3				18.5		1.9
Synthesis via electrolysis						4.3	4.3					36.0	
Biomass GSF		26.3			5.0		31.3		27.0				1.7
NG SR with CCS			26.3		0.3		26.6			18.9			9.3

Table 44. Energy-intensity breakdown for methanol production, based on [64].

Technology	Input energy-intensity (GJ/t_{MeOH})							Feedstock input (GJ/t_{MeOH})					Output energy intensity (GJ/t_{MeOH})
	LPG	Biomass	Natural gas	Coke-oven gas	Coal	Machine drive	Total	Biomass	Natural gas	LPG	Coal	Hydrogen	Steam
NG SR (2020)			15.7			0.3	16.0		21.9				2.8
NG SR (2050)			13.8			0.3	14.1		21.9				3.0
Coke oven gas SR (2020)				26.9		3.7	30.6		21.9				5.5
Coke oven gas SR (2050)				24.2		3.3	27.5		19.7				5.5
LPG POX (2020)	14.8					2.0	23.0			21.0			2.9
LPG POX (2050)	10.1					2.0	23.0			12.1			2.1
Coal GSF (2020)					26.9	3.7	30.6				19.5		5.5
Coal GSF (2050)					24.2	3.3	27.5				17.6		5.5
Synthesis via electrolysis						1.4	1.4					22.5	
Biomass GSF		28.0				5.0	33.0	28.4					5.9

Table 45. Energy-intensity breakdown for pulp and paper production technologies.

Technology	Input energy intensity (GJ/t_P *)				Material input (t/t_P)		Output energy intensity (GJ/t_P)		Material output (t/t_P)
	Process heat	Steam	Machine drive	Total	Wood	Pulp	Electricity	Steam	Solid biomass waste
Mechanical pulping* (2020)		0.9	7.4	8.3	1.2			3.3	
Mechanical pulping (2050)		0.9	6.6	7.5	1.2			6.6	
Semi-chemical pulping		2.3	1.6	3.9	1.3				
Kraft process	11.0	11.2	2.5	24.7	2.2		5.8		22.2
Sulfite process	7.1	6.5	3.2	16.8	2.0		2.9		12.3
Recycled fiber pulping		0.8	0.5	1.3					
Paper mill		4.1	2.5	6.6		0.6			

* t_P: ton of pulp/paper

Ringraziamenti

Se ripenso a tre anni fa, all'inizio di questo percorso fantastico che mi ha finalmente portato a capire cosa voglio fare da grande, non avrei potuto immaginare quanto le cose sarebbero cambiate nella mia vita, e non solo a livello professionale.

Ognuna delle persone che ho incontrato, chi se n'è andato, chi c'è ancora e chi resterà, mi ha regalato un pezzetto della propria esperienza, mi ha aiutato a crescere e capirmi (quasi) fino in fondo, e senza di voi questo viaggio sarebbe stato sicuramente meno entusiasmante.

Mamma, Papà, Alessio, Nonna, grazie per essere sempre vicini a me col cuore e con i pensieri, per sopportare i miei momenti no e per il vostro infinito amore. Il nostro legame indissolubile è la mia guida in ogni momento, nonostante i chilometri che ci separano. Vi voglio bene, anche se non ve lo dico spesso, ma senza di voi tutti i miei traguardi sarebbero impossibili da raggiungere.

Un ringraziamento speciale a Laura, una guida costante, infaticabile, in grado di andare sempre oltre il proprio ruolo formale di supervisore e di mettersi completamente a disposizione sia a livello professionale che personale. Credo che in un percorso di Dottorato in pochi abbiano la fortuna impagabile di poter contare sempre su una persona sempre pronta a farsi in quattro per tutti, anche tra i mille (e più) impegni. Hai sicuramente contribuito in maniera importante a rendermi quel che sono oggi e te ne sarò per sempre grato.

Grazie Rosella, che forse non a caso è l'anagramma di "sorella"; la sorella che non ho avuto ma che, da vicino o da lontano, è sempre pronta a regalarmi il suo entusiasmo, la sua irrefrenabile voglia di vivere, la sua sincerità e il suo supporto.

Grazie Luca per avermi insegnato che esistono tanti modi per essere amici, che non esiste un modo giusto o un modo sbagliato, ma che il migliore è quello che si può racchiudere in un abbraccio come i tuoi.

Grazie Marco, perché dietro la corazza si nasconde un amico leale, un po' sciocco, sempre pronto a volare, a squattare e a uscire con i bro. Ma grazie soprattutto perché mi hai fatto credere di nuovo che un'amicizia vera può esistere.

Grazie Mattia per la tua capacità di sostenere gli amici nei momenti bui e di rendere indimenticabili con la tua esuberanza i momenti felici. Il tuo supporto e la tua rete del pescatore sempre pronta a raccogliermi e farmi tornare sulla strada giusta sono stati una certezza per me in questi anni.

Grazie Nicola.

Oltre che per il piatto bruciato (vedi immagine sopra), grazie perché dietro il tuo essere un meme vivente non mi sarei mai aspettato di trovare un amico fantastico con cui condividere passioni (tutte tranne una) e un rapporto spontaneo e sincero.

Grazie Francesco per avermi insegnato che la serietà, il duro lavoro e la follia possono andare di pari passo.

Grazie Simone per avermi fatto capire che la focaccia barese è meglio di quella ligure e per la tua disponibilità nel tendere sempre una mano agli amici.

Ai miei due colleghi preferiti (non me ne vogliano gli altri), Matteo e Gianvito, grazie per aver reso piacevole ogni giorno di lavoro, anche se adesso

dovrò abituarmi alla vostra assenza. Sono sicuro, però, che non sarà sufficiente a scalfire l'amicizia che abbiamo costruito in questi anni fianco a fianco.

Ad Alessia e Domenico, grazie per esserci sempre, col mare sereno e tra le tempeste.

Al resto della mia famiglia torinese, Francesca, Alina, Edoardo, Daniela, Melissa, Laura, grazie per l'entusiasmo, l'allegria e la spensieratezza che sapete regalarmi, e per i momenti felici che abbiamo passato e passeremo insieme.

A tutto il gruppo MAHTEP, ricordatevi che il vostro Deputy Head sarà sempre lì a vegliare su di voi, ma che avrebbe vissuto quest'esperienza solo a metà senza persone fantastiche come voi.

Grazie a Lonia, per essere anche da lontano un punto fisso, sempre pronta a concedermi sorrisi e spensieratezza.

Grazie a Pippo per restarmi sempre accanto, per trovare sempre un momento per me e per aiutarmi a scovare potenziali fenomeni dall'Eredivisie.

E infine grazie a tutti, per citare un poeta contemporaneo.